Universidad de Concepción
Dirección de Postgrado
Facultad de Ciencias Naturales y Oceanográficas -Programa de Doctorado en Oceanografía

Metabolismos Alternativos del Carbono y del Nitrógeno en las Picocianobacterias que Habitan las Zonas Marinas Anóxicas

Tesis para optar al grado de Doctor en Oceanografía

MONTSERRAT GABRIELA ALDUNATE CHINCHÓN
CONCEPCIÓN-CHILE
2019

Profesor Guía: Osvaldo Ulloa Quijada
Dpto. de Oceanografía, Facultad de Ciencias Naturales y Oceanográficas
Universidad de Concepción

Profesor Co-Guía: Peter von Dassow
Depto. de Ecología, Facultad de Ciencias Biológicas
Pontificia Universidad Católica de Chile

Universidad de Concepción
Dirección de Postgrado

La Tesis de "*Doctorado en Oceanografía*" titulada *"Metabolismos Alternativos del Carbono y del Nitrógeno en las Picocianobacterias que Habitan las Zonas Marinas Anóxicas"*, de la Srta. *"MONTSERRAT GABRIELA ALDUNATE CHINCHÓN"* y realizada bajo la Facultad de Ciencias Naturales y Oceanográficas, Universidad de Concepción, ha sido aprobada por la siguiente Comisión de Evaluación:

Dr. Osvaldo Ulloa
Profesor Guía
Universidad de Concepción _____

Dr. Peter von Dassow
Profesor Co-Guía
Pontificia Universidad Católica de Chile _____

Dr. Carmen Morales Van de Wyngard
Miembro Comité de Tesis
Universidad de Concepción _____

Dra. Beatriz Díez
Evaluadora Externa
Pontificia Universidad Católica de Chile _____

Dra. Pamela Hidalgo
Directora
Programa de Doctorado en Oceanografía
Universidad de Concepción _____

Dedicatoria

A mis padres, Marisol Chinchón y Miguel Aldunate por ser mi apoyo y mi guía en la vida, los quiero más que a nadie.

Patricio Morales, por estar conmigo durante todo el proceso, en los buenos y malos momentos.

Mis abuelos Silvia Chinchón, Gustavo Chinchón y Eliana Hidalgo, quienes sé estarían orgullosos de estar presentes.

Mis hermanos: Anton, Pablo y Miguel Ángel y mi sobrino Raimundo.

Agradecimientos

Me gustaría agradecer a los jefes científicos de los cruceros de investigación en los que participé para el desarrollo de esta tesis: Alan Devol, Bess Ward (NBP1305), Frank Stewart (NH1410), Margie Mulholland (AT2626, RB1603), Amal Jayakumar (RB1603) y Osvaldo Ulloa (LowpHOx-I) y a los capitanes y los miembros de la tripulación de los buques de investigación RV Nathaniel B. Palmer, RV New Horizon, RV Atlantis, AGS-61 Cabo de Hornos y RV Ronald Brown. A los miembros pasados y presentes del Laboratorio de Oceanografía Microbiana: Alejandro Murillo, Marcia Astorga, Alvaro Muñoz Plominsky, Bárbara Léniz, Paula Ruiz, Francisca Olivares, Gadiel Alarcón, Carlos Henríquez, Salvador Ramírez y Cristián Venegas por su valiosa colaboración discutiendo los resultados de mi manuscrito. A mis profesores, el Dr. Osvaldo Ulloa y el Dr. Peter von Dassow por su colaboración y guía. A los profesores del Departamento de Oceanografía de la Universidad de Concepción. Al Instituto Milenio de Oceanografía por la plataforma y el cofinanciamiento.

Curriculum Vitae

Montserrat Gabriela Aldunate Chinchón

Nacida el 10 de febrero, 1984 en Linares, Chile

2002-2007: Bióloga Marina, Universidad de Concepción, Chile.

2010-2014: Magíster en Ciencias con mención en Oceanografía, Universidad de Concepción, Chile.

2013-presente: Doctorado en Oceanografía, Universidad de Concepción, Chile.

PUBLICACIONES

- **Aldunate, M.,** Henríquez-Castillo, C., Ji, Q., Lueders-Dumont, J., Mulholland, M. R., Ward, B. B., von Dassow, P. Ulloa, O. 2019. Nitrogen assimilation in picocyanobacteria inhabiting the oxygen-deficient waters of the eastern tropical North and South Pacific. Limnology and Oceanography. DOI:10.1002/lno.11315
- Ganesh S., Bertagnolli A., Bristow L., Padilla C.C., Blackwood N., **Aldunate M**., Bourbonnais A., Altabet M., Malmstrom R., Woyke T., Ulloa O., T. Konstantinidis K.T., Thamdrup B., Stewart, F.J. 2018. Genomic evidence for the use of alternative nitrogen substrates by anammox bacteria. The ISME Journal. DOI: 10.1038/s41396-018-0223-9.
- **Aldunate M**., De la Iglesia R., Bertagnolli A., Ulloa O. 2018. Oxygen modulates bacterial community composition in the coastal upwelling waters off central Chile. Deep-Sea Research Part II Top. Stud. Oceanogr. 1–12. DOI:10.1016/j.dsr2.2018.02.001.
- Garcia-Robledo, E., Padilla, C.C., **Aldunate, M**., Stewart, F.J., Ulloa, O., Paulmier, A., Gregori, G., Revsbech, N.P. 2017. Cryptic oxygen cycling in anoxic marine zones. Proc. Natl. Acad. Sci. 114, 8319–8324. DOI:10.1073/pnas.1619844114.

ÁREAS DE INVESTIGACIÓN

Principal: oceanografía biológica

Secundaria: oceanografía microbiana

Otras: ciclos biogeoquímicos; ecología microbiana.

EXPERIENCIA DOCENTE

- Coordinadora Curso: Introducción a las Ciencias del Mar, 1er año de Biología Marina, Facultad de Ciencias Naturales y Oceanográficas, Universidad de Concepción. Profesores: Silvio Pantoja, Osvaldo Ulloa, Renato Quiñones. 1er semestre 2018.
- Ayudante/"Teacher Assistant" curso internacional: "Ecology and Diversity of Marine Microorganisms (ECODIM)". Universidad de Concepción. Desde el 7 al 27 de enero de 2018, Dichato, Chile.
- Organización del curso internacional "Ecology and Diversity of Marine Microorganisms (ECODIM)", Dichato, Chile (Agosto de 2017 hasta marzo de 2018).
- Miembro de comité de proyecto de tesis de Biología Marina, Universidad de Concepción. Sr. Julio Poblete. "Variabilidad de mesoescala en la estructura de comunidades de nanoflagelados en la zona frente a Valparaiso". Julio, 2017.
- Miembro de comité de tesis de Biología Marina, Universidad de Concepción. Srta. Francisca Olivares. "Ecología molecular del bacterioplancton a través del gradiente de oxígeno en el Pacífico Sur Oriental". Marzo, 2017.
- Ayudantía Curso: Introducción a las Ciencias del Mar, Facultad de Ciencias Naturales y Oceanográficas, Universidad de Concepción. Profesor: Silvio Pantoja. 1er semestre de los años 2014, 2015, 2016 y 2017.
- Miembro de comité de proyecto de tesis de Biología Marina, Universidad de Concepción. Srta.Francisca Olivares. "Ecología molecular del bacterioplancton a través del gradiente de oxígeno en el Pacífico Sur Oriental". Septiembre, 2016.
- Ayudantía Curso: Biología de Recursos II, Facultad de Ciencias Naturales y Oceanográficas, Universidad de Concepción. Profesor: Dr. Ciro Oyarzún & Krisler Alveal. 2011-2012.
- Ayudantía Curso: Computación Básica, Facultad de Ciencias Naturales y Oceanográficas, Universidad de Concepción. Profesor: Salvador Ramírez.

CRUCEROS OCEANOGRÁFICOS

2017. Crucero TAN1711. Objetivo: Estudio de la edad y las fuentes del carbono inorgánico disuelto en aguas mesopelágicas, abisales y hadales, y de las comunidades microbianas que

habitan a esas profundidades en la fosa de Kermadec. Jefes científicos: Ronnie Glud (University of Southern Denmark) y Ashley Rowden (NIWA, Nueva Zelanda). RV. Tangaroa, Nueva Zelanda.

2016. Crucero RB1603. Objetivo: Ciclo del nitrógeno en Zona de Mínimo Oxígeno en el Océano Pacífico Nor Oriental. Jefe científico: Margaret Munholland (Old Dominium University) y Amal Jayakumar (Princeton University). RV Ronald Brown, San Diego, EE.UU.

2015. Crucero Lowphox I. "Tramas tróficas y el ciclo del carbono en aguas de bajo pH y bajo oxígeno: potencial impacto de El Niño". Jefe científico: Osvaldo Ulloa (Instituto Milenio de Oceanografía). AGS-61 Cabo de Hornos, Valparaiso, Chile.

2015. Crucero AT2626. Objetivo: Ciclo del nitrógeno en Zona de Mínimo Oxígeno en el Océano Pacífico Sur Oriental. Jefe científico: Margaret Munholland (Old Dominium University) y Amal Jayakumar (Princeton University). RV Atlantis, Arica, Chile.

2014. Crucero NH1410. Objetivo: Entendimiento filogenético y funcional del ciclo microbiano del azufre en las zonas de mínimo oxígeno. Jefe científico: Frank Stewart (Georgia Institute of Technology). RV New Horizon, San Diego, EE.UU.

2013. Crucero NBP1305. Objetivo: Estudio de los procesos de desnitrificación y anammox en el océano Pacífico Sur Oriental. Jefe científico: Alan Devol (University of Washington) y Bess Ward (Princeton University). RV Nathaniel B. Palmer, Valparaiso, Chile.

ESTADÍAS DE INVESTIGACIÓN O ENTRENAMIENTO

- Laboratorio Profesor Peter von Dassow. Departamento de Ecología, Pontificia Universidad Católica de Chile. Desde el 7 al 25 de mayo de 2018. Santiago, Chile.

- Laboratorio Profesora Bess Ward. Departamento de Geociencias, Princeton University. Desde el 30 de septiembre al 16 de octubre de 2015, Princeton, New Jersey, EE. UU.

- Laboratorio Profesora Bess Ward. Departamento de Geociencias, Princeton University. Desde el 7 de noviembre al 21 de noviembre de 2014, Princeton, New Jersey, EE. UU.

- Laboratorio Profesor Peter von Dassow. Departamento de Ecología, Pontificia Universidad Católica de Chile. Desde el 8 de septiembre al 12 de octubre de 2014. Santiago, Chile.

Índice de Contenidos

Índice de Figuras

Índice de Tablas

Resumen

Metabolismos alternativos del carbono y el nitrógeno en las picocianobacterias que habitan las zonas marinas anóxicas

Montserrat Gabriela Aldunate Chinchón

2019

Dr. Osvaldo Ulloa, Profesor Guía

Dr. Peter von Dassow, Profesor Co-Guía

Prochlorococcus y *Synechococcus* son los microorganismos fotosintéticos de vida libre más abundantes en el océano y representan aproximadamente el 25% de la productividad primaria marina. Linajes no cultivados de estas picocianobacterias también se desarrollan en la parte superior poco iluminada (< 1% de luz incidente) y alta en nutrientes de las zonas marinas anóxicas (ZMAs), generando un máximo secundario de clorofila (MSC). La disponibilidad de los nutrientes y la energía necesaria para la asimilación de estos nutrientes son factores esenciales que controlan el crecimiento del fitoplancton. *Prochlorococcus* posee divinil clorofila *a* y *b* (Chl a_2, Chl b_2) como pigmentos fotosintéticos principales, los que les permite ser muy eficientes capturando energía para desarrollar fotosíntesis en zonas más profundas. Sin embargo, estudios genómicos y otros basados en tasas de crecimiento sugieren que *Prochlorococcus* tiene el potencial para utilizar fuentes de carbono (C) alternativas, por lo que una heterotrofía complementaria no puede ser descartada. Esto es especialmente importante para los ecotipos que habitan las ZMAs, los que probablemente experimenten periodos prolongados sin la cantidad de luz necesaria para hacer fotosíntesis. Por otro lado, a diferencia de la superficie, las formas más comunes de nitrógeno (N) en las ZMAs son el nitrato (NO_3^-) y el nitrito (NO_2^-) con concentraciones nanomolares e indetectables de amonio (NH_4^+) y urea, respectivamente. Las picocianobacterias de la superficie basan su metabolismo asimilativo en fuentes reducidas de N, sin embargo, los ecotipos de *Prochlorococcus* de las ZMAs tienen el potencial genético para utilizar diferentes formas de N, incluyendo NO_3^- y NO_2^-; fuentes poco comunes para la mayoría de los ecotipos de *Prochlorococcus*, pero comunes para *Synechococcus*. Esta capacidad le conferiría a *Prochlorococcus* de ZMA una ventaja ecológica

sobre los linajes de *Prochlorococcus* que no tienen los genes necesarios para asimilar estos nutrientes.

En esta tesis se investigaron comunidades naturales del MSC y los grupos funcionales que las componen a través de isótopos estables (abundancia natural de ^{13}C y ^{15}N), citometría de flujo, y tasas de asimilación de distintas fuentes de C y N. Los resultados demostraron que las picocianobacterias del MSC de las ZMAs, en su mayoría del género *Prochlorococcus*, son muy eficientes en la captación de energía solar y en su capacidad de fijar C y que probablemente, durante los momentos de ausencia de luz, estarían asimilando glucosa como fuente de C complementaria. Además, durante el proceso de fotosíntesis, el MSC libera oxígeno (O_2) en aguas donde el O_2 es indetectable utilizando los sensores más sensibles, lo que refleja un acoplamiento estrecho entre la producción y el consumo de este gas, generando un ciclo críptico del O_2. Las tasas de producción bruta de O_2 y de fijación de C en el MSC fueron similares a las reportadas para la oxidación de NO_2^-, así como para la reducción anaeróbica de NO_3^- y SO_4^{2-}, lo que sugiere un efecto significativo de la fotosíntesis oxigénica local en los ciclos biogeoquímicos de las ZMAs del Pacífico. Además, la producción de C en el MSC puede proveer un 5-47% y 2-20% de la materia orgánica suministrada hacia las aguas anóxicas del Pacífico Nor Oriental Tropical (PNOT) y el Pacífico Sur Oriental Tropical (PSOT) respectivamente, dónde parte de ésta es remineralizada por los proceso de reducción desasimilatoria del NO_3^- a NO_2^- y desnitrificación.

Los resultados también sugieren que los ecotipos de *Prochlorococcus* de las ZMAs están utilizando una mezcla de formas reducidas y medianamente oxidadas de N (mayormente NO_2^-) para satisfacer sus necesidades nutricionales. Cuando el NH_4^+ y la urea están disponibles, *Prochlorococcus* utiliza preferentemente estas fuentes de N reducidas, a pesar de que su repertorio genómico permite la utilización de fuentes oxidadas. La preferencia por el NH_4^+ y la urea puede explicarse por la baja energía necesaria para asimilar estos nutrientes aun cuando NO_3^- es alto, un factor importante en el MSC (<1% de luz incidente). Además, la producción de O_2 por *Prochlorococcus* estaría estimulando la respiración aeróbica en la ZMA, generandose entonces el NH_4^+ que *Prochlorococcus* necesita, sin acumulación de este nutriente en el MSC. Por lo tanto, las picocianobacterias de las ZMAs podrían así representar potenciales competidores de las bacterias anammox por NH_4^+ y NO_2^-, de las arqueas amonio oxidantes por NH_4^+ y bacterias nitrito oxidantes por el NO_2^-.

Abstract

Alternative metabolisms of carbon and nitrogen in picocyanobacteria inhabiting anoxic marine zones

Montserrat Gabriela Aldunate Chinchón

2019

Dr. Osvaldo Ulloa, Thesis Advisor

Dr. Peter von Dassow, Thesis Co-Advisor

Prochlorococcus and *Synechococcus* are the most abundant free-living photosynthetic microorganisms in the ocean and represent approximately 25% of marine primary productivity. Uncultivated lineages of these picocyanobacteria also thrive in the dimly illuminated (<1% of incident light) and high nutrients upper part of the anoxic marine zones (AMZs), generating a secondary chlorophyll maximum (SCM). The availability of nutrients and the energy required for the assimilation of these nutrients are essential factors controling the growth of phytoplankton. *Prochlorococcus* have divinyl chlorophyll *a* and *b* (Chl a_2, Chl b_2) as the main photosynthetic pigments, which allows them to be very efficient capturing energy for photosynthesis in deeper zones. However, genomic studies and other studies based on *Prochlorococcus* growth rates suggests that *Prochlorococcus* lineages have the potential to use alternative carbon (C) sources, so a complementary heterotrophy cannot be ruled out. This is especially important for AMZ ecotypes, which are likely to esperience prolonged periods without the amount of light needed to perform photosynthesis. On the other hand, unlike the surface, the most common forms of nitrogen (N) in AMZs are nitrate (NO_3^-) and nitrite (NO_2^-) with nanomolar and undetectable concentrations of ammonium (NH_4^+) and urea respectively. Surface picocyanobacteria base their N assimilative metabolism on reduced N sources, however, AMZ *Prochlorococcus* ecotypes have the genetic potential to use different N forms, including NO_3^- and NO_2^-; unusual N sources for most *Prochlorococcus* ecotypes, but common for *Synechococcus*. This ability would confer ZMA *Prochlorococcus* an ecological advantage over *Prochlorococcus* lineages that do not have the genes necessary to assimilate these nutrients.

In this thesis, natural SCM communities and the functional groups composing them were investigated through stable isotopes (^{13}C and ^{15}N natural abundance), flow cytometry, and assimilation rates of several C and N sources. Results demonstrated that SCM picocyanobacteria at AMZ, composed mostly by *Prochlorococcus,* are very efficient in capturing solar energy and their ability to fix C, and also they are probably assimilating glucose as a complementary source of C during moments of absence of light. In addition, during photosynthesis, the SCM releases oxygen (O_2) in waters where O_2 is undetectable using the most sensitive sensors, reflecting a tight coupling between the production and consumption of this gas, generating then a cryptic O_2 cycle. The rates of gross O_2 production and C fixation in the SCM were similar to those reported for the oxidation of NO_2^-, as well as for anaerobic reduction of NO_3^- and SO_4^{2-}, which suggests a significant effect of local oxygenic photosynthesis in the biogeochemical cycles of the Pacific AMZs. In addition, the production of C at the SCM can provide 5-47% and 2-20% of the organic matter supplied to the anoxic waters of the Eastern Tropical North Pacific (ETNP) and the Eastern Tropical South Pacific (ETSP) respectively, where part of it is remineralized by dissimilatory NO_3^- reduction to NO_2^- and denitrification.

Our results also suggest that AMZ *Prochlorococcus* ecotypes are using a mixture of reduced and partly oxidized N forms (mostly NO_2^-) to satisfy their nutritional needs. When NH_4^+ and urea are available, *Prochlorococcus* preferably uses these reduced N sources, even though their genomic repertoire allows the use of oxidized N sources. The choice of NH_4^+ and urea can be explained by the low energy needed to assimilate these nutrients even when NO_3^- is high, a important factor in the SCM (<1% incident light). In addition, *Prochlorococcus* O_2 production could be stimulating aerobic respiration in the AMZs, thus generating the NH_4^+ that *Prochlorococcus* needs, without accumulation of this nutrient in the SCM. Accordingly, AMZ picocyanobacteria might thus represent potential competitors with anammox bacteria for NH_4^+ and NO_2^-, with ammonia-oxidizing archaea for NH_4^+, and with nitrite-oxidizing bacteria for NO_2^-.

1. INTRODUCCIÓN

1.1. Picocianobacterias y las zonas marinas anóxicas

Prochlorococcus es el fotótrofo unicelular de vida libre más pequeño del planeta (Chisholm et al. 1992). Es numéricamente importante, y junto a otra picocianobacteria llamada *Synechococcus*, representan aproximadamente el 25% de la productividad primaria marina (Flombaum et al. 2013). Aunque *Prochlorococcus* es un grupo monofilético muy relacionado con *Synechococcus* (Biller et al. 2015), ambos grupos presentan grandes diferencias fisiológicas y ecológicas. Una de estas diferencias tiene relación con su aparato fotosintético, basado en la presencia de ficobilisomas en *Synechococcus* y en el complejo Pcb/Divinil Clorofila *a* y *b* en *Prochlorococcus*, este último permitiendo una mejor absorción de la luz azul dominante en aguas profundas. Los patrones de abundancia de ambas picocianobacterias también difieren, disminuyendo la abundancia de *Synechococcus* desde aguas eutróficas a oligotróficas y al contrario, aumentando la abundancia de *Prochlorococcus* a medida que se aleja de la costa (Partensky et al. 1999; Grob et al. 2007) (Fig. 1.1).

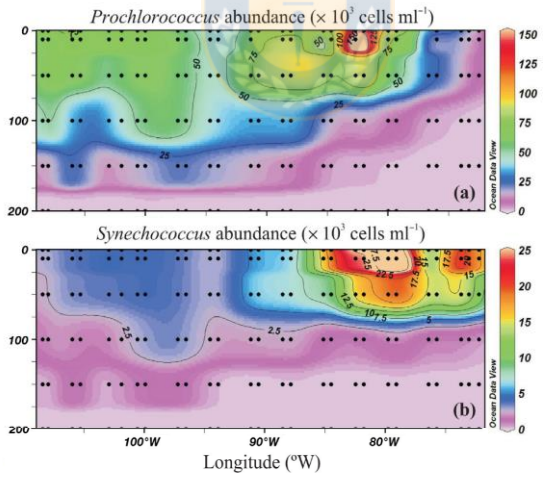

Figura 1.1. Patrón de abundancias costa-océano de *Prochlorococcus* (a) y *Synechococcus* (b) en células ml^{-1}. Modificado de Grob et al. 2007.

Latitudinalmente también presentan diferencias, mientras *Prochlorococcus* se distribuye mayormente entre los 40º de latitud norte y sur, *Synechococcus* tiene una distribución más amplia (Fig. 1.2). Así, debido a su amplia distribución y abundancia, ambas picocianobacterias

fotosintéticas contribuyen de forma importante a la biomasa y producción primaria marina de los océanos tropicales y subtropicales (Li et al. 1994; Liu et al. 1997).

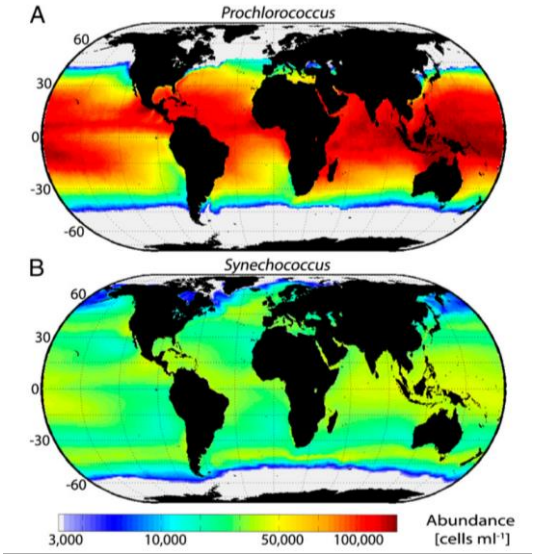

Figura 1.2. Distribución global de la abundancia promedio anual en la superficie del mar de *Prochlorococcus* (A) y *Synechococcus* (B). Extraído de Flombaum et al. 2013.

Prochorococcus y *Synechococcus* poseen una gran diversidad genética y se sugiere que esta es una de las razones de su éxito en colonizar los océanos del mundo. Por ejemplo, en *Prochorococcus* se distinguen varios ecotipos, determinados principalmente por la disponibilidad de luz y nutrientes. Los ecotipos adaptado a altas intensidades lumínica son los denominados HL (del inglés High Light), mientras que los ecotipos adaptado a bajas intensidades lumínicas (< 1% de luz incidente) son denominados LL (del inglés Low Light) (Rocap et al. 2003) (Fig. 1.3). Como la intensidad lumínica disminuye exponencialmente con la profundidad, los ecotipos HL se encuentran principalmente en la capa superficial del océano, mientras que los LL son dominantes a mayores profundidades (Goericke et al. 2000). Por otro lado, *Synechococcus* muestra una diversidad genética mayor a la de *Prochlorococcus*, con 3 grandes clusters llamados 5.1, 5.2 y 5.3, sin embargo la mayoría de los *Synechococcus* marinos pertenecen al clado 5.1 con más de 20 linajes descritos (Huang et al. 2012). A pesar de que los linajes de *Synechococcus* presentan patrones de distribución geográfica bien marcados, no muestran un patrón de distribución vertical claro como *Prochlorococcus* (Zwirglmaier et al. 2008).

En el caso de *Prochlorococcus*, hasta la fecha se han podido identificar 12

linajes/ecotipos, de los cuales 6 pertenecen al grupo de ecotipos HL (monofilético) y 6 al grupo de ecotipos LL (polifilético) (Huang et al. 2012; Biller et al. 2015). De los linajes cultivados de *Prochlorococcus* LL, el LLIV es el linaje más relacionado a *Synechococcus* filogenéticamente (Rocap et al. 2002). Incluso, se ha reportado que los genomas de algunas cepas del ecotipo LLIV son más parecidos al genoma de *Synechococcus* que a los genomas de los linajes HL del mismo *Prochlorococcus* (Zhaxybayeva et al. 2009; Partensky & Garczarek, 2010). Los linajes más basales, el LLV y LLVI, se han encontrado hasta ahora sólo en las zonas marina anóxicas (ZMA; Ulloa et al. 2012) del océano Pacífico Nor-Oriental Tropical y Pacífico Sur-Oriental Tropical (Lavin et al. 2010) y no poseen ejemplares cultivados.

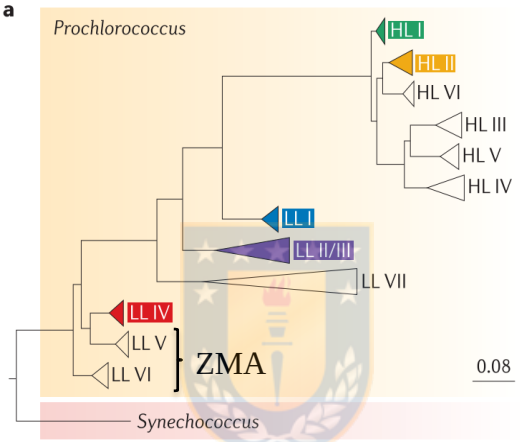

Figura 1.3. Distribución filogenética de los clados de *Prochlorococcus* determinada por la diversidad de secuencias del Espaciador Transcrito Interno de ARNr (ITS). De estos 12 clados, 5 (mostrados en color) poseen representantes cultivados, el resto ha sido identificado mediante secuencias ambientales (Modificado de Biller et al. 2015).

Las ZMAs (Fig. 1.4) se consideran un estado intermedio entre las zonas de mínimo oxígeno (ZMO) y las cuencas anóxicas sulfídicas. En las ZMOs (*e.g.* Bahía de Bengala, Pacífico Nor-Este) al contrario que las cuencas anóxicas sulfídicas (*e.g.* Mar Negro, Mar Báltico, Cuenca Cariaco, costas de Namibia) aún se puede encontrar algo de oxígeno y no presentan acumulación de nitrito (NO_2^-) ni sulfuro. En cambio, las ZMAs (Pacífico Nor-Oriental Tropical, PNOT; Pacífico Sur-Oriental Tropical, PSOT; Mar Arábigo) se caracterizan por presentar acumulaciones de NO_2^-, por poseer un ciclo críptico del azufre (Canfield et al. 2010) y por ser completamente anóxicas, no pudiendo detectarse oxígeno ni siquiera utilizando los sensores más sensibles con límites de detección que van entre 1 – 10 nM

(Revsbech et al. 2009; Thamdrup et al. 2012). La ausencia total de oxígeno permite que el nitrato (NO_3^-) actúe como aceptor de electrones terminal, participando activamente en los procesos de nitrato reducción y desnitrificación lo que representaría una pérdida de nitrógeno dentro de las ZMAs (Ward et al. 2009).

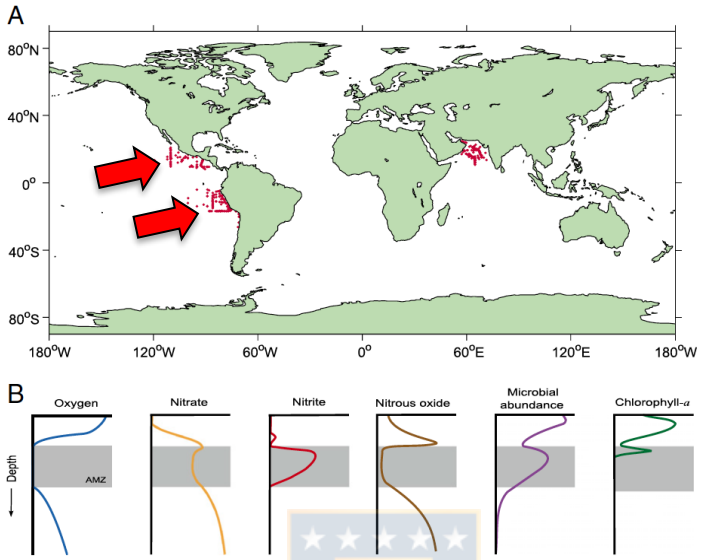

Figura 1.4. Zonas marinas anóxicas (≤ 2 µM de oxígeno y ≥ 0,5 µM de NO_2^-) en los océanos del mundo (A) y sus perfiles verticales característicos (B). Las flechas rojas destacan el Océano Pacífico Nor-Oriental Tropical (PNOT) y el Océano Pacífico Sur-Oriental Tropical (PSOT); Modificada de Ulloa et al. 2012.

En estas ZMAs también se puede identificar la presencia de un Máximo Secundario de Clorofila (MSC) (Johnson et al. 1999; Goericke et al. 2000; Lavín et al. 2010), el cual está principalmente compuesto por los linajes LL de *Prochlorococcus* IV, V y VI (Lavín et al. 2010) y, en menor medida, por los linajes I, VI y XV de *Synechococcus*. Si bien el linaje LLIV de *Prochlorococcus* ha sido encontrado en otros MSC de zonas óxicas, como en el Mar de los Sargazos y en el giro subtropical del Pacífico Norte (Rocap et al. 2003; Malmstrom et al. 2010), los linajes V y VI han sido reportados únicamente en las ZMAs (Lavín et al. 2010) del PNOT y PSOT, específicamente en el límite inferior de la capa fótica. Debido a que el Mar Arábigo también es una ZMA, es probable que estos linajes se encuentren también en esta zona.

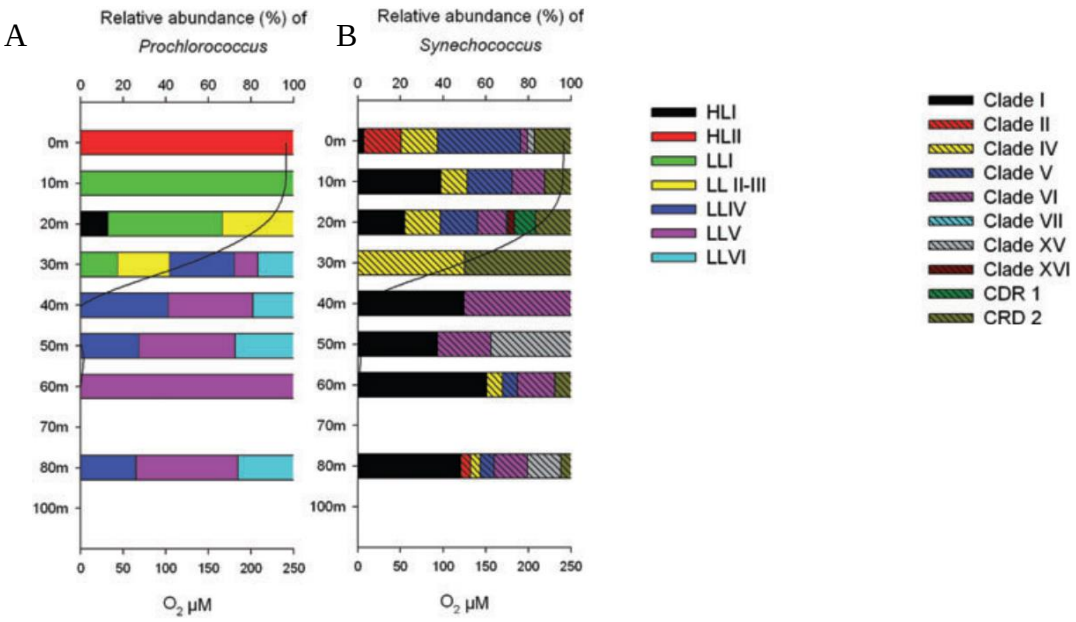

Figura 1.5. Perfiles de abundancia relativa de los linajes específicos de *Prochlorococcus* (A) y *Synechococcus* (B) obtenidos por T-RFLP y biblioteca de clones en la ZMA del océano Pacífico Sur Oriental Tropical. Modificado de Lavín et al. 2010.

1.2. Metabolismo del Carbono en picocianobacterias marinas

El pequeño tamaño de *Prochlorococcus*, junto con la presencia de divinil clorofila *a* (Chl a_2) como pigmento fotosintético principal, hace de esta picocianobacteria muy eficiente en la captación de energía solar y en su conocida capacidad de fijar C mediante fotosíntesis (Li, 1994; Bibby et al. 2003; Jardillier et al. 2010). El C fijado por estas picocianobacterias puede ser reciclado a través del anillo microbiano o exportado hacia zonas más profundas, y en el caso del MSC, el C puede ser exportado hacia el interior de las ZMAs (Garcia-Robledo et al. 2017; Fuchsman et al. 2019). Tanto *Prochlorococcus* como *Synechococcus* utilizan el ciclo de Calvin-Benson-Bassham para fijar C, siendo la enzima Rubisco la encargada de llevar a cabo la primera reacción de este ciclo, fijando el CO_2 a una molécula orgánica (Hess et al. 2001). Sin embargo, un estudio basado en experimentos de tasas de crecimiento de muestras naturales del Mar Arábigo sugiere una posible heterotrofía complementaria para *Prochlorococcus* (Johnson et al. 1999). Esto es reforzado por algunos estudios genómicos que han encontrado que la expresión de genes relacionados a la utilización de glucosa incrementa fuertemente después de la adición de esta fuente de C en cultivos de *Prochlorococcus* (Gómez-Baena et al. 2008; Muñoz-Marín et al. 2013). Una posible mixotrofía sería relevante

para los linajes de *Prochlorococcus* LL de las ZMAs ya que debido a la posición que ocupa en la columna de agua, es probable que presenten periodos con ausencia de luz y, por lo tanto, ausencia de energía para realizar fotosíntesis.

1.3. Metabolismo del Nitrógeno en picocianobacterias marinas

La disponibilidad de nutrientes es un factor esencial y limitante de la productividad primaria (Tyrrell, 1999). El amonio (NH_4^+) es la fuente de N preferida de las cianobacterias, pero se encuentra generalmente en concentraciones muy bajas. Sin embargo, las picocianobacterias como *Prochlorococcus* y *Synechococcus* han sorteado este obstáculo debido a la capacidad que tienen de utilizar una gran variedad de fuentes de N para satisfacer sus necesidades nutricionales (Moore et al. 2002). Entre estas fuentes de N alternativas al NH_4^+ se encuentran la urea (Painter et al. 2008), el NO_2^- (Moore et al. 2002; Martiny et al. 2009) y el cianato (un derivado de la descomposición de la urea; Berube et al. 2015). Incluso fuentes orgánicas de N, como algunos aminoácidos, pueden ser importantes para la síntesis de proteínas, haciendo de estas picocianobacterias organismos mucho más versátiles de lo que inicialmente se pensaba (Zubkov et al. 2003; Zubkov et al. 2004).

El NO_3^- es un nutriente escaso en la superficie del océano, pero muy abundante a medida que aumenta la profundidad. Hasta hace poco se pensaba que de las dos picocianobacterias sólo *Synechococcus* era capaz de utilizar NO_3^- como fuente de N (Moore et al. 2002). Sin embargo, en estos últimos años se ha proporcionado evidencia de que algunos linajes de *Prochlorococcus* tendrían también esta capacidad. Uno de los primeros estudios es el de Casey et al. (2007) quienes demostraron, utilizando muestras ambientales del máximo profundo de clorofila del Mar de los Sargazos, que los linajes de *Prochlorococcus* que habitan en esa comunidad estarían utilizando entre el 10 y 20% de NO_3^- con respecto a las otras fuentes de N disponibles. Posteriores estudios genómicos (también en muestras ambientales) han ido confirmando esta capacidad en *Prochlorococcus*, utilizando como base la presencia de genes de asimilación de NO_3^- en algunos de sus linajes (Martiny et al. 2009; Widner et al. 2018). Incluso, otro trabajo mostró que algunos linajes cultivados de *Prochlorococcus* sobrevivirían en presencia de NO_3^- como única fuentes de N (Berube et al. 2015). En el caso específico de los linajes de *Prochlorococcus* asociados al MSC de las ZMAs, existen dos estudios que evidencian el potencial genético que tienen estos linajes para asimilar NO_3^-. El primero estuvo

basado en la reconstrucción del metagenoma de un linaje presente en el PSOT que presentó un repertorio completo de genes involucrados en el transporte (*napA*) y asimilación (*narB*) de NO_3^- (Astorga-Eló et al. 2015). En el segundo, Widner et al. (2018b) demostró además la presencia de genes para la utilización de NH_4^+ y NO_2^- y no se encontraron genes relacionados con la utilización de cianato. Así, pareciera ser que los distintos linajes de *Prochlorococcus* y *Synechococcus* han evolucionado para utilizar distintas fuentes de N.

1.4. Abundancia natural de isótopos estables

Los isótopos son átomos de un mismo elemento cuyo núcleo tiene cantidad diferente de neutrones, por lo que presentan diferente masa (Fig. 1.6). Los elementos como el C y N poseen dos o más isótopos los que pueden ser estables o radioactivos diferenciándose en que el último presenta desintegración nuclear.

En el ambiente se pueden encontrar naturalmente los distintos isótopos de un elemento, sin embargo, los más livianos son los más abundantes (Tabla 1.1). Las diferencias de masas, aunque parezcan pequeñas, afectan las propiedades químicas y físicas de los elementos, permitiendo que los distintos isótopos de un mismo elemento sean utilizados por los microorganismos de forma diferenciada, con la mayoría de los procesos bioquímicos favoreciendo la utilización del isótopo más liviano. Por ejemplo, si los microorganismos necesitan NO_3^- para cubrir sus necesidades metabólicas, utilizarán preferentemente $^{14}NO_3^-$ (liviano), dejando al ambiente más enriquecido en el isótopo pesado ($^{15}NO_3^-$), este proceso es denominado *fraccionamiento isotópico*.

Tabla 1.1. Abundancia de los isótopos del C y N en la naturaleza (Berglund & Wieser, 2011)

Elemento	Isótopo	Abundancia (%)
Carbono	^{12}C	98,89
	^{13}C	1,11
Nitrógeno	^{14}N	99,63
	^{15}N	0,37

Dado que naturalmente la abundancia del isótopo pesado es muy pequeña con respecto a la abundancia del isótopo liviano (Tabla 1.1) es usual trabajar con la notación "delta" (δ), que representa las abundancias de estos isótopos con respecto a un estándar, donde *R* representa la proporción entre el isótopo pesado y el liviano:

$$\delta^{A}X = \left((R_{muestra} | R_{está□□□□}) - 1\right) \cdot 1000$$

Estos $\delta^{A}X$ pueden cambiar dependiendo del origen del elemento, su abundancia en el ambiente, de si es una fuente limitante o no y de los procesos biogeoquímicos involucrados en su formación.

Así, el uso de isótopos permite comparar por ejemplo los $\delta^{15}N$ de las distintas fuentes de N que naturalmente se encuentran en un ecosistema en particular (*e.g.* $\delta^{15}N\text{-}NO_3^-$, $\delta^{15}N\text{-}NO_2^-$, $\delta^{15}N\text{-}NH_4^+$, $\delta^{15}N$-urea) con los $\delta^{15}N$ de la comunidad picoplanctónica de interés (nitrógeno orgánico particulado <3 μm), y los $\delta^{15}N$ de grupos picoplanctónicos específicos (*i.e.* $\delta^{15}N$-*Prochlorococcus*, $\delta^{15}N$-*Synechococcus*, $\delta^{15}N$-Picoeucariontes fotosintéticos). Con esta comparación, se puede entonces determinar la marca isotópica que deja la fuente de N utilizada en la materia orgánica de los microorganismos (Fig 1.6).

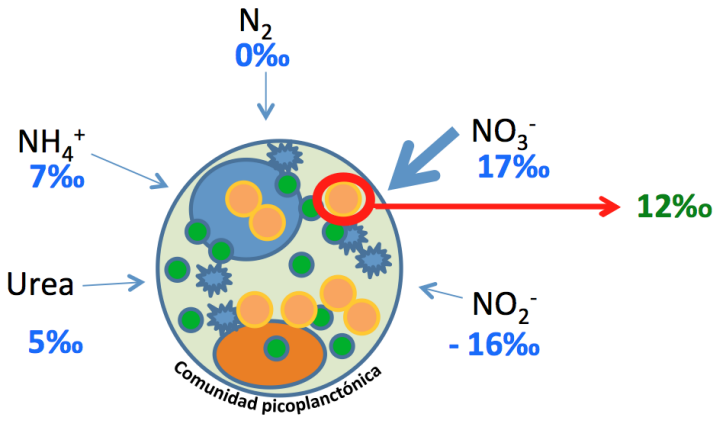

Figura 1.6. Ejemplo ilustrativo del estudio de los microorganismos por medio de isótopos estables. La comunidad picoplanctónica está expuesta naturalmente a distintas fuentes de N en el ambiente las cuales tienen sus respectivos $\delta^{□□}N$ (en azul). Si por ejemplo, un grupo de microorganismos miembro de esa comunidad (círculo naranjo) está utilizando preferentemente

una fuente de N como el NO_3^- ($\delta^{\square\square}N$ =17‰), el grupo de microorganismos en cuestión (círculo naranjo) tendrá en su N-orgánico una señal isotópica similar a la de la fuente de N que utilizó (N-orgánico=12‰).

1.5. Experimentos con trazadores isotópicos

El estudio de la abundancia isotópica natural de los microorganismos y sus fuentes de C y/o N nos ayuda a comprender cuál(es) fuente(s) de C y/o N están estos microorganismos utilizando. Sin embargo, los datos son insuficientes para determinar cuán rápido o a qué tasas están fijando o asimilando estas fuentes. Una forma de cuantificarlo es a través de experimentos con trazadores isotópicos dónde muestras de agua que contienen la comunidad bajo estudio se incuban en condiciones simuladas de luz y temperatura. Cada muestra es incubada además añadiendo distintas fuentes de C y N radiactivas (^{14}C) y/o estables ($^{13}C/^{15}N$). Así, se pueden obtener las tasas de fijación/asimilación de distintas fuentes de C/N, hasta su incorporación en la célula.

1.6. Separación de células por citometría de flujo

Un potencial problema en este tipo de estudios es que, si bien la comunidad picoplanctónica está dominada por *Prochlorococcus*, también está compuesta por otros organismos que pueden contribuir en forma diferenciada al fraccionamiento isotópico de la comunidad, como *Synechococcus*, picoeucariontes o bacterias y arqueas heterotróficas. Actualmente, existen técnicas que permiten distinguir y separar componentes específicos de una comunidad de microorganismos, una de las más utilizadas en oceanografía es el "Cell Sorting" o separación o aislamiento de células por citometría de flujo (Davey & Kell, 1996; Shapiro et al. 2003). Esta técnica está basada en la detección de grupos celulares por medio de la excitación de sus pigmentos naturales o tinciones fluorescentes, utilizando haces de luz láser con distintas longitudes de onda. También pueden ser utilizados otros parámetros, como la dispersión de la luz en la célula, la cual es diferencial dependiendo de la morfología celular. En el caso de *Prochlorococcus*, éste puede ser identificado en un citograma primeramente por su tamaño (< 0,8 μm) que genera una dispersión de la luz menor que en *Synechococcus* y por la ausencia de ficoeritrina (Scanlan et al. 2009; Biller et al. 2015) (Fig. 1.7).

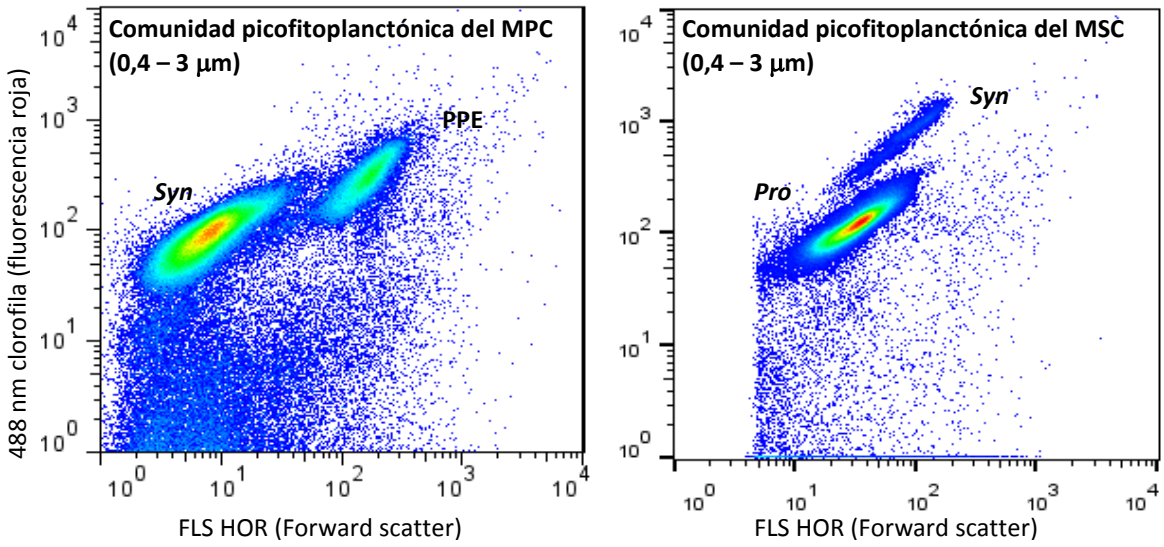

Figura 1.7. Citograma que muestra grupos autofluorescentes en muestras recolectadas desde la Estación 8 en el crucero AT2626 en el PSOT. El eje X (FLS HOR) representa la dispersión de la luz horizontal y el eje Y (488 nm clorofila) representa la fluorescencia roja. Los grupos identificados son: *Synechococcus* (*Syn*), Picoeucariontes fotosintéticos (PPE) y *Prochlorococcus* (*Pro*). A) Máximo primario de clorofila y B) Máximo secundario de clorofila.

1.7. Acoplamiento de citometría de flujo e isótopos estables del N.

La técnica de "cell sorting" de grupos celulares puede ser acoplada a análisis de isótopos radiactivos (Li, 1994) y estables (Lomas et al. 2011; Fawcett et al. 2011); esta última es conocida como FLOW-SIP (del inglés "Flow" o flujo, y "Stable Isotope Probing" o Rastreo con Isótopos Estables) (Casey et al. 2007). Como la cantidad de N-orgánico es muy pequeña (nmoles) luego del "sorting" o selección de células, las muestras quedarían bajo del límite de detección del espectrómetro de masas. Es por esto que el uso de nuevas metodologías más sensibles, como el *método desnitrificante*, son esenciales para obtener mediciones de abundancia natural y enriquecida (experimentos) para este tipo de muestras (Sigman et al. 2001). El método en su conjunto consiste en cuatro pasos que se detallan en la Figura 1.8.

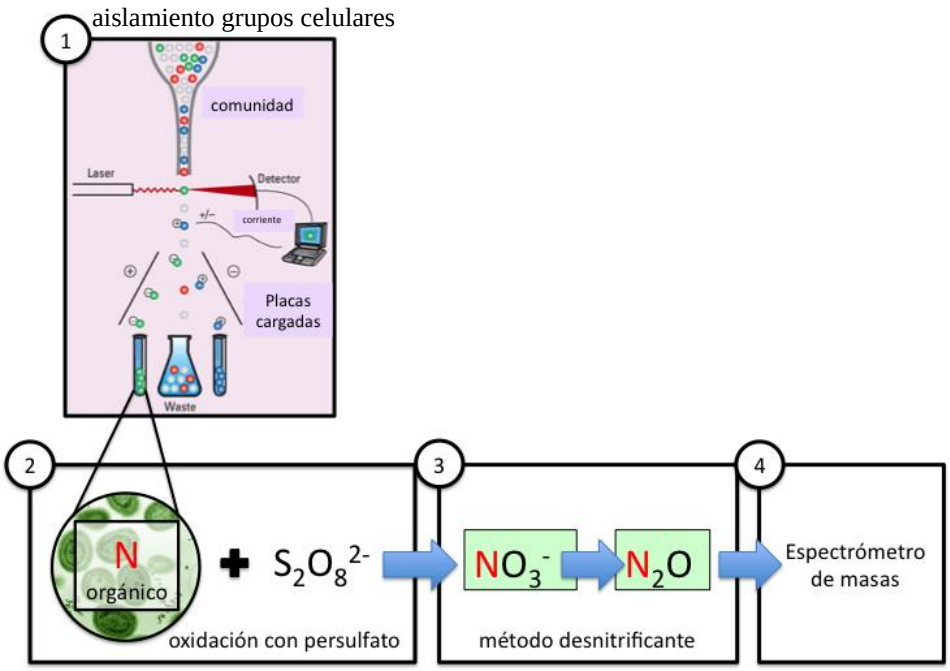

Figura 1.8. Resumen de la técnica FLOW-SIP. (1) identificación, selección y aislamiento de los grupos celulares en estudio a través de un citómetro de flujo con "cell-sorting" (2) oxidación del N orgánico de las células aisladas hasta NO_3^- utilizando $S_2O_8^{2-}$ (Knapp et al. 2005) (3) Reducción de NO_3^- a N_2O a través de bacterias desnitrificantes (Sigman et al. 2001) (4) lectura de los isótopos del N en el N_2O utilizando el espectrómetro de masas.

Con los antecedentes expuestos surgen las siguientes preguntas:

¿Estarán las picocianobacterias que habitan las ZMAs fijando C para sus requerimientos metabólicos? ¿Utilizan otras fuentes complemetarias de C?

¿Cuáles son las fuentes de N que utilizan las picocianobacterias que habitan las ZMAs?

¿Cuál es la contribución de las picocianobacterias al ciclo del C y del N en la comunidad picoplanctónica del MSC en las ZMAs?

1.9. Objetivo general

Como objetivo general se pretende:

Establecer la presencia y actividad a granel y célula específica de metabolismos alternativos del C y N en poblaciones naturales de *Prochlorococcus* y *Synechococcus* y su contribución a los ciclos del C y N en ZMA. Para ello se complementarán los métodos basados en la utilización de isótopos estables y citometría de flujo.

2. HIPÓTESIS Y OBJETIVOS ESPECÍFICOS

2.1. Hipótesis

H_1: La picocianobacteria *Prochlorococcus* LL que habita en el MSC de las ZMAs posee un metabolismo del C basado en la fijación de C y una heterotrofía complementaria que les permitiría vivir en zonas de baja luminosidad y bajo oxígeno.

H_2: La picocianobacteria *Prochlorococcus* LL que habita en el MSC de las ZMAs posee un metabolismo del N basado en la utilización de NO_3^-, a diferencia del conocido para los linajes que habitan las zonas óxicas iluminadas que está basado principalmente en amonio.

2.2. Objetivos específicos

Objetivo 1. Determinar las fuentes de C y N que utiliza las comunidad picoplanctónica que habita en el máximo primario y secundario de clorofila en las zonas marinas anóxicas a través de la señal en la abundancia isotópica natural de C y N en la materia orgánica particulada.

Objetivo 2. Determinar las fuentes de C y N específicas que utilizan los grupos de picocianobacterias que habita en el máximo primario y secundario de clorofila en las zonas marinas anóxicas a través de la señal en la abundancia isotópica natural de C y N en las células.

Objetivo 3. Determinar las tasas de utilización de distintas fuentes de C (*i.e.*, bicarbonato, glucosa, aminoácidos, piruvato, acetato) y de N (*i.e.*, NO_3^-, NO_2^-, NH_4^+, urea) en la comunidad picoplanctónica que compone el máximo primario y secundario de clorofila.

Objetivo 4. Determinar las tasas de utilización de las distintas fuentes de C (bicarbonato, glucosa, aminoácidos, piruvato, acetato) y de N (NO_3^-, NO_2^-, NH_4^+, urea) en

los componentes de la comunidad picoplanctónica (*e.g. Prochlorococcus* y *Synechococcus*) que habitan el máximo primario y secundario de clorofila.

3. MATERIALES Y MÉTODOS

3.1. Sitio de estudio y obtención de muestras

Las hipótesis planteadas fueron contrastadas por medio de la recolección y análisis de muestras desde las ZMAs presentes en el Océano Pacífico Nor-Oriental Tropical (PNOT) y el Pacífico Sur-Oriental Tropical (PSOT) durante seis cruceros oceanográficos: AMOP (Enero de 2014), NH1410 (Mayo de 2014) y RB1603 (Abril de 2016) en el PNOT; NBP1305 (Junio de 2013), AT2626 (Enero de 2015) y LowpHOx-I (Noviembre de 2015) para el PSOT (ver mapa con estaciones de muestreo en la Fig. 1 de los capítulos de resultados 1 y 2). De cada estación de muestreo se seleccionaron dos profundidades utilizando el perfil de fluorescencia y oxígeno: una de las profundidades corresponde al máximo primario de clorofila (MPC) y la otra profundidad al máximo secundario de clorofila (MSC). En el caso del crucero LowpHOx-I, donde no hubo desarrollo de MSC, las muestras fueron recolectadas desde la capa superficial de la ZMA, por debajo de la oxiclina. Las muestras de agua fueron recolectadas utilizado un Sistema Perfilador con Bomba del inglés "Pumping Profiling System (PPS)", compuesto por una bomba y un CTD (Seabird SBE-19 plus para el PNOT y Seabird SBE-25 para el PSOT). El PPS es óptimo para este tipo de muestreo ya que se minimiza la contaminación con oxígeno en las muestras de las ZMAs. Cuando el PPS no estuvo disponible se utilizó una roseta oceanográfica con CTD. En todos los cruceros al CTD se le incorporó un sensor de oxígeno (Seabird SBE 43 y STOX cuando estuvo disponible) y de fluorescencia (WET Labs, modelo WETStar para el PNOT y ECO-AFL/FL para el PSOT) (Objetivos específicos 1, 2, 3 y 4).

3.2. Determinación de abundancia natural de isótopos estables del C y del N

Parte del agua extraída desde el MPC y el MSC se utilizó para la determinación del $\delta^{13}C$ del Carbono Orgánico Particulado (COP) y del $\delta^{15}N$ del Nitrógeno Orgánico Particulado (NOP) de la comunidad picoplanctónica (fracción de tamaño celular: 0,3 – 3 μm). Estas muestras se obtuvieron por medio de la filtración de aproximadamente 2 L de agua de mar con prefiltros de policarbonato de 3-μm de tamaño de poro, concentrando así la biomasa picoplanctónica en filtros de fibra de vidrio de 0,3 μm (Sterlitech GF-75) previamente combustionados (500ºC por 6 h). Estos filtros GF-75 fueron secados a bordo del buque de

investigación y guardados en un lugar oscuro, fresco y seco o congelados en nitrógeno líquido. Una vez en el laboratorio, los filtros fueron acidificados con los vapores de HCl fumante, y luego introducidos en cápsulas de estaño para por último ser enviados a las Instalaciones de Isótopos Estables de la Universidad de California en Davis, Estados Unidos para su análisis (Objetivo específico 1).

Para determinar el $\delta^{15}N$ de grupos picoplanctónicos específicos, se concentraron los microorganismos de aproximadamente 4 L de agua de mar del MPC y el MSC utilizando pre-filtros de membrana de policarbonato de 3 μm y recolectando la biomasa picoplanctónica en filtros de membrana de policarbonato de 0,4 μm. Estos últimos fueron transferidos a crioviales de 4 mL y las células agregadas en el filtro fueron fijadas utilizando 200 μL de solución de formaldehido al 10% y 3,8 mL de agua de mar filtrada por 0,22-μm (concentración final de formaldehido= 0,5%). Después de 1 h de incubación en oscuridad y a 4ºC, los crioviales se agitaron y se conservaron en nitrógeno líquido hasta llegar al laboratorio dónde fueron almacenados a -80ºC hasta ser procesados (Objetivo específico 2).

3.3. Experimentos de incubación con isótopos estables del C y del N

Para los experimentos de incubación se recolectó agua desde el MSC en un botellón de vidrio de 20 L. Para evitar la contaminación por oxígeno, el botellón fue llenado previamente con una mezcla de gases compuesta por He y CO_2 (800 ppm) permaneciendo este flujo de gas durante el llenado del botellón y luego de 20 min terminado el muestreo para asegurar la eliminación de cualquier traza de oxígeno. Esta agua fue redistribuida en 6 – 12 botellas de vidrio de 1,1 L especialmente diseñadas para la incubación de muestras en anoxia (detalles de las botellas en la sección materiales y métodos de los capítulos 1 y 2 de resultados). Las botellas fueron transferidas a un incubador con temperatura controlada (~14-16 ºC) e iluminación LED azul con regulación de intensidad (10 – 30 μmol fotones m^{-2} s^{-1}) simulando las condiciones *in situ* del MSC. Además, se utilizaron agitadores magnéticos para evitar la estratificación de la muestra dentro de las botellas (Objetivos específicos 3 y 4).

Para determinar las tasas de fijación de C y asimilación de N por la comunidad picoplanctónica se hicieron experimentos de incubación dónde se agregaron simultáneamente una fuente de C ($NaH^{13}CO_3^-$; ^{13}C-glucosa, ^{13}C-acetato y ^{13}C-cianato) Cambridge Isotope Laboratories) y una de N ($^{15}NO_3^-$, $^{15}NO_2^-$, $^{15}NH_4^+$ ó ^{15}N-urea; Cambridge Isotope

Laboratories). La concentración final de $NaH^{13}CO_3^-$ fue de aproximadamente un 14,9-20,3%, 17,7% para la ^{13}C-glucosa, 16,5% para el ^{13}C-acetato y 83,8% para el ^{13}C-cianato, mientras que la concentración de los trazadores de N varió entre un 19,6-27,2% para $^{15}N\text{-}NO_3^-$, 47,6% para $^{15}N\text{-}NO_2^-$, 88,2% para $^{15}N\text{-}NH_4^+$ y un 74,1% para la ^{15}N-urea. Luego de 12 h de incubación, el picoplancton de cada botella fue concentrado, almacenado y analizado de igual forma que las muestras de abundancia natural de ^{13}C y ^{15}N en la comunidad del MSC y que se detalla en la sección 3.2. (Objetivo específico 3).

Para las incubaciones asociadas al metabolismo asimilativo del N por los grupos que componen la comunidad picoplanctónica del MSC se utilizaron las mismas cuatro fuentes de N marcadas con ^{15}N y el mismo sistema y tiempo de incubación que se utilizaron en los experimentos de tasas de asimilación comunitarias. Sin embargo, para estos experimentos, el picoplancton de cada botella fue prefiltrado utilizando filtros de policarbonato de 3 μm de tamaño de poro, concentrado en filtros de policarbonato de 0,4 μm de tamaño de poro y luego preservados de igual forma que las muestras de abundancia natural de ^{15}N que se detalla en la sección 3.2. para el caso de grupos que componen la comunidad picoplanctónica (Objetivo específico 4).

3.4. Identificación, selección y aislamiento de grupos picoplanctónicos por citometría de flujo

Para la determinación del δ^{15}N de grupos celulares específicos (Objetivo específico 2), como para la determinación de tasas de asimilación de distintas fuentes de N de estos grupos (muestras enriquecidas) (Objetivo específico 4) se utilizó la metodología de Fawcett et al. (2011) con algunas modificaciones. Las muestras almacenadas en crioviales se descongelaron a temperatura ambiente y se agitaron suavemente para despegar las células adheridas al filtro de policarbonato. Cada muestra fue analizada utilizando un citómetro de flujo con capacidad de aislamiento de células de marca InFlux® flow Cytometer-Cell Sorter (anteriormente Cytopeia y ahora de BD Biosciences) equipado con cinco lasers [488-nm (200mW), 457-nm (300 mW), 532-nm (150 mW), 355-nm (100mW), 640-nm (50 mW)] y utilizando una punta de cerámica de 86 μm de diámetro de apertura y una presión del fluido de 227,5 kPa. Como fluido matriz se preparó diariamente una solución de NaCl al 3,5 % (NaCl grado biología + agua purificada Milli Q) filtrada con filtros Steripak de 0,22 μm tamaño de poro (Merck Millipore, SPGPM20RJ). Como medida adicional, se agregó al sistema de tuberías del

citómetro un filtro Sterivex de 0,22 μm tamaño de poro (Merck Millipore, SVGVL10RC). Para el alineamiento y la calibración de los lasers se utilizaron nanoesferas fluorescentes de 1 y 3 μm (Partículas fluorescentes Ultra Rainbow; Spherotech, Lake Forest, IL, USA).

Prochlorococcus fue identificado basado en su fluorescencia roja (692/40 nm) usando una combinación de los laser azules de 457 nm y 488 nm. *Synechococcus* fue identificado basado en su fluorescencia naranja (579/36 nm) usando los laser 488 (azul) y 532 nm (verde); los picoeucariontes fotosintéticos (PPE) fueron identificados basados en la fluorescencia roja (692/40 nm) usando el laser azul de 488 nm. Los eventos fueron activados utilizando la dispersión de la luz (Forward Light Scatter; FLS). Para detectar las células no fluorescentes se utilizó la tinción fluorescente Sybr Green I (Marie et al. 2001), y los eventos fueron activados basados en la fluorescencia verde (530/40 nm) exitada por el laser azul (488 nm) y la ausencia de fluorescencia roja. Las muestras se analizaron a un flujo promedio de 30 μL min^{-1}, monitorizado por un flujómetro (Sensirion, US) y la tasa de eventos fue de 10.000-15.000 eventos s^{-1}. Luego de identificados los grupos, las células fueron aisladas utilizando el modo "purity" del citómetro y la configuración de dos tubos, mientras que el retraso en la caída de la gota fue calculado usando el procedimiento de calibración del Software Spigot y un microscopio de epifluorescencia. Los archivos de resultados fueron analizados con el Software FlowJo (FlowJo LLC, Ashland, OR, USA) y graficados usando el Software R (paquete ggplot). Los grupos aislados se concentraron en filtros de fibra de vidrio de 0,3 μm previamente combustionados (Sterlitech GF-75), los filtros fueron secados en una estufa a 40ºC, transferidos a sobres de aluminio previamente combustionado y almacenados libres de humedad hasta la oxidación con persulfato.

3.5. Oxidación con persulfato y método desnitrificante

Los filtros con las células aisladas por citometría de flujo correspondientes a las muestras naturales y enriquecidas en ^{15}N (experimentos de incubación), como también los estándares (USGS40, USGS41) y blancos (filtros sin células) fueron transferidos a un vial de vidrio pre combustionado de 4 mL. A cada uno de estos viales se les agregó 2 mL del reactivo de persulfato oxidación (3 g de NaOH en 60 mL de agua desionizada + 3g de persulfato recristalizado 5X en 60 mL de agua desionizada) y luego fueron autoclavados a 121ºC por 30 min. En este punto del proceso, todo el N orgánico de las células se han oxidado a NO_3^-. Para

obtener las mediciones de $\delta^{15}N$, se utilizó el "método desnitrificante" (Sigman et al. 2001) basado en el análisis isotópico del óxido nitroso (N_2O) generado por la acción de una bacteria desnitrificante que convierte el NO_3^- en N_2O y sin actividad N_2O reductasa. La composición isotópica del N_2O fue analizada por cromatografía de gases/espectrómetía de masas (ThermoFinnigan GasBench II and DeltaV. Las mediciones finales fueron corregidas con los blancos.

3.6. Cálculo de las tasas de asimilación

Las tasas de asimilación de C y N para la comunidad picoplanctónica del MSC fueron calculadas según las ecuaciones de Dugdale & Wilkerson (1986) utilizando los datos de C y N respectivamente. Estas ecuaciones fueron modificadas para la estimación de las tasas de asimilación de fuentes de N célula-específica de la siguiente manera:

$$V = \frac{R_{(\text{células})}}{R_{(\text{ND})}} \times T \qquad (1)$$

$$\rho\text{NDcélulas} = V \times \frac{N}{CA} \qquad (2)$$

Dónde V es la tasa de asimilación específica (h-1), $R_{(\text{células})}$ y $R_{(\text{ND})}$ el porcentaje de enriquecimiento en exceso de los átomos de ^{15}N en las células y en el nitrógeno disuelto (ND), respectivamente (%); T representa el tiempo de incubación (h); N representa la cantidad de N en las células aisladas analizadas (fg N); CA representa el número de células aisladas para el análisis isotópico (células).

Las tasas de asimilación grupo-específicas (ρND_{grupo}; nmol L^{-1} d^{-1}) se calcularon de la siguente forma:

$$\rho\text{NDgrupo} = \rho\text{NDcélulas} \times AIS \qquad (3)$$

Dónde AIS es la abundancia *in situ* promedio de cada grupo de células aisladas (células L^{-1}).

Cuando las adiciones de trazadores isotópicos excedieron el 50% de las concentraciones encontradas *in situ*, las tasas se consideraron como tasas potenciales.

3.7. Análisis estadísticos

Las diferencias significativas entre δ^{13}C-POC de las distintas estaciones de muestreo fueron analizadas utilizando la prueba de Kruskal-Wallis. Las correlaciones entre los datos de δ^{15}N de *Prochlorococcus*, δ^{15}N de *Synechococcus* y los factores ambientales (concentración de nutrientes y porcentaje de luz) se calcularon utilizando el análisis de correlación de Pearson. Las variables fueron previamente transformadas logarítmicamente como Log10 (X+1) y los coeficientes de correlación de Pearson fueron probados para su significancia usando un α=0,05 y el software XLStat (AddinSoft SARL).

4. RESULTADOS

4.1. Capítulo 1. "Ciclo críptico del oxígeno en zonas marinas anóxicas"

Artículo científico publicado en la revista "Proceedings of the National Academy of Sciences of the United States of America" **(114)**: 8319–8324, 2017. https://doi.org/10.1073/pnas.1619844114

Autores: Emilio Garcia-Robledo, Cory C. Padilla, **Montserrat Aldunate**, Frank J. Stewart, **Osvaldo Ulloa**, Aurélien Paulmier, Gerald Gregori and Niels Peter Revsbech

Resumen

La disponibilidad de oxígeno impulsa cambios en la diversidad microbiana y ciclos biogeoquímicos entre la capa superficial aeróbica y el núcleo anaeróbico en zonas marinas anóxicas (ZMAs) ricas en nitrito, que constituyen grandes regiones sin oxígeno en los océanos tropicales. El paradigma actual es que la producción primaria y la nitrificación dentro de la capa superficial óxica estimulan los procesos anaeróbicos en el núcleo anóxico de las ZMAs, donde ocurre entre 30-50% de la pérdida global de nitrógeno marino. Aquí demostramos que la fotosíntesis oxigénica en el máximo secundario de clorofila (MSC) emite cantidades significativas de O_2 a un ambiente que de otro modo es anóxico.

El MSC, comúnmente encontrado dentro de las ZMA, estaba dominado por la picocianobacteria *Prochlorococcus* spp. Niveles de O_2 libres en esta capa fueron, sin embargo, indetectables por las técnicas convencionales, lo que refleja un estrecho acoplamiento entre la producción de O_2 y el consumo por procesos aeróbicos en condiciones anóxicas aparentes. Análisis transcriptómicos de la comunidad microbiana en el MSC aparentemente anóxico reveló el aumento de la expresión de genes para procesos aeróbicos, como la oxidación de nitrito. Las tasas de producción bruta de O_2 y la fijación de carbono en el MSC fueron similares a los reportados para la oxidación de nitrito, así como para la reducción de nitrato disimilatoria anaeróbica y reducción de sulfato, sugiriendo un efecto importante de la fotosíntesis oxigénica local en los ciclos biogeoquímicos de la ZMA del Pacifico.

Cryptic oxygen cycling in anoxic marine zones

Emilio Garcia-Robledo[a,1,2], Cory C. Padilla[b], Montserrat Aldunate[c,d], Frank J. Stewart[b], Osvaldo Ulloa[d], Aurélien Paulmier[e], Gerald Gregori[f], and Niels Peter Revsbech[a]

[a]Microbiology Section, Department of Bioscience, Aarhus University, 8000 Aarhus, Denmark; [b]School of Biological Sciences, Georgia Institute of Technology, Atlanta, GA 30332-0230; [c]Graduate Program in Oceanography, Department of Oceanography, University of Concepción, 4070386 Concepcion, Chile; [d]Departamento de Oceanografía, Instituto Milenio de Oceanografía, Universidad de Concepción, 4070386 Concepción, Chile; [e]Laboratoire d'Etudes en Géophysique et Océanographie Spatiales, Institut de Recherche pour le Développement, CNRS, Centre National d'Etudes Spatiales, University of Toulouse, 31400 Toulouse, France; and [f]Aix Marseille Université, Université de Toulon, CNRS, Institut pour la Recherche et le Développement, Mediterranean Institute of Oceanography UM 110, 13288 Marseille, France

Edited by David M. Karl, University of Hawaii, Honolulu, HI, and approved June 21, 2017 (received for review December 2, 2016)

Oxygen availability drives changes in microbial diversity and biogeochemical cycling between the aerobic surface layer and the anaerobic core in nitrite-rich anoxic marine zones (AMZs), which constitute huge oxygen-depleted regions in the tropical oceans. The current paradigm is that primary production and nitrification within the oxic surface layer fuel anaerobic processes in the anoxic core of AMZs, where 30–50% of global marine nitrogen loss takes place. Here we demonstrate that oxygenic photosynthesis in the secondary chlorophyll maximum (SCM) releases significant amounts of O_2 to the otherwise anoxic environment. The SCM, commonly found within AMZs, was dominated by the picocyanobacteria *Prochlorococcus* spp. Free O_2 levels in this layer were, however, undetectable by conventional techniques, reflecting a tight coupling between O_2 production and consumption by aerobic processes under apparent anoxic conditions. Transcriptomic analysis of the microbial community in the seemingly anoxic SCM revealed the enhanced expression of genes for aerobic processes, such as nitrite oxidation. The rates of gross O_2 production and carbon fixation in the SCM were found to be similar to those reported for nitrite oxidation, as well as for anaerobic dissimilatory nitrate reduction and sulfate reduction, suggesting a significant effect of local oxygenic photosynthesis on Pacific AMZ biogeochemical cycling.

Prochlorococcus | oxygen minimum zone | secondary chlorophyll maximum | metatranscriptomics | aerobic metabolism

In coastal zones of the eastern tropical Pacific Ocean, the upward transportation of nutrient-rich waters results in relatively high primary productivity at surface depths. Sinking of organic matter produced by surface production coupled with sluggish circulation leads to the formation of oxygen-deficient water masses at intermediate depths below the mixed layer. Due to strong stratification, these oxygen minimum zones (OMZs) extend far offshore over vast swaths of the eastern Pacific. In these regions, oxygen availability plays a major role in structuring organism distributions and biogeochemical processes in the pelagic ocean (1).

Recently developed sensor techniques (2) show that in much of the OMZ water column, from about 30–100 m to about 800 m, O_2 concentrations fall below sensor-specific detection limits of down to 3 nmol·L^{-1} ($3{\cdot}10^{-9}$ moles per liter) (3, 4). OMZs in the eastern tropical North and South Pacific (ETNP and ETSP, respectively) and in the Arabian Sea are subject to such intense O_2 depletion and therefore have been redefined as anoxic marine zones (AMZs) (5). In other oceanic OMZs, including in the Bay of Bengal and northeast Pacific, oxygen concentrations may decrease to a few micromolar, but total O_2 depletion occurs only occasionally (6). AMZs are often distinguished from more oxygen-replete OMZs by the accumulation of nitrite, which is typically most pronounced when O_2 falls below the nanomolar detection limit (5–8). Nitrite is a key substrate in microbial N_2 and N_2O production by either denitrification or anaerobic ammonium oxidation (anammox), which together in AMZs mediate 30–50% (9) of the marine recycling of inorganic nitrogen compounds (nitrate, nitrite, and ammonium) to atmospheric N_2.

Nitrite is also produced and consumed in the aerobic nitrification pathway involving the two-step process of aerobic ammonia and nitrite oxidation (10, 11). Despite the absence of measureable O_2 in the core of eastern Pacific AMZs, biomolecular evidence (DNA, RNA, and proteins) indicates the presence of aerobic microbial processes. The expression of genes encoding for nitrification and other O_2-dependent microbial metabolisms, potentially including heterotrophic respiration, have been found well below the oxycline (12, 13), raising the question of how aerobic processes could persist under apparent anoxia.

In the three oceanic AMZs of the Arabian Sea, ETNP, and ETSP, dense populations of phototrophs have been observed at the base of the photic zone but below the oxycline that separates oxic from anoxic waters (14–16). This deep secondary chlorophyll maximum (SCM) is mainly composed of novel, yet uncultivated, lineages of the cyanobacterium *Prochlorococcus* (14), with chlorophyll concentrations that can equal that of the primary chlorophyll peak near the surface (16). The presence of this large population of putative oxygenic phototrophs has suggested a mechanism by which aerobic metabolism can be maintained in a zone where in situ measurements indicate anoxic conditions (5). Although an active photosynthetic community produces and releases oxygen to the environment, coupled O_2 consumption by an aerobic microbial community may keep seawater O_2 concentration at very low and possibly subnanomolar levels, thereby resulting in a cryptic O_2 cycle. The existence of such a cryptic

Significance

Anoxic marine zones (AMZs) create expansive habitats for microbes whose anaerobic metabolisms help drive global nutrient cycles, for example, by removing nitrogen from the oceans by producing N_2 gas. AMZ cycles may also be shaped by oxygen intrusion from outside the AMZ, creating opportunities for aerobic microbial metabolisms. Here we show that aerobic processes in AMZs are linked to oxygen production within the anoxic zone. Oxygen is produced during daytime in a layer of photosynthetic cyanobacteria near the top of the AMZ and then rapidly consumed by aerobic processes without accumulating. Oxygen turnover and carbon fixation rates are comparable to those of microbial N_2 production, suggesting an important role for internal oxygen cycling in AMZ transformations of matter and energy.

Author contributions: E.G.-R., F.J.S., O.U., A.P., and N.P.R. designed research; E.G.-R., C.C.P., M.A., and N.P.R. performed research; E.G.-R., C.C.P., M.A., A.P., and G.G. analyzed data; and E.G.-R., F.J.S., O.U., and N.P.R. wrote the paper.

The authors declare no conflict of interest.

This article is a PNAS Direct Submission.

Data deposition: The sequences have been deposited in the National Center for Biotechnology Information (NCBI, www.ncbi.nlm.nih.gov). For a list of accession numbers, see Table S5.

[1]Present address: Ecology Section, Department of Biology, University of Cadiz, 11510 Cadiz, Spain.

[2]To whom correspondence should be addressed. Email: emilio.garcia@uca.es.

This article contains supporting information online at www.pnas.org/lookup/suppl/doi:10.1073/pnas.1619844114/-/DCSupplemental.

oxygen cycle has been suggested by biomolecular evidence (12) but has not yet been demonstrated.

In this study we used a combination of high-resolution oxygen profiling, metabolic rate measurements, and community mRNA sequencing to explore the potential for oxygen cycling in the SCMs of the ETNP off Mexico and the ETSP off Peru. Our results show that the photosynthetic community of the SCM produces significant amounts of O_2, sufficient to maintain an aerobic community in an otherwise anoxic environment. Rates of O_2 production and carbon fixation in the SCM in both ETNP and ETSP AMZs are comparable to previously measured rates of aerobic processes like nitrite and ammonium oxidation (8, 17), as well as anaerobic AMZ processes like denitrification, anammox, and sulfate reduction (7, 8). Although the measured metabolic rates exhibit large spatial and temporal variability, our data collectively suggest a significant effect of local photosynthesis on the biogeochemical cycling in Pacific Ocean AMZs.

Results and Discussion

Sampling in both the ETNP and ETSP revealed a typical AMZ O_2 distribution in the upper 200 m of the water column. Oxygen concentrations in the 0–35 m surface layer in the ETNP were stable at ~200 μmol·kg^{-1}, before declining along a clearly defined oxycline from 35–45 to 60–80 m, and then falling below the detection limit of the switchable trace amount oxygen (STOX) sensors (few nanometers) at 80–100 m (Fig. 1*B*). In the ETSP AMZ off Peru, O_2 concentrations and the depth of the oxycline were more variable and clearly influenced by proximity to the shore, with anoxic depths beginning at ~30 m at the coastal station but at ~70 m for the more oceanic station (Fig. 1*H*). In both the ETNP and ETSP, the chlorophyll concentration below the primary maximum decreased in parallel with O_2 concentration, reaching a minimum before complete O_2 depletion and then increasing again to form an SCM in which 90% of the phototrophs were *Prochlorococcus* (Fig. 1 and Table S1). Although the upper region of the SCM was consistently located near the oxic–anoxic interface, maximum in vivo fluorescence and *Prochlorococcus* abundance were usually localized within the anoxic zone a few meters below. Low O_2 concentrations (<500 nmol·L^{-1}) were occasionally found inside the SCM (Table S2), suggesting intrusion of overlying oxygenated waters or in situ O_2 production and accumulation.

Oxygenic Photosynthesis and Carbon Fixation in the SCM. Shipboard experiments using water from the SCM incubated under trace O_2 conditions revealed that O_2 concentration with time differed substantially between dark- and light-incubated samples (Fig. 2 *A* and *D*). Net community production (NCP), corresponding to the slope of the O_2 concentration curves and hence the balance between O_2 production and consumption, gradually increased to more positive values with increasing irradiance. NCP was also variable between stations, reflecting the spatial and temporal variability of the metabolic activity in terms of photosynthesis and respiration rates (Fig. 2 *B* and *E*). At several stations, net consumption of O_2 occurred at all applied irradiances, although a clear decrease in consumption rate was always measured with increasing light intensities. At other stations, a net increase in O_2 was measured when the samples were exposed to an irradiance of only 10 μmol photons·m^{-2}·s^{-1}. The observed maximum irradiance in situ was, however, only in the range of 2–5 μmol photons·m^{-2}·s^{-1} at most stations (see examples in Fig. S1); at such low light levels, net O_2 consumption was always observed.

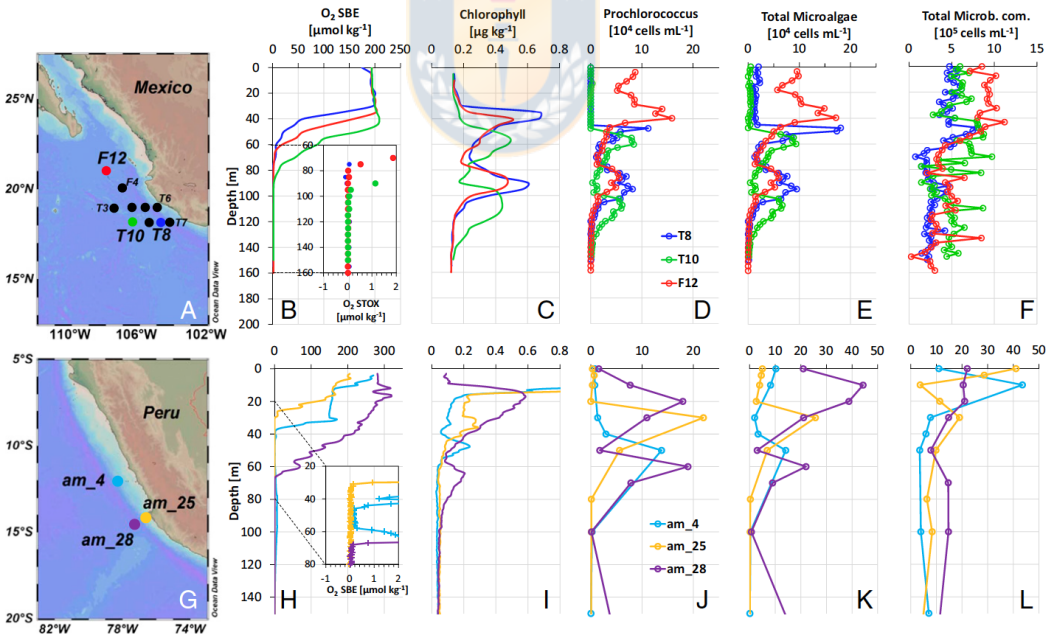

Fig. 1. Maps with sampled stations and main characteristics of the upper part of the (*A–F*) ETNP AMZ and (*G–L*) ETSP AMZ. Stations off Mexico (*A*) and Peru (*G*) where the SCM was found and sampled. (*B* and *H*) Dissolved oxygen profiles, based on SBE43 and STOX sensors (zooming in at low STOX O_2 values in *B* or corrected SBE O_2 in *H*). (*C* and *I*) Profiles of chlorophyll concentration inferred from in vivo fluorescence. (*D* and *J*) *Prochlorococcus* abundance. (*E* and *K*) Total microalgae (*Prochlorococcus*, *Synechococcus*, and picoeukaryotes) and (*F* and *L*) total microbial community (Total Microb. com.) abundance measured by flow cytometry.

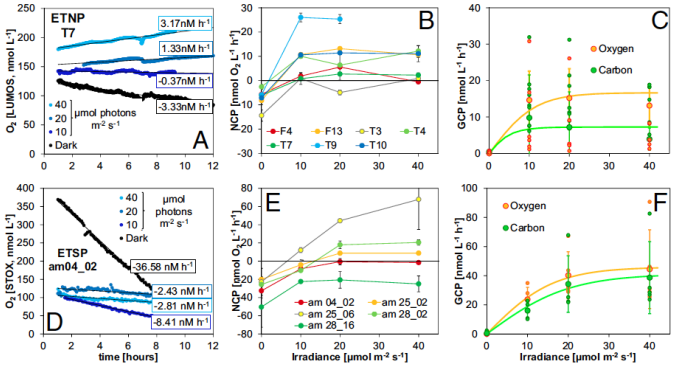

Fig. 2. Oxygen production and carbon fixation during incubations of samples from the SCM off (*A*–*C*) Mexico and (*D*–*F*) Peru. (*A* and *D*) Evolution of O_2 concentration during incubation of SCM samples exposed to a range of scalar irradiances (0–40 µmol photons·m^{-2}·s^{-1}). (*B* and *E*) Net community production (NCP) rates versus scalar irradiance. (*C* and *F*) Gross community production (GCP): O_2-GCP was measured as the net O_2 production, and C-GCP was measured by the incorporation of ^{13}C (at ETNP) or ^{14}C (ETSP). Data were fitted to a photosynthesis–irradiance model to calculate maximum rates (GCP_{max}) and the initial slope of the curve (α), an index of the photosynthetic efficiency at low light (values in the main text). Error bars represent the SE.

Tracking O_2 consumption during our experiments allowed for estimates of aerobic respiration rates. O_2 consumption curves were linear down to about 50 nmol·L^{-1} during dark incubations (Fig. 2 *A* and *D*). Aerobic respiration by prokaryotes is generally driven by two classes of terminal oxidases: low-affinity terminal oxidases (LATO) with a half saturation constant (K_m) of about 200 nmol O_2·L^{-1} and high-affinity terminal oxidases (HATO) with K_m values of 3–8 nmol O_2·L^{-1} (18). Marine bacteria possessing HATO can decrease apparent K_m values of aerobic respiration down to less than 10 nmol O_2·L^{-1} (19), and a linear O_2 decrease may thus be expected down to about 50 nmol O_2·L^{-1}. Therefore, O_2 consumption rates (referred to as respiration for simplicity) obtained at concentrations >50 nmol·L^{-1} represent potential respiration rates (R^*) because they were measured above the threshold of O_2 limitation. The estimated R^* rates were significantly higher in the ETSP compared with the ETNP (Fig. 2 and Table S2), consistent with a higher microbial and particle abundance measured in the ETSP (Fig. 1 and Tables S1 and S2).

Experiments under the unique, almost anoxic conditions, of AMZs have not been performed in previous measurements of photosynthetic activity in the SCM (20). We conducted our experiments at O_2 levels below those sporadically detected by in situ measurements (up to 500 nmol·L^{-1}) but far above the K_m values for HATO. In this range, we can assume that gross community production of O_2 (GCP-O_2) can be calculated as the sum of NCP and R^*. We also validated these production calculations by simultaneously measuring the incorporation of inorganic carbon (using ^{13}C or ^{14}C) into biomass [gross community carbon production (GCP-C)], as has been done previously to quantify *Prochlorococcus* carbon fixation (20, 21). Both GCP-O_2 and GCP-C followed a classical photosynthesis–irradiance curve (Fig. 2 *C* and *F*), with maximum (GCP_{max}) values above saturating light intensities (E_k) of 10.5 ± 2.0 and 21.4 ± 9.3 µmol photons·m^{-2}·s^{-1} (0.5 and 1% of the incident light) for the ETNP and ETSP, respectively. The low E_k values reflect adaptation to the dim light environment, being similar to values found for the SCM community in the Arabian Sea (20) or in *Prochlorococcus* cultures (21). Above E_k, mean GCP_{max}-O_2 values in the ETNP and ETSP were 16.6 ± 9.1 and 52.5 ± 30.4 nmol O_2·L^{-1}·h^{-1}, respectively, and were generally consistent with maximum GCP-C rates (GCP_{max}-C: 8.1 ± 11.2 and 44.4 ± 30.3 nmol C·L^{-1}·h^{-1} in the ETNP and ETSP, respectively) (mean values of all stations ± SD in Table S3 and model in Fig. 2 *C* and *F*). The parameters describing the photosynthesis characteristics of the SCM community (maximum gross production rates, photosynthetic efficiency, and E_k) were similar to the values previously found for the SCM community of the Arabian Sea and the characterization of several *Prochlorococcus* isolates from the Pacific Ocean (20, 21). The values found for the ETNP were similar to those found for the SCM of the Arabian Sea (20), whereas the ETSP SCM values were more similar to those from the laboratory cultures.

Although it is not yet possible to directly quantify in situ O_2 transformations in the AMZ, in situ GCP rates can be estimated based on water column chlorophyll concentrations and light conditions (Fig. S1). The light intensity at the SCM was variable and almost always substantially below 10 µmol photons·m^{-2}·s^{-1}. Under such conditions, O_2 production rates are lower than potential respiration rates (R^*), and the O_2 produced is immediately consumed by the microbial community, resulting in a cryptic O_2 cycle in the seemingly anoxic environment of the SCM (Fig. 1). However, at some stations the irradiance in the SCM was similar or close to the E_k. The occasional detection of low O_2 concentrations in the SCM (4, 8) (Table S2) may thus be explained by photosynthetic activity in the SCM increasing O_2 concentrations to measurable levels. Such daily changes are difficult to measure by discrete sampling, but recurrent measurements in the same water mass might reveal hourly and daily changes in the SCM.

Oxygen Production Coupling with Aerobic Microbial Processes. Even if undetectable, O_2 production in the SCM may support important (micro)aerobic metabolisms. To explore this prediction, we looked for signatures of such aerobic metabolism in available metatranscriptomes along the AMZ depth gradient in the ETNP during two cruises in 2014 and 2013, focusing on station T6 where the SCM was well developed and for which the metatranscriptome dataset was most comprehensive. Transcripts encoding terminal oxidases, including both LATO and HATO (Table S4), were detected at all depths (Fig. 3 and Fig. S2), including deep within the AMZ, where the transcript pool was dominated by sequences affiliated with diverse Gammaproteobacteria and Alphaproteobacteria (Fig. S3). The presence of oxidase transcripts within anoxic marine waters has been reported previously (13) and may reflect constitutive expression by groups at high abundance in the AMZ core, potentially to capitalize quickly on O_2 if it becomes available (22). The relative abundance of both LATO and HATO transcripts exhibits a local peak within the SCM compared with depths immediately above (base of oxycline) and below the SCM (Fig. 3 and Fig. S2). Similar trends were observed at stations T4 and T10, although limited sampling affected our ability to fully resolve oxidase distributions immediately above the SCM at these sites (Fig. S2). Together, these data provide evidence of a local peak in O_2 scavenging within the SCM.

Oxygen produced in the SCM may also be consumed through key steps of the OMZ nitrogen cycle. Comparatively high rates of autotrophic nitrification (ammonia and nitrite oxidation) are known to occur close to the oxic–anoxic boundary of AMZs (10). Here transcripts affiliated with ammonia oxidizing bacteria

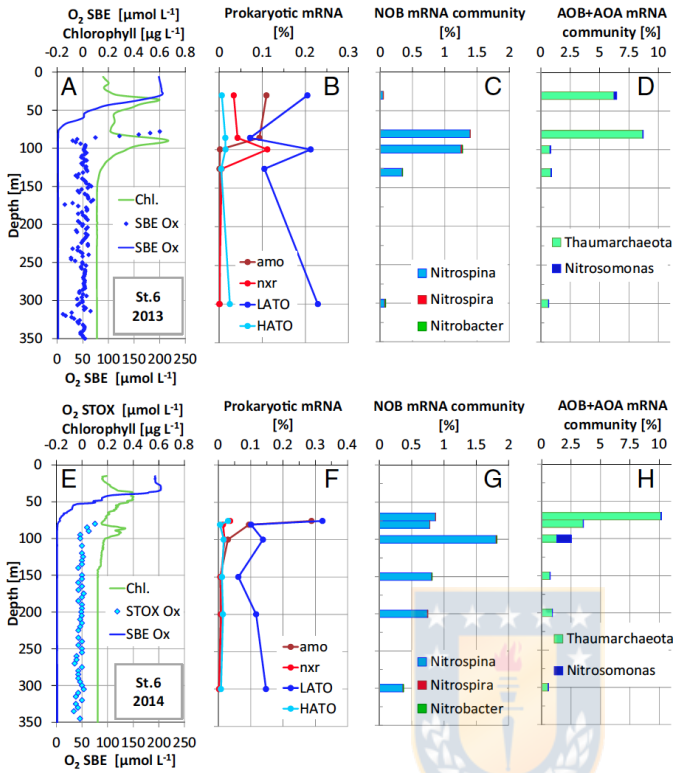

Fig. 3. Water column dissolved oxygen (O_2), chlorophyll concentrations (Chl.), and microbial transcript abundances at station T6 in the ETNP in (*A–D*) 2013 and (*E–H*) 2014. (*A* and *E*) O_2 based on SBE and STOX sensor measurement and chlorophyll inferred from in vivo fluorescence. (*B* and *F*) Abundances of transcripts encoding LATO and HATO, *amo*, and *nxr*, as a percentage of total prokaryotic mRNA. (*C* and *G*) Taxonomic classification of total mRNA affiliated with NOB and (*D* and *H*) AOB (Nitrosomonas) and AOA (Thaumarchaeota), as a percentage of total prokaryotic mRNA.

(AOB) and ammonia oxidizing archaea (AOA), notably those encoding the ammonia monooxgynease (*amo*) enzyme catalyzing aerobic ammonia oxidation, peaked in the upper part of the oxycline and declined in abundance into the core of the ETNP AMZ (Fig. 3 and Fig. S2). In contrast, transcripts of nitrite oxidizing bacteria (NOB), primarily those of the marine NOB genus *Nitrospina*, spiked within the SCM, coinciding in most cases with a local enrichment in transcripts encoding nitrite oxidoreductase (*nxr*) (Fig. 3 and Fig. S2). A prior study showed that potential nitrite oxidation rates at station T6 in the ETNP peaked in the anoxic SCM at 10.8 nmol $N{\cdot}L^{-1}{\cdot}h^{-1}$, a rate approximately double that of the maximal O_2 respiration rate measured in this study (Table S3). Taking the stoichiometry of nitrite oxidation into account, we can infer that most of the measured O_2 consumption (R^*) could be due to nitrite oxidation. The nitrite oxidation rates reported at the same stations were measured at low O_2 concentrations (<80 $nmol{\cdot}L^{-1}$), and we assume that the conditions were similar to our incubations, suggesting that the previous nitrite oxidation and our present R^* rates are directly comparable. The balance between heterotrophic and nitrite oxidizer O_2 consumption may, however, vary as a function of the actual O_2 concentration in the 0 to ~100 $nmol{\cdot}L^{-1}$ range that we measured in the ETNP SCM (Table S2). The cooccurrence of elevated *Nitrospina* transcription and nitrite oxidation rates in the SCM suggests that NOB is fueled by local O_2 production.

Implications for Oxygen Minimum Zones. The results of this study indicate that the SCM is a significant source of O_2 for both nitrite and organic matter oxidation, as well as a source of fixed carbon. Total productivity in terms of O_2 released and C fixed in the SCM was calculated by integrating the GCP profiles (Fig. S1) over a diel cycle, using measured (ETSP) or estimated (ETNP) scalar irradiance profiles (Fig. S4 and Table 1). Higher chlorophyll and estimated irradiance values at the SCM in the ETNP off Mexico resulted in higher mean production rates (0.83/0.39 mmol $O_2/C{\cdot}m^{-2}{\cdot}d^{-1}$) compared with the ETSP off Peru (0.32/0.31 mmol $O_2/C{\cdot}m^{-2}{\cdot}d^{-1}$). Although in situ light attenuation profiles were used for the ETNP, cloud coverage and other local factors reducing the incident light could not be included in the calculations,

Table 1. Depth-integrated oxygen production and carbon fixation rates

	GCP, $mmol{\cdot}m^{-2}{\cdot}d^{-1}$	
Station	O_2	C
ETNP–Mexico		
T4	0.43	0.15
F4	1.70	0.19
T7	0.48	0.13
T9	0.97	0.93
T10	0.59	0.55
	0.83 ± 0.53	0.39 ± 0.35
ETSP–Peru		
am_04	0.03	0.02
am_25	0.03	0.03
am_28	0.91	0.87
	0.32 ± 0.51	0.31 ± 0.49

and therefore, the production values should be taken as maximum values. Productivity was also highly variable among sites (0.43–1.70/0.15–0.95, and 0.03–0.91/0.02–0.87 mmol O_2/C·m^{-2}·d^{-1} for ETNP and ETSP, respectively), reflecting the heterogeneous spatial distribution of the SCM (Fig. 1 and Tables S1 and S2).

Although primary production in surface waters largely exceeds these values (23), the vast majority of surface production is remineralized before reaching the AMZ core. Indeed, the range of particulate organic carbon supply to the AMZ is 0.83–7.81 mmol C·m^{-2}·d^{-1} (11, 24) in the ETNP or 1.52–14.70 mmol C·m^{-2}·d^{-1} in the ETSP (25). This wide range highlights the variability in export rates in these regions. Nonetheless, comparing these estimations with our data, the carbon production in the SCM could provide 5–47% and 2–20% of the organic matter supplied to the anoxic waters of the ETNP and ETSP, respectively, where part of it is then mineralized by dissimilatory nitrate reduction to nitrite and denitrification (8, 11, 23, 26). Nitrate respiration to nitrite appears as the dominant mineralization step in the ETNP (8), and mineralization rates of about 1 mmol C·m^{-2}·d^{-1} can be calculated from published data (7, 23). These rates are close to the C fixation rate in the SCM, highlighting the relevance of the SCM in OMZ metabolism.

Global warming is expected to result in shoaling of the OMZ oxycline and overall expansion of OMZ volumes (27). Mesoscale physical processes such as local upwelling and anticyclonic eddies that shoal the oxic–anoxic boundary have been shown to enhance the development of SCMs (15, 16). Oxycline shoaling increases the light intensities in the anoxic cores of the AMZs, thereby potentially stimulating the photosynthetic community. The effects of these changes on microbial communities and microbial biogeochemical cycling in AMZs are difficult to predict, although significant changes in carbon, nitrogen, and sulfur cycling are expected (27). Our data show a significant carbon supply to the anoxic core of the Pacific AMZs by SCM photosynthetic activity, and it is likely that the situation is similar in the Arabian Sea. Although we did not measure nitrogen transformation processes, the nitrifying community was also enriched at the SCM, potentially reflecting elevated metabolic rates. A shoaling of the AMZ coupled with increases in irradiance and SCM photosynthetic activity would increase the carbon and daytime oxygen supply to the upper part of the AMZ. Shoaling of the AMZ due to global warming could thus lead to more extensive areas with high rates of SCM biological activity, with the diel oxic/anoxic cycles of these SCMs influencing marine productivity and coupled global nitrogen cycling.

Materials and Methods

Sampling Sites and in Situ Measurements. The two main oxygen minimum zones of the ETSP and ETNP were investigated during two cruises during 2014: the Activities of Research Dedicated to the Minimum of Oxygen in the Eastern Pacific (AMOP) cruise on the R/V *L'Atalante* to the ETSP off Peru during late January and February 2014 and the Oxygen Minimum Zone Microbial Biogeochemistry Expedition 2 (OMZoMBiE2) cruise on the R/V *New Horizon* to the ETNP region off Mexico during May–June 2014. Profiles of physical and chemical variables were obtained with a Seabird SBE-911 CTD system, equipped with a SBE 43 oxygen sensor and a Seapoint Chlorophyll Fluorimeter (R/V *New Horizon*) or a Chelsea Aqua 3 fluorimeter (R/V *L'Atalante*). CTD sensors were calibrated according to the manufacturer. The fluorometers used for the determination of chlorophyll were calibrated using pure chlorophyll solutions in 90% acetone (from 0.1 to 100 μg/L). In the ETNP, a pump profiling system (PPS) was also used for water collection. High-resolution O_2 profiling was performed during the CTD and PPS casts during the ETNP cruise. A high-resolution STOX sensor (2, 28) was used to measure O_2 concentration at nanomolar levels as described previously (2, 4).

Flow Cytometry Analysis. Samples for cell counts were taken at several depths from the rosette (ETNP and ETSP) and the PPS (ETNP), fixed with glutaraldehyde and stored at –80 °C until analysis. Cell abundance was determined by flow cytometry using a FACSCalibur flow cytometer (Beckton Dickinson). *Prochlorococcus*, *Synechococcus*, and other autofluorescent cells (identified as picoeukaryotes) were counted in untreated samples, whereas autofluorescent plus nonautofluorescent cells (bacteria + archaea, referred as total microbial community) were analyzed by staining the cells with SYBR Green (Molecular Probes) as described previously (29, 30).

Oxygen Production and Carbon Fixation Measurements. Water samples from the SCM (summarized in Table S1) were collected using Niskin bottles or a PPS. To minimize the O_2 leaking from the polymers of the Niskin bottles, the water was transferred to a 20-L glass bottle previously purged with N_2 gas as soon as the rosette was on deck. If the samples were collected using the PPS, the 20-L glass bottle purged with N_2 gas was filled directly from the outlet of the PPS. A certain O_2 contamination (1–5 μmol·L^{-1}) during the sampling procedure could not be avoided, and the seawater was therefore immediately degassed in the 20-L bottle by bubbling with N_2 + 0.05% CO_2. A STOX sensor was inserted inside the bottle to determine when anoxia was approached (<100 nmol O_2·L^{-1}). After adjusting the O_2 concentration to 100–400 nmol·L^{-1}, samples were siphoned to custom made incubation vessels (n = 12–16) (Fig. S5) (31, 32), containing either STOX sensors (ETSP) or a combination of STOX and optode sensors with a measuring range of 0–1,000 nmol·L^{-1} (32, 33) (ETNP). Each vessel was placed inside a light incubation tube immersed in a constant temperature water bath, enabling maintenance of in situ temperature (14–15 °C) and quantification of very low O_2 transformation rates. The light incubation tubes consisted of a black PVC tube with white LEDs (LF06S-W3F-850; OSRAM) installed along the whole periphery of the tube and with a custom-built waterproof magnetic stirrer fitted at the bottom. The LEDs were covered with a blue filter (131 Marine Blue filter; LEE Filters) to simulate the in situ light spectrum. Oxygen concentrations (Fig. 2) throughout the incubation period (8–12 h) were measured in treatments spanning a range of bluish light intensities slightly above maximum in situ levels (10, 20, and 40 μmol photons·m^{-2}·s^{-1}) and in darkness (n = 3–4, per treatment). Rates of oxygen consumption or production (here named NCP) were obtained by linear regression of the oxygen evolution during the incubations. GCP rates were calculated by subtracting the mean respiration value (NCP rate measured in darkness) from the NCP rates measured at different irradiances.

Rates of carbon incorporation were measured simultaneously during the incubations for oxygen measurements using stable (ETNP) or radioactive (ETSP) isotopes. Incubations amended with Na^{14}C-HCO$_3$ (450 μCi/L final concentration) were done in parallel incubation bottles of only 110 mL (but otherwise similar to the one described in Fig. S5) following the procedure described by Telling et al. (34). Incubations amended with Na^{13}C-HCO$_3$ (0.27 mM ^{13}C final concentration) were done in the same incubation bottles used for O_2 measurements. Incorporation of ^{14}C was measured by counting on a Perking Elmer Tri-Carb 2900 TR scintillation counter, whereas the ^{13}C incorporation was analyzed in an Elemental Analyzer (Thermo Elemental Analyzer Flash EA 1112 HT) coupled to an Isotope Ratio Mass Spectrometer (Delta V; Thermo Scientific). The ^{13}C enrichment in the produced organic carbon was calculated as the difference between the amounts of ^{13}C in the sample minus the natural ^{13}C abundance measured on blank filters. Decays per minute values (^{14}C incubations) and ^{13}C incorporation were converted to ^{12}C uptake values or GCP (nmol C·L^{-1}·h^{-1}) rates using the formula described in Telling et al. (34).

Rates Modeling and Upscaling of Processes. The photosynthesis–irradiance model described by Jassby and Platt (35) was fitted to the measured GCP (nmol·L^{-1}·h^{-1}) rates for both O_2 production and C assimilation (Fig. 2), being

$$GCP = GCP_{max} \times \tanh(\alpha \times E / GCP_{max}),$$

where GCP_{max} (nmol·L^{-1}·h^{-1}) is the maximum gross community production rate, reached at saturating irradiances, tanh is the hyperbolic tangent, α [(nmol·L^{-1}·h^{-1})(μmol photons·m^{-2}·s^{-1})$^{-1}$] is an index of the photosynthetic efficiency, and E (μmol photons·m^{-2}·s^{-1}) is the spherical irradiance.

The obtained parameters were normalized by the chlorophyll concentration and used to estimate the in situ O_2 production and C fixation using the light and chlorophyll profiles measured in the SCM by the fluorescence and photosynthetic active radiation (PAR) sensors connected to the CTD (ETSP cruise) or the PPS (ETNP cruise). During the ETSP cruise off Peru, casts were consistently repeated every 3–4 h, and thus, the light profiles from the CTD were used in our calculations. During the ETNP cruise, light profiles measured with the PPS during daytime were normalized to the incident irradiance at the surface. The light attenuation profiles were assumed to be constant at each station, and the incident irradiance was used to calculate the change in light profile during the day. The values of incident irradiance were taken from the closest National Radiation station located in San Diego (National Solar Radiation Database, National Oceanic and Atmospheric Administration, United States).

Metatranscriptome Analysis. Community cDNA sequencing was used to characterize microbial gene transcription in biomass (retained on 0.22-μm filters) from a subset of AMZ samples at the ETNP region off Mexico (Tables S4 and S5). These included samples collected during the OMZoMBiE2 cruise (2014) and a subset of samples previously reported by Padilla et al. (36). Seawater from discrete depths spanning the oxic zone, SCM, lower oxycline, upper AMZ, and AMZ core was collected using Niskin bottles or the PPS. The sampling, preservation, RNA extraction, and sequencing were done following the procedure described by Padilla et al. (36). Barcoded sequences were demultiplexed, and low-quality reads (Phred score < 25) were removed. Paired-end sequences were merged using custom scripts incorporating the FASTX toolkit (hannonlab.cshl.edu/fastx_toolkit/index.html) and USEARCH algorithm, with criteria of minimum 10% overlap and 95% nucleotide identity within the overlapping region. Ribosomal RNA (rRNA) transcripts were identified with riboPicker (37) and removed from the analysis. Merged nonrRNA sequences were queried via DIAMOND using sensitive search parameters (38) against the National Center for Biotechnology Information (NCBI)-nr database (November 2013). DIAMOND-identified protein-coding transcripts were assigned a functional annotation based Kyoto Encyclopedia of Genes and Genomes (KEGG) orthology (KO) identifiers (39) using Metagenome Analyzer 5 (MEGAN5) (40), with taxonomic classification assigned using the lowest common ancestor (LCA) algorithm in MEGAN5 based on the NCBI taxonomy. Counts per KO were normalized to the total number of protein coding transcripts classified within bacteria and archaea (i.e., prokaryotes). Transcripts encoding LATO and HATO, *nxr*, and *amo* (all subunits) were identified by the KO identifiers listed in Table S4. NOB abundances were determined by taxonomic LCA assignment according to NCBI taxonomy of DIAMOND-identified mRNA transcripts normalized to the total number of prokaryotic mRNA sequences. Taxonomic affiliation of both LATO and HATO were also assigned according to NCBI taxonomy via the LCA algorithm in MEGAN5.

ACKNOWLEDGMENTS. We thank P. Sørensen and L. B. Pedersen for the fabrication of sensors and conscientious and continuous technical support. We are grateful for the support from P. Lehner, S. Borisov, and I. Klimant in enabling high-resolution optode measurements. We also thank the captains and crews of the R/V *New Horizon* and *L'Atalante*. We additionally thank J. C. Kondrup for making the glass bottles and G. Alarcón, C. Venegas, M. Soto, C. Henry, M. Dugenne, D. Lefevre, A. Franco-Garcia, J. Grelet, O. Depretz-De-Gesincourt, and A. Barani for operational and experimental support. We are also grateful to H. Maske and G. Rodriguez for the logistical support dealing with radioactive compounds, as well as K. B. Oest and J. Pedersen for the support and analysis of isotopes samples. We thank M. Altabet, B. Dewitte, C. Maes, and V. Garçon. This work was supported by the European Research Council Grant 267233 and European Union Seventh Framework Programme Project 614141; the National Science Foundation 1151698 and 1558916 (to F.J.S.); the Sloan Foundation RC944 (to F.J.S.); the Chilean National Commission for Scientific and Technological Research 1130784 (to O.U.) and a graduate fellowship (to M.A.); the Millennium Science Initiative IC120019 (to O.U.); and Activity of Research Dedicated to the Minimum of Oxygen in the Eastern Pacific project supported by Institut de Recherche pour le Développement, CNRS/Institut National des Sciences de l'Univers, and Laboratoire d'Etudes en Géophysique et Océanographie Spatiales.

1. Paulmier A, Ruiz-Pino D (2009) Oxygen minimum zones (OMZs) in the modern ocean. *Prog Oceanogr* 80:113–128.
2. Revsbech NP, Thamdrup B, Dalsgaard T, Canfield DE (2011) Construction of STOX oxygen sensors and their application for determination of O_2 concentrations in oxygen minimum zones. *Research on Nitrification and Related Processes*, Methods in Enzymology, ed Klotz MG (Elsevier, San Diego), Part A, Vol 486, pp 325–341.
3. Thamdrup B, Dalsgaard T, Revsbech NP (2012) Widespread functional anoxia in the oxygen minimum zone of the Eastern South Pacific. *Deep Sea Res Part I Oceanogr Res Pap* 65:36–45.
4. Tiano L, et al. (2014) Oxygen distribution and aerobic respiration in the north and south eastern tropical Pacific oxygen minimum zones. *Deep Sea Res Part I Oceanogr Res Pap* 94:173–183.
5. Ulloa O, Canfield DE, DeLong EF, Letelier RM, Stewart FJ (2012) Microbial oceanography of anoxic oxygen minimum zones. *Proc Natl Acad Sci USA* 109:15996–16003.
6. Bristow LA, et al. (2017) N2 production rates limited by nitrite availability in the Bay of Bengal oxygen minimum zone. *Nat Geosci* 10:24–29.
7. Canfield DE, et al. (2010) A cryptic sulfur cycle in oxygen-minimum-zone waters off the Chilean coast. *Science* 330:1375–1378.
8. Ganesh S, et al. (2015) Size-fraction partitioning of community gene transcription and nitrogen metabolism in a marine oxygen minimum zone. *ISME J* 9:2682–2696.
9. Codispoti L, et al. (2001) The oceanic fixed nitrogen and nitrous oxide budgets: Moving targets as we enter the anthropocene? *Sci Mar* 65:85–105.
10. Dalsgaard T, Thamdrup B, Farias L, Revsbech NP (2012) Anammox and denitrification in the oxygen minimum zone of the eastern South Pacific. *Limnol Oceanogr* 57: 1331–1346.
11. Babbin AR, Keil RG, Devol AH, Ward BB (2014) Organic matter stoichiometry, flux, and oxygen control nitrogen loss in the ocean. *Science* 344:406–408.
12. Stewart FJ, Ulloa O, DeLong EF (2012) Microbial metatranscriptomics in a permanent marine oxygen minimum zone. *Environ Microbiol* 14:23–40.
13. Kalvelage T, et al. (2015) Aerobic microbial respiration in oceanic oxygen minimum zones. *PLoS One* 10:e0133526.
14. Lavin P, González B, Santibáñez JF, Scanlan DJ, Ulloa O (2010) Novel lineages of Prochlorococcus thrive within the oxygen minimum zone of the eastern tropical South Pacific. *Environ Microbiol Rep* 2:728–738.
15. Goericke R, Olson RJ, Shalapyonok A (2000) A novel niche for Prochlorococcus sp in low-light suboxic environments in the Arabian Sea and the Eastern Tropical North Pacific. *Deep Sea Res Part I Oceanogr Res Pap* 47:1183–1205.
16. Cepeda-Morales J, Beier E, Gaxiola-Castro G, Lavín M, Godínez V (2009) Effect of the oxygen minimum zone on the second chlorophyll maximum in the Eastern Tropical Pacific off Mexico. *Cienc Mar* 35:389–403.
17. Bristow LA, et al. (2016) Ammonium and nitrite oxidation at nanomolar oxygen concentrations in oxygen minimum zone waters. *Proc Natl Acad Sci USA* 113: 10601–10606.
18. Morris RL, Schmidt TM (2013) Shallow breathing: Bacterial life at low O(2). *Nat Rev Microbiol* 11:205–212.
19. Gong X, Garcia-Robledo E, Schramm A, Revsbech NP (2015) Respiratory kinetics of marine bacteria exposed to decreasing oxygen concentrations. *Appl Environ Microbiol* 82:1412–1422.
20. Johnson Z, et al. (1999) Energetics and growth kinetics of a deep Prochlorococcus spp. population in the Arabian Sea. *Deep Sea Res Part II Top Stud Oceanogr* 46:1719–1743.
21. Moore LR, Chisholm SW (1999) Photophysiology of the marine cyanobacterium Prochlorococcus: Ecotypic differences among cultured isolates. *Limnol Oceanogr* 44: 628–638.
22. Tsementzi D, et al. (2016) SAR11 bacteria linked to ocean anoxia and nitrogen loss. *Nature* 536:179–183.
23. Kalvelage T, et al. (2013) Nitrogen cycling driven by organic matter export in the South Pacific oxygen minimum zone. *Nat Geosci* 6:228–234.
24. Devol AH, Hartnett HE (2001) Role of the oxygen-deficient zone in transfer of organic carbon to the deep ocean. *Limnol Oceanogr* 46:1684–1690.
25. Escribano R, et al. (2004) Biological and chemical consequences of the 1997–1998 El Niño in the Chilean coastal upwelling system: A synthesis. *Deep Sea Res Part II Top Stud Oceanogr* 51:2389–2411.
26. Ward BB (2013) Oceans. How nitrogen is lost. *Science* 341:352–353.
27. Gilly WF, Beman JM, Litvin SY, Robison BH (2013) Oceanographic and biological effects of shoaling of the oxygen minimum zone. *Annu Rev Mar Sci* 5:393–420.
28. Revsbech NP, et al. (2009) Determination of ultra-low oxygen concentrations in oxygen minimum zones by the STOX sensor. *Limnol Oceanogr Methods* 7:371–381.
29. Lebaron P, Parthuisot N, Catala P (1998) Comparison of blue nucleic acid dyes for flow cytometric enumeration of bacteria in aquatic systems. *Appl Environ Microbiol* 64: 1725–1730.
30. Grégori G, Denis M, Seorbati S, Citterio S (2001) Resolution of viable and membrane-compromised free bacteria in aquatic environments by flow cytometry. Curr Protoc Cytom 11:11.15.1–11.15.7.
31. Tiano L, Garcia-Robledo E, Revsbech NP (2014) A new highly sensitive method to assess respiration rates and kinetics of natural planktonic communities by use of the switchable trace oxygen sensor and reduced oxygen concentrations. *PLoS One* 9: e105399.
32. Garcia-Robledo E, Borisov S, Klimant I, Revsbech NP (2016) Determination of respiration rates in water with sub-micromolar oxygen concentrations. *Front Marine Sci* 3:244.
33. Lehner P, et al. (2015) LUMOS—A sensitive and reliable optode system for measuring dissolved oxygen in the nanomolar range. *PLoS One* 10:e0128125.
34. Telling J, et al. (2010) Measuring rates of gross photosynthesis and net community production in cryoconite holes: A comparison of field methods. *Ann Glaciol* 51: 153–162.
35. Jassby A, Platt T (1976) Mathematical formulation of the relationship between photosynthesis and light for phytoplankton. *Limnol Oceanogr* 21:540–547.
36. Padilla CC, et al. (2016) NC10 bacteria in marine oxygen minimum zones. *ISME J* 10: 2067–2071.
37. Schmieder R, Lim YW, Edwards R (2012) Identification and removal of ribosomal RNA sequences from metatranscriptomes. *Bioinformatics* 28:433–435.
38. Buchfink B, Xie C, Huson DH (2015) Fast and sensitive protein alignment using DIAMOND. *Nat Methods* 12:59–60.
39. Kanehisa M, Goto S (2000) KEGG: Kyoto encyclopedia of genes and genomes. *Nucleic Acids Res* 28:27–30.
40. Huson DH, Mitra S, Ruscheweyh H-J, Weber N, Schuster SC (2011) Integrative analysis of environmental sequences using MEGAN4. *Genome Res* 21:1552–1560.

Supporting Information

Garcia-Robledo et al. 10.1073/pnas.1619844114

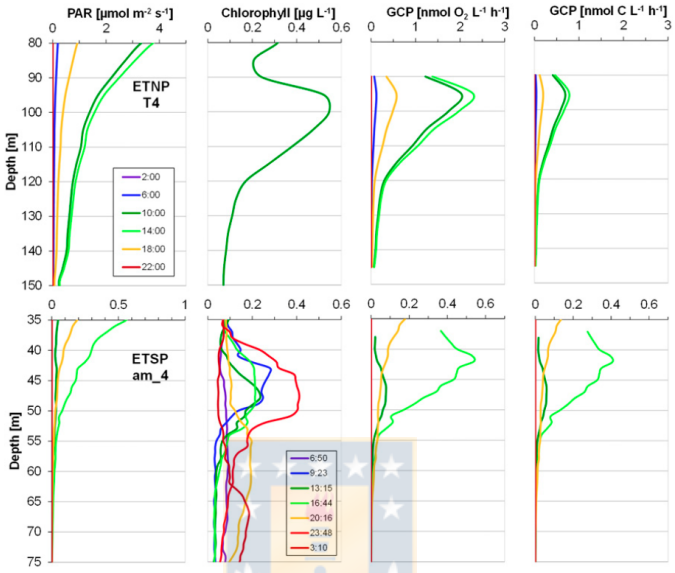

Fig. S1. PAR, chlorophyll, and in situ gross oxygen production and carbon fixation rates in the SCM estimated from onboard experimental data for O_2 metabolism and C fixation. GCP rates were calculated only at the SCM, considered as the water layer extending from the minimum fluorescence value between the peaks to the bottom of the photic layer. An oceanic station with a deeper SCM (T4) off Mexico (ETNP, *Upper*) and a coastal station with a shallow SCM (am_4) off Peru (ETSP, *Lower*). Note the different scales.

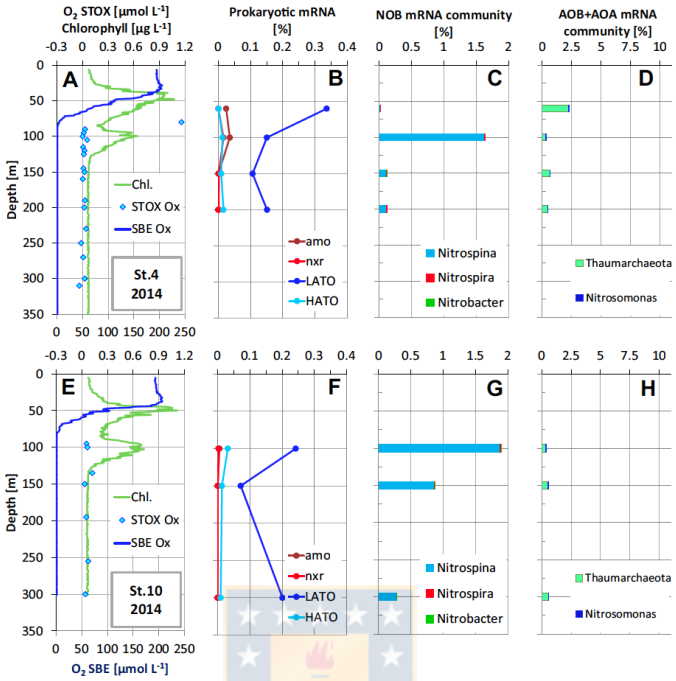

Fig. S2. Water column dissolved oxygen (O_2) and chlorophyll concentrations and microbial transcript abundances at stations (*A–D*) T4 and (*E–H*) T10 in the ETNP in 2014. (*A* and *E*) O_2, based on SBE and STOX senor measurement, and chlorophyll inferred from in vivo fluorescence. (*B* and *F*) Abundances of transcripts encoding LATO and HATO, *amo*, and *nxr*, as a percentage of total prokaryotic mRNA. (*C* and *G*) Taxonomic classification of total mRNA affiliated with NOB and (*D* and *H*) AOB and AOA, as a percentage of total prokaryotic mRNA.

Fig. S3. Taxonomic identities of terminal oxidases. Taxonomic assignment of (*Upper*) HATO and (*Lower*) LATO at stations T4, T6, and T10 off Mexico in 2014 and T6 in 2013 as determined via lowest common ancestor binning in MEGAN5. Abundances are presented as the percentage of total prokaryotic mRNA from each sample.

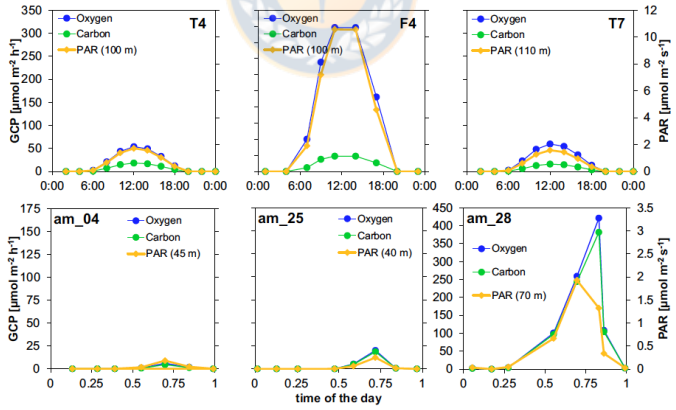

Fig. S4. Depth integration of in situ gross oxygen production and carbon fixation rates. Three stations off Mexico (T4, F4, T7; *Upper*) and off Peru (am_04, am_25, and am_28; *Lower*) were selected as examples. Modeled in situ gross oxygen production and carbon fixation rate profiles were integrated with depth to calculate the aerial contribution of the SCM. We used only GCP rates from the SCM, being delimited as the water layer extending from the minimum fluorescence value between the primary and secondary chlorophyll maxima to the bottom of the photic layer. Light at the depth where the maximum fluorescence value was measured is also shown as reference.

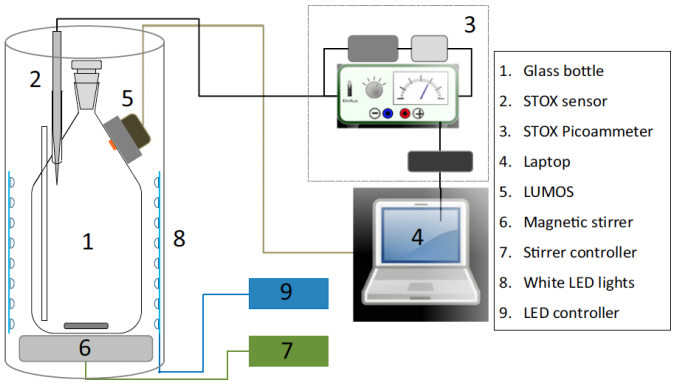

Fig. S5. Experimental setup for measurement of O_2 production/consumption. Glass bottle (labeled as 1) with a volume of 1160 mL. A series of modifications were done to a standard Schott–Duran glass bottle including (*i*) the insertion of a long open glass tube (internal diameter 2.5 mm) for pressure compensation and for the injection of calibration solution or tracers; (*ii*) the addition of a short 8.1-mm (inner diameter) glass tube for insertion of the STOX sensor (labeled as 2) or a solid 8-mm glass bar if STOX sensors were not used; (*iii*) a modification of the bottle neck to accommodate a ground glass stopper (internal diameter 12 mm) so that the inner part of the bottle could be accessed; and (*iv*) insertion of a sensing dot for optode-based measurements that was glued onto the inner surface of the bottle, whereas the reading device (LUMOS) was positioned on the outside, held by a PVC frame glued to the bottle. STOX sensors (labeled as 2) were connected to a picoammeter (labeled as 3) equipped with an external battery and a switch for the periodic polarization of the front guard of the sensor. The signal from the picoammeter was fed into an A/D converter connected to a laptop (labeled as 4). The LUMOS (labeled as 5) device was directly connected to the laptop. A magnetic stirrer (labeled as 6) and a controller (labeled as 7) ensured homogeneous mixing of the water in the bottle by a glass coated magnet. A white LED system surrounded the bottle (labeled as 8) to ensure a homogeneous light distribution. The light intensity was modulated by an external controller (labeled as 9), and the light spectrum of the SCM was simulated by coating the LEDs with a Marine Blue filter (LEE Filters). The LEDs were installed within a nontransparent PVC tube. The incubation bottles and associated lighting and stirring equipment were immersed into a water bath held at the in situ temperature (14 °C).

Table S1. Flow cytometry analysis of the SCM microbial community

Cruise	Station	Depth, m	Prochl., 10^4 cells per mL	Syn., 10^4 cells per mL	P.euk., 10^4 cells per mL	T.Microb., 10^5 cells per mL	Prochl., % photot.	Prochl., % total	Chl., $\mu g \cdot L^{-1}$
OMZoMBiE2 (ETNP)	T4	100	5.06	0.29	0.001	3.56	94.5	12.4	0.55
	T7	80	2.99	0.66	0.000	3.95	81.8	6.9	0.15
	T9	90	6.97	0.74	0.009	4.76	90.3	12.6	0.67
	T10	110	5.99	0.45	0.002	8.67	93.0	6.4	0.52
	T3	115	1.76	0.08	0.001	2.12	95.4	7.6	0.20
	F12	85	5.56	0.43	0.000	6.49	92.8	7.8	0.43
Mean		97	4.72	0.44	0.002	4.92	91.3	9.0	0.42
SD		14	1.96	0.24	0.003	2.33	5.0	2.8	0.21
AMOP'14 (ETSP)	am_4	50	13.80	0.30	0.006	3.49	97.8	28.1	0.13
	am_25	30	21.97	3.70	0.035	19.02	85.5	10.2	0.16
	am_28	60	18.96	3.06	0.012	14.66	86.0	11.2	0.21
Mean		47	18.25	2.35	0.018	12.39	89.8	16.5	0.16
SD		15	4.13	1.81	0.015	8.01	7.0	10.1	0.04

The abundance of *Prochlorococcus sp.* (Prochl.), *Synechococcus sp.* (Syn.), photosynthetic pico-eukaryotes (P.euk.), and total microbial community (T.Microb.) are expressed as cells per mL. The percentage of *Prochlorococcus sp.* in the phototrophic microbial community (% photot.) and in the total microbial community (% total) were also calculated. Mean chlorophyll values (Chl.) from in situ CTD measurements were added for comparison.

Table S2. Descriptive data and CTD measurements from within the SCM at sampled stations in both the ETNP and ETSP

Cruise	Station	Date (2014)	Offshore (K_m)	Depth, m	Beam transmission, %	Chlorophyll, $\mu g \cdot L^{-1}$	O_2, $\mu mol \cdot kg^{-1}$	T, °C	Density (σ_θ), $kg \cdot m^{-3}$
OMZoMBiE2 (ETNP)	T4	15/05	140	100	88.92	0.54	0.002	14.2	26.0
	F4	18/05	150	100	88.93	0.54	0.013	14.1	25.8
	T7	21/05	70	95	89.10	0.38	0.439	15.6	25.6
	T7	21/05	70	90	89.04	0.24	—	15.1	25.8
	T9	22/05	125	90	—	0.67	0.002	14.3	26.0
	T10	24/05	190	100	88.61	0.64	0.000	14.6	25.9
	T3	27/05	230	110	89.49	0.25	0.314	14.1	26.0
	T3	27/05	230	105	88.94	0.44	0.102	14.5	25.9
	F13	01/06	280	90	88.62	0.75	0.006	14.4	25.9
Mean				98	88.96	0.49	0.112	14.6	25.9
SD				7	0.28	0.18	0.170	0.5	0.1
AMOP'14 (ETSP)	am_4	31/01	97	46	80.73	0.21	0.16	14.7	26.3
	am_25	14/02	30	45	79.68	0.30	0.07	14.7	25.8
	am_25	15/02	30	53	79.82	0.30	0.22	14.6	26.2
	am_28	17/02	125	70	80.25	0.20	0.04	13.6	26.2
	am_28	19/02	125	70	80.95	0.12	68.56	13.6	26.2
Mean				57	80.29	0.23	0.123	14.3	26.2
SD				12	0.55	0.08	0.083	0.6	0.2

Table S3. Summary of metabolic rates calculated from oxygen and carbon incorporation data

Cruise	Station	Depth, m	R^*, nmol $O_2 \cdot L^{-1} \cdot h^{-1}$	GCP_{max}, $nmol \cdot L^{-1} \cdot h^{-1}$		α, $(nmol \cdot L^{-1} \cdot h^{-1})$ $(\mu mol\ photons \cdot m^{-2} \cdot s^{-1})^{-1}$	
				O_2	C	O_2	C
OMZoMBiE2 (ETNP)	T4	100	2.6	13.3	2.4	1.26	0.2
	F4	100	5.7	8.8	1.1	0.75	0.1
	T7	95	5.3	8.0	2.6	0.61	0.2
	T7	90	6.9	10.0	0.0	0.76	0.0
	T9	90	3.2	35.5	30.3	3.19	3.1
	T10	100	7.1	19.4	9.2	1.77	0.8
	T3	110	17.4	16.8	3.1	1.32	0.4
	T3	105	11.4	—	—	1.60	—
	F13	90	8.2	21.3	—	1.89	—
Mean		98	7.5	16.6	6.9	1.46	0.69
SD		7	4.5	9.1	10.7	0.80	1.09
AMOP'14 (ETSP)	am_4	46	32.6	32.5	28.5	2.4	1.9
	am_25	45	20.1	32.1	33.1	1.61	1.02
	am_25	53	22.8	105.0	98.3	3.49	3.25
	am_28	70	25.7	51.9	35.2	2.11	2.01
	am_28	70	63.2	41.0	27.1	4.08	2.28
Mean		57	32.9	52.5	44.4	2.74	2.09
SD		12	17.6	30.4	30.3	1.02	0.80

Table S4. KEGG orthology identifiers used to screen metatranscriptomic datasets for terminal oxidase and nitrification marker genes

Function	Protein	Abbreviation	KEGG orthology identifier (KO)
Terminal oxidase	Cytochrome C	*LATO*	K02277, K02276, K02274, K15408, K02275, K02258, K02259
Terminal oxidase	cbb3	*HATO*	K00404, K00405, K15862, K00407, K00406
Terminal oxidase	bd	*HATO*	K00425, K00246
Nitrification	Nitrite oxidoreducatase	*nxr*	K00370, K00371
Nitrification	Ammonia monooxygenase	*amo*	K10944, K10945, K10946

Table S5. ETNP sequencing statistics

Year	Stn	Depth, m	Total	Read length, bp	nonrRNA	DIAMOND	MEGAN bacteria	MEGAN archaea	MEGAN Prok	Accession
2013	6	30	1,521,531	203	1,053,980	108,873	62,934	5,476	68,410	PRJNA263621*
		85	1,364,985	201	294,080	175,178	115,127	4,935	120,062	PRJNA263621*
		100	1,024,593	214	218,551	158,677	115,316	1,922	117,238	PRJNA263621*
		125	1,494,459	204	377,156	256,113	174,678	4,559	179,237	PRJNA263621*
		300	712,020	212	159,091	110,937	78,842	2,389	81,231	PRJNA263621*
2014	4	60	2,302,732	197	417,033	232,758	126,802	6,986	133,788	PRJNA305951
		100	2,520,169	199	805,179	359,336	258,010	15,993	274,003	PRJNA305951
		150	1,291,622	208	310,389	183,424	128,402	6,995	135,397	PRJNA305951
		200	1,212,126	205	253,637	155,219	110,453	5,938	116,391	PRJNA305951
	6	75	4,786,146	164	957,802	298,788	187,702	63,517	251,219	PRJNA277357†
		80	1,407,348	183	591,754	165,806	80,047	41,583	121,630	PRJNA305951
		100	1,601,640	183	611,712	192,294	133,385	13,799	147,184	PRJNA305951
		150	1,452,296	202	359,133	169,271	113,485	14,564	128,049	PRJNA305951
		200	2,325,341	177	482,694	210,303	158,319	5,971	164,290	PRJNA305951
		300	18,781,558	185	7,710,908	1,645,992	1,540,161	51,789	1,591,950	PRJNA277357†
	10	100	2,149,661	192	439,535	106,713	62,268	3,823	66,091	PRJNA277357†
		150	4,523,472	166	1,276,310	495,416	416,236	14,970	431,206	PRJNA277357†
		300	1,335,682	194	439,535	226,427	187,523	6,458	193,981	PRJNA277357†

Stn, stations in the ETNP; Total, number of sequences post trimming, merging, and quality control; Read length, average read length (bp) of merged and quality controlled sequences; nonrRNA, number of nonrRNA reads; DIAMOND, number of sequences with DIAMOND matches (bit score >50) to protein-coding sequences in the NCBI-nr database; MEGAN bacteria, number of reads assigned to the bacteria node using the lowest common ancestor (LCA) algorithm in MEGAN5; MEGAN archaea, number of reads assigned to the archaea node using the LCA algorithm in MEGAN5; MEGAN Prok, the sum of bacteria and archaea-assigned reads by the LCA algorithm; and Accession, NCBI accession number or BioProject ID.

*Samples collected in 2013 published in Ganesh et al. (8).

†Samples collected in 2014 published in Padilla et al. (35).

4.2. Capítulo 2. “Asimilación de nitrógeno en picocianobacterias que habitan aguas deficientes de oxígeno del Pacífico Norte y Sur Oriental Tropical”

Artículo científico publicado en línea en la revista “Limnology and Oceanography”

Autores: **Montserrat Aldunate**, Carlos Henríquez-Castillo, Qixing Ji, Jessica Lueders-Dumont, Margaret R. Mulholland, Bess B. Ward, Peter von Dassow, Osvaldo Ulloa.

Resumen

Prochlorococcus y *Synechococcus* son los microorganismos fotosintéticos de vida libre más abundantes en el océano. Linajes no cultivados de estas cianobacterias también se desarrollan en la parte superior poco iluminada de las zonas marinas anóxicas (ZMAs), dónde una parte importante de la pérdida de nitrógeno (N) del océano tiene lugar a través de los procesos de desnitrificación y la oxidación anaeróbica del amonio. Un estudio metagenómico reciente reveló que *Prochlorococcus* de ZMAs tiene el potencial genético para usar diferentes formas de N, incluido el nitrato, una fuente de N poco común para *Prochlorococcus*, pero común en *Synechococcus*. Para determinar qué fuentes de N están utilizando realmente las picocianobacterias de ZMAs en la naturaleza, se determinaron la abundancia natural celular de ^{15}N ($\delta^{15}N$) y las tasas de asimilación de los distintos compuestos de N utilizando células aisladas por citometría de flujo y espectrometría de masas. El $\delta^{15}N$ natural de *Prochlorococcus* de ZMAs varió desde -4,0‰ a 13,0‰ (n=9), con un 50% de los valores en el rango de -2,1‰ a 2,6‰. Mientras que los valores más altos sugieren el uso de nitrato por las picocianobacterias de ZMAs, la mayoría de las observaciones indican el uso de nitrito, amonio o una mezcla de fuentes de N. Los experimentos de incubación revelaron tasas potenciales de asimilación de amonio y urea en el mismo orden de magnitud que la esperada para el total de N en varios ambientes, incluyendo las ZMAs, mientras que las tasas de asimilación de nitrato y nitrito fueron muy bajas. Por lo tanto, nuestros resultados indican que las formas reducidas de N y el nitrito son las fuentes dominantes para las picocianobacterias de ZMAs, aunque el nitrato podría ser importante en algunas ocasiones. Las picocianobacterias de ZMAs podrían representar competidores potenciales de bacterias anammox o arqueas oxidantes del amonio y/o bacterias oxidantes de nitrito.

LIMNOLOGY
and
OCEANOGRAPHY

Limnol. Oceanogr. 00, 2019, 1–17

doi: 10.1002/lno.11315

Nitrogen assimilation in picocyanobacteria inhabiting the oxygen-deficient waters of the eastern tropical North and South Pacific

Montserrat Aldunate,[1,2,3] Carlos Henríquez-Castillo,[1,3] Qixing Ji,[4,a] Jessica Lueders-Dumont,[4] Margaret R. Mulholland,[5] Bess B. Ward,[4] Peter von Dassow,[3,6,7] Osvaldo Ulloa[1,3]*

[1]Departamento de Oceanografía, Universidad de Concepción, Concepción, Chile
[2]Programa de Postgrados en Oceanografía, Universidad de Concepción, Concepción, Chile
[3]Instituto Milenio de Oceanografía, Universidad de Concepción, Concepción, Chile
[4]Department of Geosciences, Princeton University, Princeton, New Jersey, USA
[5]Department of Ocean, Earth and Atmospheric Sciences, Old Dominion University, Norfolk, Virginia, USA
[6]Departmento de Ecología, Pontificia Universidad Católica de Chile, Santiago, Chile
[7]UMI 3614, Evolutionary Biology and Ecology of Algae, Centre National de la Recherche Scientifique-UPMC Sorbonne Universités, PUCCh, UACH, Station Biologique de Roscoff, Roscoff, France

Abstract

Prochlorococcus and Synechococcus are the most abundant free-living photosynthetic microorganisms in the ocean. Uncultivated lineages of these picocyanobacteria also thrive in the dimly illuminated upper part of oxygen-deficient zones (ODZs), where an important portion of ocean nitrogen (N) loss takes place via denitrification and anaerobic ammonium oxidation. Recent metagenomic studies revealed that ODZ Prochlorococcus have the genetic potential for using different N forms, including nitrate and nitrite, uncommon N sources for Prochlorococcus, but common for Synechococcus. To determine which N sources ODZ picocyanobacteria are actually using in nature, the cellular ^{15}N natural abundance ($\delta^{15}N$) and assimilation rates of different N compounds were determined using cell sorting by flow cytometry and mass spectrometry. The natural $\delta^{15}N$ of the ODZ Prochlorococcus varied from −4.0‰ to 13.0‰ (n = 9), with 50% of the values in the range of −2.1–2.6‰. While the highest values suggest nitrate use, most observations indicate the use of nitrite, ammonium, or a mixture of N sources. Meanwhile, incubation experiments revealed potential assimilation rates of ammonium and urea in the same order of magnitude as that expected for total N in several environments including ODZs, whereas rates of nitrite and nitrate assimilation were very low. Our results thus indicate that reduced forms of N and nitrite are the dominant sources for ODZ picocyanobacteria, although nitrate might be important on some occasions. ODZ picocyanobacteria might thus represent potential competitors with anammox bacteria for ammonium and nitrite, with ammonia-oxidizing archaea for ammonium, and with nitrite-oxidizing bacteria for nitrite.

Prochlorococcus and Synechococcus are the most abundant free-living photosynthetic microorganisms in the euphotic zone of oligotrophic tropical and subtropical ocean waters (Partensky et al. 1999a,b). These picocyanobacteria represent ~ 25% of marine primary productivity (Flombaum et al. 2013) and their successful colonization of the global ocean has been attributed to their small size and ability to take up nutrients at high rates (Chisholm 1992), as well as their high within species genetic diversity (Scanlan 2003; Biller et al. 2014).

The structure and pigment content of their photosynthetic apparatus differs between the two picocyanobacteria: Synechococcus uses a phycobilisome as the main light-harvesting antenna while Prochlorococcus lacks phycobilisomes and uses a complex of chlorophyll-binding proteins (Pcb) (Partensky et al. 1999b). The Pcb complex contains divinyl chlorophyll a (Chl a_2) and divinyl chlorophyll b (Chl b_2). This complex allows them to capture light more efficiently at greater depths (Moore and Chisholm 1999). Indeed, some lineages of Prochlorococcus with high ratios of Chl b_2/a_2 content are able to grow at extremely

*Correspondence: oulloa@udec.cl

Additional Supporting Information may be found in the online version of this article.

[a]Present address: Helmholtz Centre for Ocean Research Kiel, Kiel, Germany

low irradiances (< 10 mol quanta m^{-2} s^{-1}), where low Chl b_2/a_2 lineages are incapable of such growth. Conversely, low Chl b_2/a_2 lineages are able to grow maximally at higher light intensities where high Chl b_2/a_2 isolates are inhibited (Moore and Chisholm 1999). Thus, the depth distributions of *Prochlorococcus* lineages are consistent with these characteristics: members of the high light (HL) ecotypes are found mainly in the nutrient-depleted surface waters of the ocean, while members of the low light (LL) ecotypes are dominant at the base of the euphotic zone where nutrients are replete (Goericke et al. 2000; West et al. 2001; Rocap et al. 2003; Johnson et al. 2006; Lavin et al. 2010). While *Prochlorococcus* shows a clear vertical partitioning of ecotypes related principally with light and the availability of nutrients, *Synechococcus* lineages do not show a clear spatial partitioning with depth (Moore et al. 1998; Biller et al. 2014).

As for other phytoplankton, the assimilation of N is central to picocyanobacteria nutrition, with ammonium (NH_4^+) as the preferred N source due to the low energy needed for its assimilation into organic N (Moore et al. 2002). There are indications that *Prochlorococcus* and *Synechococcus* lineages have diverged in the ability to use also other forms of N that are available in the ocean, such as nitrate (NO_3^-) and nitrite (NO_2^-) (Moore et al. 2002; Martiny et al. 2009), cyanate (Fuhrman 2003; Kamennaya and Post 2011), and amino acids (Zubkov et al. 2003). Initially, *Prochlorococcus* was considered unable to use nitrate (NO_3^-), because the original cultured isolates could not use it (Moore et al. 2002). Nevertheless, more recent studies have demonstrated genomic (Martiny et al. 2009; Batmalle et al. 2014; Berube et al. 2015) and indirect physiological (Casey et al. 2007) evidence of NO_3^- assimilation, in both cultured *Prochlorococcus* and natural assemblages of *Prochlorococcus*. Analyzing the genomes of different strains of *Prochlorococcus*, Berube et al. (2015) showed that the genomic configuration of the genes related to the NO_3^- assimilation differed among *Prochlorococcus* strains. They presented evidence of acquisition, loss, and horizontal transfer of NO_3^- assimilation related genes for some HL strains, as well as evidence of retention of those genes in some members of the LL ecotypes during the evolutionary diversification from their common ancestor with *Synechococcus*.

The most basal *Prochlorococcus* lineages found to date are noncultured representatives (LLV and LLVI) inhabiting the secondary chlorophyll maximum (SCM) in the oxygen-deficient waters of the eastern tropical North and South Pacific (ETNP and ETSP), which are characterized as adapted to very low-light and nutrient-rich conditions (Lavin et al. 2010; Ulloa et al. 2012). These SCMs have been found specifically in the oxygen-deficient zones (ODZs), also known as anoxic marine zones (AMZs), that are distinguished from other oxygen minimum zones by the accumulation of nitrite and the complete absence of detectable oxygen using the most sensitive detectors such as the STOX oxygen sensor (detection limits 1–10 nmol L^{-1}; Revsbech et al. 2009; Thamdrup et al. 2012; Ulloa et al. 2012). Nevertheless, these *Prochlorococcus* have recently been shown to drive a cryptic oxygen cycle that possibly fuels aerobic processes such as NO_2^--oxidation (Garcia-Robledo et al. 2017).

In the ODZs, there is an accumulation of NO_2^-, mainly due to dissimilatory nitrate reduction (Ward et al. 2009; Lam and Kuypers 2011) that only takes place when oxygen levels are below 50 nmol L^{-1} (Thamdrup et al. 2012). Within the ODZs, there are high concentrations of inorganic nutrients and a very active nitrogen (N) cycle mediated by anaerobic microorganisms (Lam and Kuypers 2011). The forms and abundance of bioavailable N present, as well as the sources of energy supporting their assimilation, are important factors controlling the growth of *Prochlorococcus* and *Synechococcus*. Any inorganic N taken up must be converted to NH_4^+ for incorporation into vital compounds such as amino acids or nucleic acids (Berges and Mulholland 2008), so assimilation of reduced forms of N such as NH_4^+ or urea is metabolically favored when they are available (García-Fernández et al. 2004; García-Fernández and Diez 2004; Berges and Mulholland 2008). However, the most common forms of N in such extremely ODZs are NO_3^- and NO_2^- (Ulloa et al. 2012) with very low (nmol L^{-1}) to undetectable concentrations of NH_4^+ and undetectable concentrations of urea using standard methods (Thamdrup et al. 2006; Hamersley et al. 2007; Widner et al. 2018*b*). Thus, in contrast to the picocyanobacteria in the primary chlorophyll maximum (PCM) above the oxycline, the ODZ cyanobacteria inhabit a high NO_3^- and NO_2^- environment.

Reconstruction of a metagenome using environmental samples collected from the SCM in the ETSP showed that these ODZ lineages have the genetic potential to assimilate urea and NO_3^- (Astorga-Eló et al. 2015), having a full repertoire of genes involved in NO_3^- transport (*napA*), NO_3^- assimilation (*narB*), and biosynthesis of the Mo-cofactor (*moeA* and *mobA*) necessary for the *narB* function (Flores and Herrero 2005). Astorga-Eló et al. (2015) also suggested that this pathway was retained during *Prochlorococcus* divergence from *Synechococcus* rather than a secondary horizontal gain (Astorga-Eló et al. 2015). This scenario is similar to what occurred in lineage LLIV, a lineage that appears not to be affected by the genome reduction documented in the more recently diverged lineages of *Prochlorococcus* (e.g., HL strain MED4) (Partensky and Garczarek 2010). Lately, Widner et al. (2018*a*) showed that LLIV *Prochlorococcus* inhabiting the ODZ also have genes for the utilization of NH_4^+ and NO_2^-, although no cyanate assimilation related genes were found.

The capacity for utilization of NO_3^- or NO_2^- might confer to ODZ *Prochlorococcus* an ecological advantage over *Prochlorococcus* lineages that do not have the genes needed to assimilate these compounds, allowing them to take advantage of the high NO_3^- concentrations (with respect to NH_4^+ and/or urea) present in the SCM in the ODZs. This capability might also allow ODZ *Prochlorococcus* to avoid competition for NH_4^+ with important groups of microorganisms recycling N in these regions, such as anammox bacterial and ammonia-oxidizing archaea. Thus,

a further knowledge about the metabolic capabilities and physiology of ODZ *Prochlorococcus* and the less abundant, but present, *Synechococcus*-like lineages inhabiting the SCM within the ODZ is essential for understanding their role in ODZs and how they may use this niche as an advantage over other lineages that cannot consume NO_3^-. Therefore, in this work, we focus on testing the hypothesis, based on apparent genomic potential, that *Prochlorococcus* uses NO_3^- as a N source for its assimilative metabolism.

Stable isotopes analysis is a powerful tool for investigating this hypothesis. $\delta^{15}N$ notation represents the deviation between the ratio of the two stable isotopes of N ($^{15}N/^{14}N$) contained in the samples (particulate organic nitrogen and/or selected sorted picoplanktonic groups) compared with the ratio of these same two stable isotopes of N contained in the atmospheric N_2 (standard) (Owens 1987). Comparing the $\delta^{15}N$ of the organisms that inhabit an environment with the $\delta^{15}N$ of the different N sources available for assimilation in a specific environment (e.g., $\delta^{15}N$ of NO_3^- and NO_2^-) can help determine which sources of N are being used by the organisms. Previous work has coupled the use of stable isotopes and cell sorting, allowing the characterization of the N content and the natural abundance $\delta^{15}N$ signature of distinct components of the particulate nitrogen suspended in Sargasso Sea surface waters (Fawcett et al. 2011) and specific uptake rates of different $\delta^{15}N$-labeled sources of N by *Prochlorococcus* (Casey et al. 2007). In this study, we analyzed the natural abundance of $\delta^{15}N$ of suspended particulate organic nitrogen (PON_{sus}) and *Prochlorococcus* and *Synechococcus*-like cells sorted from the microbial community inhabiting the SCM (and PCM when SCM was present) at several stations in the ODZ in both ETNP and ETSP. These $\delta^{15}N$ data were compared with literature values of $\delta^{15}N$ natural abundance signatures of different sources of N. Complementary experimental evidence for the uptake of N compounds was derived from onboard tracer incubations in which natural seawater samples collected from the SCM were amended with ^{15}N-labeled NO_3^-, NO_2^-, NH_4^+, and urea to measure potential assimilation rates in flow cytometrically sorted groups of picoplankton.

Materials and methods

Sampling site and field collection

Samples were obtained from the ODZs of the ETNP and ETSP, during four cruises: NH1410 (May 2014) and RB1603 (April 2016) for the ETNP, and NBP1305 (June 2013) and AT2626 (January 2015) for the ETSP (see station map in Fig. 1). Samples were taken from two depths, one from the PCM and the other from the SCM. The collection of water samples at both depths was performed using a pump profiler system (PPS); an instrument that pumps water directly from the desired depth while profiling the water column with an attached conductivity-temperature-depth (CTD) system (Seabird SBE-19 plus for ETNP and Seabird SBE-25 for ETSP), which provides

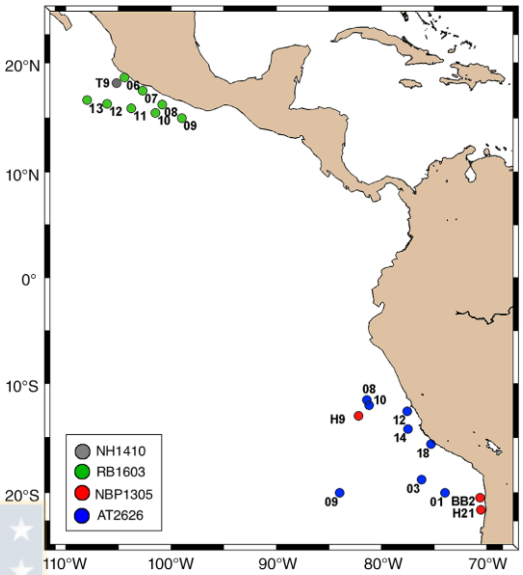

Fig. 1. Map with the sampled stations in the ETNP (cruises: NH14010 and RB1603) and the ETSP (cruises: NBP1305 and AT2626). [Color figure can be viewed at wileyonlinelibrary.com]

continuous determinations of salinity, temperature, depth, as well as dissolved oxygen (Seabird SBE 43 oxygen sensor; all cruises) and in vivo fluorescence (WETStar for ETNP cruise and ECO-AFL/FL for ETSP cruises, both WET Labs fluorometers).

NO_3^-, NO_2^-, and urea samples were run on an Astoria Pacific autoanalyzer using standard colorimetric methods according to the manufacturers specifications. NH_4^+ was determined using the fluorometric method of Holmes et al. (1999). In April 2016 (ETNP; cruise RB1603), seawater was pumped into the laboratory and connected to an auto analyzer for nutrients continuous profiles for NO_3^-, NO_2^-, and NH_4^+, binned to one measurement per second.

$\delta^{15}N$ natural abundance

PON_{sus} (0.3–3 μm size fraction) $\delta^{15}N$ natural abundance was determined by filtering 2–3 L of seawater though a 3-μm pore size polycarbonate membrane filter and collecting the microbial biomass on a precombusted (500°C for 6 h) 0.3-μm glass fiber filter (Sterlitech GF-75; 0.3 μm nominal pore size). The GF-75 filters were dried onboard or frozen in liquid nitrogen. Once in the laboratory, GF-75 filters were fumed with HCl vapors for 8 h to drive off inorganic C and then dried and encapsulated in tin capsules for analysis at the University of California Davis Stable Isotope Facility (mass detection limit 20 μg of N).

For determining $\delta^{15}N$ natural abundance of sorted groups of cells, 4 L of seawater from the PCM and SCM depths were collected in plastic carboys protected from sunlight. This water was immediately filtered at a very low speed using a peristaltic pump in order to concentrate the cells of this community on 0.4 μm pore size polycarbonate filters after a 3-μm pore size polycarbonate prefilter. To fix the cells, the filters were placed in 4-mL cryovials with 200 μL of 10% formaldehyde solution and filled to 4 mL using 0.22-μm prefiltered seawater (0.5% formaldehyde final concentration). After 1 h of incubation in the dark at 4°C, the samples were gently agitated and stored in liquid nitrogen until reaching land, upon which the samples were stored at −80°C until processing.

Incubation experiments

For incubation experiments, water was collected in a 20-liter glass bottle and purged for 20 min with a mixture of 800 ppm CO_2 balanced He in order to avoid any oxygen contamination during the sampling. This water was siphoned to 6–12 custom-made incubation bottles (1.1 liter) for anoxic experiments. These bottles were previously purged with the same mixture of He/CO_2 and were filled overflowing the water approximately 1.5 times their volume. Finally, the bottles were placed in an incubator inside a temperature-controlled cold van (see diagram in Supporting Information Fig. S1). The incubator was composed of a temperature-controlled water bath, two blue LED panels with controlled intensities of light, as well as of magnetic stirrers that prevent stratification of the water inside each incubation bottle. The incubation conditions were set to simulate in situ temperature (ranging between 14°C and 16°C depending on the station) and light intensities (10–30 μmol photons m^{-2} s^{-1}). Four different ^{15}N-labeled compounds (Cambridge Isotope Laboratories) were used to assess the potential N assimilation rates in the picoplanktonic community. Because environmental nutrient concentrations were measured only after incubations were started, the enrichment of the N sources exceeded 10–15% -the enrichment recommended for in situ assimilation rates- and so represents potential assimilation rates (Dugdale and Wilkerson 1986). Measured final concentrations of ^{15}N-NO_3^- and ^{15}N-NO_2^- were 5.5 μmol L^{-1} and 0.2 μmol L^{-1}, respectively. These concentrations represented enrichments of 19.6–27.2% for ^{15}N-NO_3^- and 47.6% for ^{15}N-NO_2^-. The in situ concentrations of urea were undetectable (detection limit 70 nmol L^{-1}) and in the nmol L^{-1} ranges for NH_4^+ (detection limit 10 nmol L^{-1}). The additions of ^{15}N-Urea and ^{15}N-NH_4^+ were 0.2 μmol L^{-1} and 0.18 μmol L^{-1} final concentration, respectively, representing an enrichment of 74.1% for ^{15}N-urea and 88.2% for ^{15}N-NH_4^+. Since urea was undetectable, the detection limit of the method (70 nmol L^{-1}) was used for the enrichment calculation. After 12 h of incubation, the picoplankton from each bottle was concentrated by filtration and stored as described above for ^{15}N natural abundance measurements.

Flow cytometric cell sorting

Both the natural abundance and isotopically enriched samples were analyzed following Fawcett et al. (2011) with some modifications: samples were thawed to room temperature and were gently stirred to detach the cells from the filter. When necessary, samples were diluted using 0.22 μm filtered NaCl (3.5% by weight). Isolation of groups was performed using an InFlux® Flow Cytometer-Cell Sorter (formerly Cytopeia, BD Biosciences, San Jose, CA, U.S.A.) equipped with five lasers (488-nm [200 mW], 457-nm [300 mW], 532-nm [150 mW], 355-nm [100 mW], and 640-nm [50 mW]) using an 86-μm ceramic black nozzle tip and a sheath pressure of 227.5 kPa. Sheath fluid was prepared daily using molecular biology grade NaCl (3.5% by weight) and purified (Milli-Q) water, filtered through 0.22-μm Steripak filter unit (Merck Millipore, SPGPM20RJ) and passed through an in-line 0.22-μm Sterivex filter unit (Merck Millipore, SVGVL10RC). Ultra rainbow fluorescent particles (1 and 3 μm, Spherotech, Lake Forest, IL, U.S.A.) were used for alignment and calibration. For picophytoplanktonic cells, sort gates were optimized based on the autofluorescence of each group. *Prochlorococcus* cells were gated based on their red fluorescence (692/40 nm; for each fluorescence emission filter, the center wavelength and band-pass width are given) using a combination of the 457 and 488 nm blue lasers. *Synechococcus*-like cells were gated based on their orange fluorescence (530/40 nm) using the 488 (blue) and 532 nm (green) lasers and photosynthetic picophytoeukaryotes (PPEs) were gated based on their red fluorescence (692/40 nm) using the 488 nm blue laser. Events were triggered on the forward light scatter. Nonpigmented cells were stained with Sybr Green I as described in Marie et al. (1999). Events were triggered based on green (530/15) fluorescence excited by the 488 nm laser and cells detected by their green fluorescence (530/15 nm) and absence of red fluorescence. Samples were run at an average flow rate of 30 μL min^{-1}, monitored with a liquid flowmeter (Sensirion, U.S.A.) and the event rate was 10,000–15,000 events s^{-1}. Cells were sorted in purity mode using two tubes configuration, the drop delay was calculated using the calibration procedure with the Spigot Software and an epifluorescence microscope. Cytometry files were analyzed with the FlowJo Software (FlowJo, Ashland, OR, U.S.A.) and plotted using R software (ggplot package). The groups isolated were filtered on 0.3 μm pore size precombusted glass fiber filters (Sterlitech GF-75; 0.3 μm nominal pore size) and dried in an oven at 40°C. These filters were placed in precombusted aluminum envelopes and stored free of humidity until persulfate oxidation.

Persulfate oxidation and denitrifier method

The filters containing both natural abundance and ^{15}N-enriched cells were placed in 4-mL precombusted (500°C for 5 h) glass vials. Two milliliters of persulfate-oxidation reagent (POR; 3 g of NaOH in 60 mL of deionized water + 3 g of 5X recrystallized persulfate in 60 mL of deionized water) was added to each vial. Isotopic reference for organic-bound

nitrogen (USGS40, USGS41, L-glutamic acid) and blanks filters were treated with the same 2 mL of POR. All samples, standards, and blanks were autoclaved at 121°C for 30 min. At this point, all the organic nitrogen content was oxidized to NO_3^- and its concentration was measured by reduction to nitric oxide and detection in a chemiluminescent detector (Teledyne model #200 EU; Garside 1982). To obtain $\delta^{15}N$ values, we used the "denitrifier method" (Sigman et al. 2001; 10–20 nmol N optimal), which is based on the isotopic analysis of nitrous oxide (N_2O) generated by the action of denitrifying bacteria that convert NO_3^- to N_2O and lack N_2O-reductase. The isotopic composition of the N_2O was measured by gas chromatography-isotope ratio mass spectrometry using a modified ThermoFinnigan GasBench II and Delta V. Final measurements were corrected by blanks.

N assimilation rates calculations

The cell-specific uptake rates (ρDINcells; fg N cell^{-1} h^{-1}) of dissolved inorganic nitrogen (DIN) were calculated for each N source. The equations used are provided in Dugdale and Wilkerson (1986) with some modification applied to cell-specific assimilation rates:

$$V = \frac{R_{(\text{cells})}}{R_{(\text{DIN})}} \times T \quad (1)$$

$$\rho\text{DINcells} = V \times \frac{N}{\text{CS}} \quad (2)$$

where V is the specific uptake rate (h^{-1}); $R_{(\text{cells})}$ = ^{15}N atom percent in the cells at the end of the incubation – ^{15}N atom percent in the cells initial; $R_{(\text{DIN})}$ = ^{15}N atom percent enrichment in DIN – ^{15}N atom percent in the cells initial; T represents the incubation time (hours); N represents the amount of N in the analyzed sorted cells (fg N); and CS = number of sorted cells for isotope analysis (cells).

Group-specific uptake rates (ρDIN group; nmol L^{-1} d^{-1}) were calculated as follows:

$$\rho\text{DINgroup} = \rho\text{DINcells} \times \text{ISA} \quad (3)$$

where ISA is the average in situ abundance of each group of sorted cells (cells L^{-1}).

When the tracer additions resulted in initial enrichments exceeding 50%, rates should be considered as potential uptake.

The detection limit of each uptake rate was calculated in order to determine if those rates were significantly different from zero. The detection limit was calculated following the specifications of Santoro et al. (2013) as the N (NH_4^+, urea, NO_3^-, NO_2^-) uptake rate necessary to cause a 1‰ increase in $\delta^{15}N$ of sorted cells from the initial value ($\delta^{15}N$ natural abundance). The 1‰ value represents twice the precision of $\delta^{15}N$ analysis using the denitrifier method (precision = 0.5‰; Sigman et al. 2001; McIlvin and Casciotti 2011).

Statistical analysis

Statistical differences among natural $\delta^{15}N$ for PON_{sus} and sorted groups of cells (*Pro*, *Syn*) were tested using Wilcoxon and the Kruskal-Wallis test. Statistical significance was set at the 0.05 level. The correlations between $\delta^{15}N$ of *Prochlorococcus*, $\delta^{15}N$ *Synechococcus*-like, and environmental factors (nutrient concentrations and light %) were calculated using Pearson's correlation analysis. The variables were logarithmic transformed as $\text{Log}_{10}(X + 1)$ and the Pearson's correlation coefficients were tested for significance at $\alpha = 0.05$ using XLStat software (AddinSoft SARL).

Results

Water column structure and nutrient content

The structure of the water column at all experimental stations exhibited a SCM in the ODZ like the examples represented in Fig. 2 (summarized in Tables 1–2). The O_2 profile shows the typical distribution with a surface oxygenated layer ranging in depth between 22 and 80 m for the ETNP, and 34 and 89 m for the ETSP, with O_2 concentrations ranging from 197 to 215 μmol L^{-1} for the ETNP and 208 to 267 μmol L^{-1} for the ETSP. Below the mixed layer, O_2 concentrations decreased rapidly depth, reaching anoxia at 62–130 m depth (depending of the station and proximity to the coast). The SCM was found within the upper anoxic layer, with the peak at average depths of 114 m (SD = 28 m; min = 90 m; max = 160 m) for the ETNP and 100 m (SD = 21 m; min = 68 m; max = 130 m) for the ETSP. The SCM varied in intensity (see examples in Fig. 2A,D) with a maximum fluorescence equaling or almost doubling that of the PCM at some stations (Table 1).

NH_4^+ concentrations (detection limit = 10 nmol L^{-1}) for the SCM presented no major differences between the two regions, reaching an average of 18.4 nmol L^{-1} for the ETNP (SD = 28.3 nmol L^{-1}; min = bdl; max = 72.4 nmol L^{-1}) and 27.5 nmol L^{-1} for the ETSP (SD = 29.2 nmol L^{-1}; min = bdl; max = 88.4 nmol L^{-1}). NH_4^+ concentrations in the PCM tended to be higher, reaching on average 36.2 nmol L^{-1} (SD = 62.3 nmol L^{-1}, min = bdl, max = 191.9 nmol L^{-1}) in the ETNP and one order of magnitude more abundant in the ETSP with 481.2 nmol L^{-1} (SD = 211.2 nmol L^{-1}; min = 108.2 nmol L^{-1}; max = 822.7 nmol L^{-1}) (Table 2). Samples for urea determination were obtained from both oceans in two cruises (ETNP-RB1603 and ETSP-AT2626), but almost all measurements for the SCM were below the detection limit of the method (70 nmol L^{-1}) with only two stations of the cruise RB1603 reaching concentrations of 0.22 μmol L^{-1} (Sta. 9) and 1.02 μmol L^{-1} (Sta. 10). NO_3^- and NO_2^- profiles (Fig. 2B,E) showed the typical structure for an ODZ (Ulloa et al. 2012). In the surface, both nutrients were depleted, with an accumulation for NO_3^- below the oxycline and of NO_2^- in anoxic waters. In the ETNP (Fig. 2, upper panels), the NO_2^- accumulation (and secondary drop in NO_3^-) was below the *Prochlorococcus* SCM, while in the ETSP (Fig. 2, lower panels), the SCM was small and NO_2^- accumulated (and NO_3^- decreased) within the

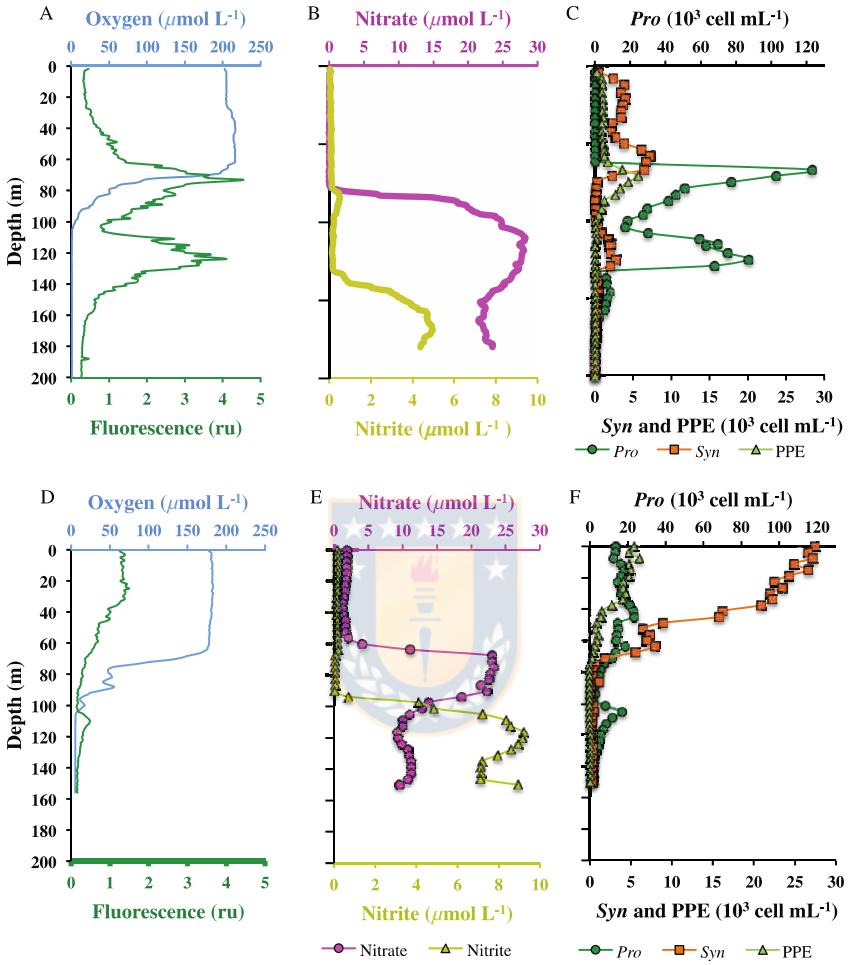

Fig. 2. Examples of environmental conditions of microbial communities inhabiting the SCM in the ODZs from the ETNP (top panels) and ETSP (bottom panels). Panels (**A**) and (**D**) show oxygen and fluorescence (in relative units, ru) profiles (CTD + fluorometer). Panels (**B**) and (**E**) show nitrate and nitrite profiles measured in continuous flow coupling the PPS and an autoanalyzer (**B**) and a high-resolution sampling (**E**). Panels (**C**) and (**F**) show cell count ($\times 10^3$ cell mL^{-1}) profiles of picophytoplankton components obtained by a high-resolution sampling analyzed by flow cytometry. Dark green circles indicate *Prochlorococcus*, light green triangles indicate PPE, and orange squares represent *Synechococcus*-like. [Color figure can be viewed at wileyonlinelibrary.com]

SCM. Nutrient concentrations within the PCM and SCM for all station sampled are shown in Table 2.

Flow cytometric analysis of picoplankton composition

Flow cytometric analysis showed that the picophytoplanktonic communities in anoxic subsurface waters differed consistently from those in oxic surface waters in both abundance and composition (see examples in Fig. 2C,F): picocyanobacteria were numerically dominant in the PCM, while PPEs were also present with abundances ranging between 800 and 96,000 cells mL^{-1} (Supporting Information Table S1). In contrast, SCM communities were mainly composed of *Prochlorococcus* cells and to a lesser extent of *Synechococcus*-like cells (yellow/orange fluorescent), with almost no detectable PPE

Table 1. Flow cytometric analysis of the microbial community at the peak depth of the SCM for the ETNP and ETSP, including: cruise name; station; position (latitude and longitude); peak depth of the SCM reported in meters; the percent of incident light at the SCM peak depth (light%); *Prochlorococcus* (*Pro*), *Synechococcus*-like (*Syn*), PPE, fluorescent picoplankton (Fluor. Picoplank. = *Pro* + *Syn* + PPE), NFP, total picoplanktonic community (Total Picoplank. = *Pro* + *Syn* + PPE + NFP) abundances (10^3 cells mL^{-1}); *Prochlorococcus* relative abundance (in %) to the fluorescent picoplankton and to the total picoplankton; fluorescence of SCM relative to PCM. ND indicates none were detected.

Cruise	Station	Lat. (N)	Long. (W)	Peak depth (m)	Light (%)	*Pro* (× 10^3 cells mL^{-1})	*Syn* (× 10^3 cells mL^{-1})	PPE (× 10^3 cells mL^{-1})	Fluor. Picoplank. (×10^3 cells mL^{-1})	NFP (× 10^3 cells mL^{-1})	Total picoplankton (×10^3 cells mL^{-1})	*Pro* Rel. Ab. to Fluor. Picoplank. (%)	*Pro* Rel. Ab. to Total Picoplank. (%)	Fluor. of SCM relative to PCM
ETNP														
NH1410	T9	18.200	105.199	90	1.39	70	7.4	0.09	77.5	476	553	90	12.7	1.30
RB1603	6	18.688	104.417	90	0.01	53	1.3	0.00	54.3	372	426	98	12.4	0.57
RB1603	7	17.500	102.700	93	0.02	78	2.0	0.00	80.0	664	744	98	10.5	0.71
RB1603	8	16.251	100.843	97	ND	58	1.8	0.00	59.8	586	646	97	9.0	0.06
RB1603	9	15.000	99.000	98	ND	40	0.9	0.00	40.9	511	552	98	7.2	0.21
RB1603	10	15.471	101.503	128	ND	13	0.5	0.00	13.5	671	684	96	1.9	0.36
RB1603	11	15.903	103.800	115	ND	70	2.1	0.00	72.1	421	493	97	14.2	0.90
RB1603	12	16.316	106.092	156	ND	22	0.2	0.00	22.2	402	424	99	5.2	0.45
RB1603	13	16.778	108.397	160	ND	7	0.2	0.00	7.2	398	405	97	1.7	0.17
Min	**—**	**—**	**—**	**90**	**—**	**7**	**0.2**	**0.00**	**7.2**	**372**	**405**	**90**	**1.7**	**0.06**
Max	—	—	—	**160**	—	**78**	**7.4**	**0.09**	**80.0**	**671**	**744**	**99**	**14.2**	**1.30**
Average	**—**	**—**	**—**	**114**	**—**	**46**	**1.8**	**0.01**	**47.5**	**500**	**548**	**97**	**8.3**	**0.52**
SD	**—**	**—**	**—**	**28**	**—**	**26**	**2.2**	**0.03**	**27.9**	**116**	**123**	**2**	**4.6**	**0.40**
ETSP														
NBP1305	H9	13.002	82.199	110	0.35	17	0.5	0.00	17.5	673	691	97	2.5	0.33
NBP1305	H21	21.500	70.582	79	0.69	7	0.7	0.00	7.7	436	444	91	1.6	0.33
NBP1305	BB2	20.526	70.712	80	0.31	13	1.8	0.04	14.8	896	911	88	1.4	0.18
AT2626	1	20.002	74.005	105	0.01	15	2.0	0.00	17.0	217	234	88	6.4	0.31
AT2626	3	18.798	76.200	98	0.01	144	37.6	3.98	185.6	5220	5406	78	2.7	1.91
AT2626	8	11.502	81.411	112	0.01	98	1	0.00	99.0	661	760	99	12.9	0.62
AT2626	9	11.999	84.001	130	ND	24	2	0.00	26.0	329	355	92	6.8	0.36
AT2626	10	11.998	81.198	110	0.07	46	1	0.82	47.8	196	244	96	18.9	1.12
AT2626	12	12.545	77.593	127	ND	28	0.2	0.00	28.2	497	525	99	5.3	0.15
AT2626	14	14.198	77.499	78	ND	18	1.1	0.00	19.1	492	511	94	3.5	0.02
AT2626	18	15.591	75.335	68	0.05	20	1.0	0.00	21.0	878	899	95	2.2	0.39
Min	—	—	—	**68**	—	**7**	**0.2**	**0.00**	**7.7**	**196**	**234**	**78**	**1.4**	**0.02**
Max	**—**	**—**	**—**	**130**	**—**	**144**	**37.6**	**3.98**	**185.6**	**5220**	**5406**	**99**	**18.9**	**1.91**
Average	**—**	**—**	**—**	**100**	**—**	**39**	**4.4**	**0.44**	**44.0**	**954**	**998**	**93**	**5.8**	**0.52**
SD	—	—	—	**21**	—	**43**	**11.0**	**1.20**	**53.3**	**1434**	**1481**	**6**	**5.5**	**0.54**

Table 2. Nutrient analysis at the peak depth of the PCM and SCM for stations sampled in the ETNP and ETSP. Cruise name, station, peak depth, and NH_4^+, urea, NO_3^- and NO_2^- concentrations. NA indicates no available data and bdl is below detection limit.

		PCM					SCM				
Cruise	Station	Peak depth (m)	NH_4^+ (nmol L^{-1})	Urea (μmol L^{-1})	NO_3^- (μmol L^{-1})	NO_2^- (μmol L^{-1})	Peak depth (m)	NH_4^+ (nmol L^{-1})	Urea (μmol L^{-1})	NO_3^- (μmol L^{-1})	NO_2^- (μmol L^{-1})
ETNP											
NH1410	T9	40	191.9	NA	NA	NA	90	63.0	NA	NA	NA
RB1603	6	30	14.6	NA	0.1	0.0	90	bdl	NA	28.2	0.0
RB1603	7	49	25.7	bdl	5.4	0.8	93	bdl	bdl	26.5	0.4
RB1603	8	35	bdl	bdl	0.1	0.2	97	bdl	NA	29.4	0.2
RB1603	9	45	70.7	0.01	0.0	0.5	98	72.4	0.22	27.6	1.0
RB1603	10	76	9.4	0.10	0.1	0.0	128	11.0	1.02	26.8	0.2
RB1603	11	78	bdl	bdl	0.1	0.1	115	bdl	bdl	24.9	0.2
RB1603	12	95	bdl	0.07	0.0	0.1	156	bdl	bdl	26.8	0.2
RB1603	13	69	bdl	bdl	0.1	0.1	160	bdl	bdl	26.2	0.1
Min		30	bdl	bdl	0.0	0.0	90	bdl	bdl	24.9	0.0
Max		95	191.9	0.10	5.4	0.8	160	72.4	1.02	29.4	1.0
Average		**57**	**36.2**	**0.06**	**0.7**	**0.2**	**114**	**18.4**	**0.62**	**27.0**	**0.3**
SD		**23**	**62.3**	**0.05**	**1.9**	**0.3**	**28**	**28.3**	**0.57**	**1.3**	**0.3**
ETSP											
NBP1305	H9	25	225.5	NA	1.5	0.1	110	bdl	NA	9.9	8.3
NBP1305	H21	23	504.4	NA	2.9	0.1	79	88.4	NA	8.2	5.1
NBP1305	BB2	24	570.0	NA	3.9	0.2	80	63.0	NA	10.9	3.9
AT2626	1	41	108.2	NA	NA	1.0	105	56.7	NA	NA	0.4
AT2626	3	35	513.2	bdl	NA	0.3	98	22.8	bdl	14.6	0.1
AT2626	8	40	668.7	bdl	8.8	2.0	112	bdl	bdl	24.2	0.5
AT2626	9	34	598.7	bdl	5.5	0.5	130	bdl	bdl	29.3	0.2
AT2626	10	50	237.9	bdl	15.4	0.3	110	bdl	bdl	17.8	5.2
AT2626	12	25	567.7	bdl	4.6	0.1	127	11.1	bdl	25.6	1.5
AT2626	14	20	476.3	bdl	1.0	0.2	78	22.2	bdl	20.6	1.2
AT2626	18	29	822.7	bdl	7.1	1.6	68	24.1	bdl	5.0	11.4
Min		20	108.2	bdl	1.0	0.1	68	bdl	bdl	5.0	0.1
Max		50	822.7	bdl	15.4	2.0	130	88.4	bdl	29.3	11.4
Average		**31**	**481.2**	**bdl**	**5.6**	**0.6**	**100**	**27.5**	**bdl**	**16.6**	**3.4**
SD		**9**	**211.2**	**bdl**	**4.4**	**0.7**	**21**	**29.2**	**bdl**	**8.2**	**3.8**

(Table 1; Supporting Information Fig. S2). The abundance of *Prochlorococcus* at the peak of the SCM varied among stations (Table 1). On average, the abundance of *Prochlorococcus* was 46×10^3 cells mL^{-1} (SD = 26×10^3 cells mL^{-1}) for the ETNP and 39×10^3 cells mL^{-1} (SD = 43×10^3 cells mL^{-1}) for the ETSP, representing 8.3% and 5.8% of the total picoplanktonic community respectively. Moreover, *Prochlorococcus* represented 97% and 93% of the total fluorescent picoplankton for the ETNP and ETSP, respectively (Table 1). Despite this variability, *Prochlorococcus* were always one order of magnitude more abundant than *Synechococcus*-like within the SCM. The remaining 91.7–94.2% of the picoplankton community is referred to as nonfluorescent picoplankton (NFP) and is composed of heterotrophic or chemoautotrophic bacteria and archaea.

$\delta^{15}N$ of PON_{sus} and sorted components of the PCM and SCM picoplanktonic community

The natural abundance $\delta^{15}N$-PON_{sus} in both the PCM and SCM showed a high variability ranging from 5.8‰ to 18.9‰ in the PCM and from 4.3‰ to 16.6‰ in the SCM (Fig. 3). These $\delta^{15}N$ values were always positive, and, in the case of the SCM, far from the $\delta^{15}N$ previously measured for NO_2^- (negative) (Table 3), but in some cases as high as those reported for NO_3^- (Table 3; Peters et al. 2018).

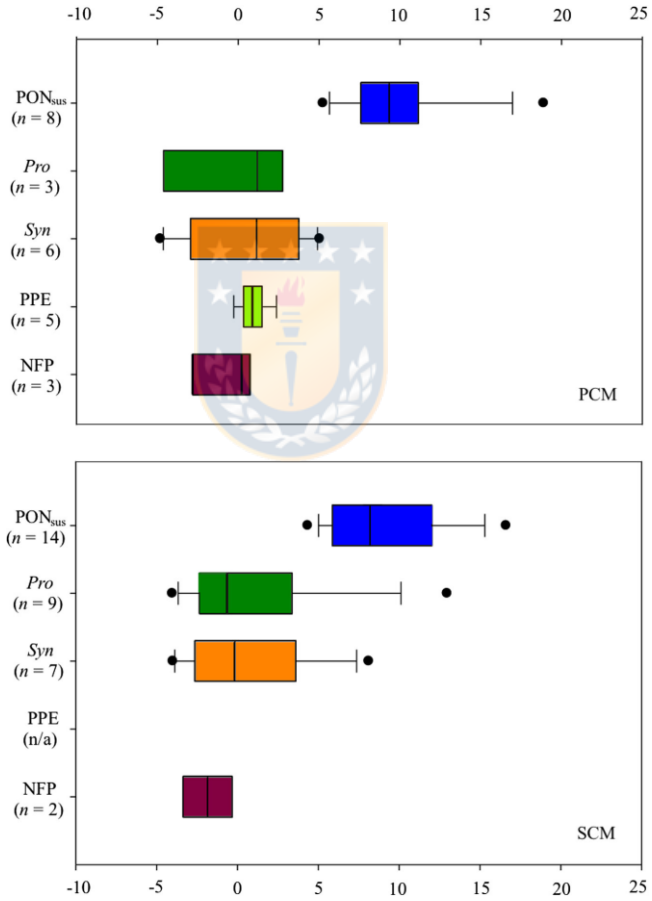

Fig. 3. Boxplot of the $\delta^{15}N$ natural abundance from PON_{sus} (0.3–3.0 μm size fraction) and the $\delta^{15}N$ of sorted picoplankton components from the PCM (top panel) and SCM (bottom panel): *Prochlorococcus* (*Pro*) and *Synechococcus*-like (*Syn*), PPE, and NFP. *n* is the number of measurements per group and n/a indicates that data were not available. [Color figure can be viewed at wileyonlinelibrary.com]

Table 3. $\delta^{15}N$ (‰) for different dissolved N sources in the ODZs and kinetic isotope effect ε (‰) during the assimilation of these sources.

N source	$\delta^{15}N$ (‰)	Study area	Reference	ε_{assim} (‰)	Reference
Nitrate	12.4 ± 0.6 and 17.2 ± 0.6 (ETNP)	TOP ODZ	Casciotti and McIlvin (2007) (ETNP)	2–5	Granger et al. (2010)
	8.2–30.1 (ETSP)		K. Casciotti pers. comm. (ETSP)		
Nitrite	−16.0 ± 2.6 and −17.8 ± 0.9	TOP ODZ ETNP	Casciotti and McIlvin (2007)	1	Sigman and Casciotti (2001)
Ammonium*	Estimated by ~7.1 ± 4.2 (PON_{sus})	TOP ODZ ETNP/ETSP	This study	20	Waser et al. (1998)
	Estimated by ~5.1 (PON_{sk})		Fuchsman et al. (2018) (ETNP)		
Urea*	Estimated by ~7.1 ± 4.2 (PON_{sus})	TOP ODZ ETNP/ETSP	This study	0–0.7	Waser et al. (1998)
	Estimated by ~5.1 (PON_{sk})		Fuchsman et al. (2018) (ETNP)		

*No measurements are available in literature. The estimations are on base of the average obtained by suspended PON in the SCM (PON_{sus} ~ 10‰) and sinking PON (PON_{sk} ~ 8.1‰) minus ε < 3‰ estimated for degradation (Sigman and Casciotti 2001) More details are available in Supporting Information Table S1.

Using a flow cytometer cell sorter, we were able to identify and sort different groups comprising the picophytoplanktonic community inhabiting the SCM. Once the groups were identified, we sorted them and analyzed them to obtain the natural abundance $\delta^{15}N$ for each group (Fig. 3; see summary of the oceans, cruises, stations, and chlorophyll peaks of the samples considered in this study and the isotopic analyses available in each one in Supporting Information Table S2). The values of $\delta^{15}N$ for sorted *Prochlorococcus* and *Synechococcus*-like also showed a high variability among different stations in both the PCM and SCM (Fig. 3 and Supporting Information Table S2). *Prochlorococcus* variability in the SCM was 23% higher than the variability shown by PON_{sus} (the total seston community from which *Prochlorococcus* was sorted) whereas *Synechococcus*-like variability was 8% lower. The $\delta^{15}N$ for *Prochlorococcus* inhabiting the SCM ranged from −4.0‰ to 13.0‰ (Fig. 3). However, the distribution of the data shows that 50% of the values (n = 9) ranged from −2.1‰ to 2.6‰, with a median of −0.6‰ and an average of 1.2‰. In the case of *Synechococcus*-like, $\delta^{15}N$ values presented a similar distribution to *Prochlorococcus*, with total values ranging from −4.0‰ to 8.1‰ and 50% of the data (n = 7) were distributed between −1.9‰ and 2.9‰, with a median of −0.2‰ and an average of 0.9‰. Despite the similar distribution, the highest value of $\delta^{15}N$ for *Synechococcus*-like was not as high as the highest $\delta^{15}N$ value for *Prochlorococcus* (Fig. 3). The multiple-pairwise comparisons among $\delta^{15}N$-PON_{sus}, $\delta^{15}N$-*Pro*, and $\delta^{15}N$-*Syn* for the SCM indicate that there are significant differences between $\delta^{15}N$-PON_{sus} vs. $\delta^{15}N$-*Pro* and $\delta^{15}N$-PON_{sus} vs. $\delta^{15}N$-*Syn* at a 95% confidence level. However, no significant differences were found between $\delta^{15}N$-*Pro* vs. $\delta^{15}N$-*Syn* (Supporting Information Table S3). Only three measurements of $\delta^{15}N$ were available for *Prochlorococcus* inhabiting the PCM, and these measurements present no significant differences with the measurements available for *Prochlorococcus* inhabiting the SCM (Supporting Information Table S4). PPEs were only found in the PCM and exhibited $\delta^{15}N$ values ranging from −0.3‰ to 2.4‰, while 50% of the data (n = 5) ranged from 0.5‰ to 1.2‰. Few measurements for $\delta^{15}N$-NFP were obtained from the PCM and SCM, with average values of −0.9 (n = 3) and −1.8 (n = 2), respectively. The NFP was not included in the statistical analysis due to the low number of measurements available for this group.

Nitrogen assimilation rates

All N uptake rates were above the detection limit (for detection limit results, see Supporting Information Table S5). In the case of the oxidized N forms (Fig. 4A; Table 4), *Prochlorococcus* showed the lowest cell-specific uptake rates of oxidized N forms while NFP showed a preference for NO_3^-, assimilating up to 7.1 times more NO_3^- than NO_2^-. This rate was approximately 7.6 times higher than the NO_3^- uptake rates calculated for *Prochlorococcus* and almost 4.3 times higher than rates calculated for *Synechococcus*-like. *Prochlorococcus* showed very low uptake rates for both NO_2^- and NO_3^-. In contrast, while NO_3^- uptake rates by *Synechococcus*-like were low, NO_2^- uptake rates were 11.4 and 12.5 times higher than those observed for *Prochlorococcus* and NFP, respectively.

The potential cell-specific uptake rates of reduced N forms (Fig. 4B; Table 4) show that NFP and *Prochlorococcus* have higher uptake rates for NH_4^+ compared with urea. In the case of NFP, uptake of NH_4^+ exceeded uptake of urea by 2.0-fold, while in *Prochlorococcus* NH_4^+ uptake exceeded urea uptake by only 1.2-fold. *Synechococcus*-like showed a strong preference for urea uptake and rates were 5.2 times the urea uptake rates measured for NFP and 4.1 times those of *Prochlorococcus*.

We also estimated the group-specific uptake rates (ng N L^{-1} d^{-1}) by multiplying the cell-specific uptake rates (fg N $cell^{-1}$ h^{-1}) by the average in situ abundance of each group (cells L^{-1}) observed in the SCM (Table 4). As the NFP were the most abundant group (5.39×10^8 cell L^{-1}) compared with *Prochlorococcus* (5.53×10^7 cell L^{-1}) and *Synechococcus*-like (1.05×10^7 cell L^{-1}), they dominated uptake rates for all forms of N measured (Table 4). The uptake rates of oxidized forms of N were 14.07 ng N L^{-1} d^{-1} for NO_3^- and 1.86 ng N L^{-1} d^{-1} for NO_2^-, 2–3 orders of magnitude higher

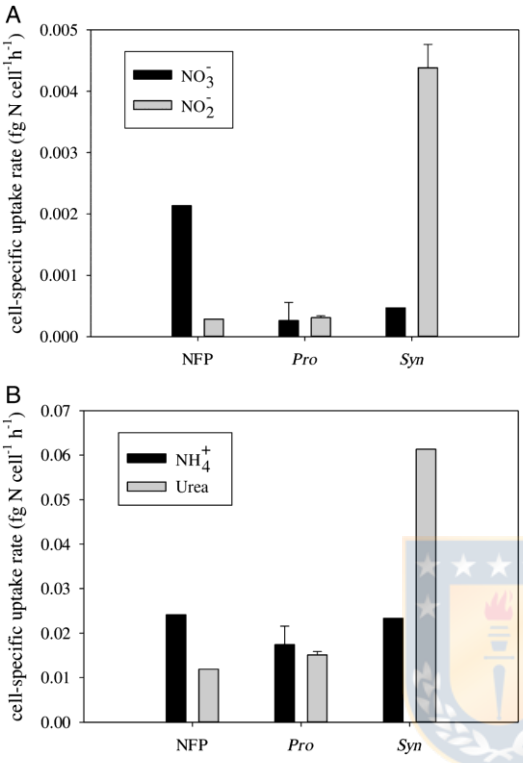

Fig. 4. Cell-specific uptake rates (fg N cell^{-1} h^{-1}) for NFP, *Prochlorococcus* (*Pro*), and *Synechococcus*-like (*Syn*) collected from the SCM: (**A**) NO_3^- and NO_2^- uptake and (**B**) NH_4^+ and urea uptake.

than the uptake rates measured for *Prochlorococcus* and *Synechococcus*-like groups. The potential uptake rates of reduced forms of N by NFP were 313.74 ng N L^{-1} d^{-1} for NH_4^+ and 154.84 ng N L^{-1} d^{-1} for urea, 1–2 orders of magnitude higher than those estimated for *Prochlorococcus* and *Synechococcus*-like. For *Prochlorococcus*, the potential uptake rates for NH_4^+ and urea were similar to each other, at 23.23 ng N L^{-1} d^{-1} and 20.16 ng N L^{-1} d^{-1}, respectively. *Synechococcus*-like had a potential uptake rates similar to *Prochlorococcus* for urea (15.53 ng N L^{-1} d^{-1}) but lower for NH_4^+ (5.91 ng N L^{-1} d^{-1}).

δ^{15}N vs. environmental variables

Pearson correlation analyses revealed a strong negative correlation between the δ^{15}N of *Prochlorococcus* and NO_3^- concentrations ($r = -0.82$; p value = 0.01) and positive correlation with NH_4^+ concentrations ($r = 0.72$; p value = 0.03) (Supporting Information Table S6). However, there were no significant correlations between δ^{15}N of *Prochlorococcus* and percent light or NO_2^- concentrations. There were no significant correlations between the δ^{15}N of *Synechococcus*-like inhabiting the SCM and any of the tested variables.

Discussion

Oceanographic conditions and SCM

Previous studies that analyzed SCMs found conditions within the range observed here (Lavin et al. 2010; Garcia-Robledo et al. 2017; Widner et al. 2018*a*,*b*). Dissolved oxygen shows saturation conditions at the surface layer, followed by a pronounced oxycline. Between 62 and 130 m depth (depending on the station) oxygen decreases to undetectable levels. Bellow this depth, a SCM develops in oxygen-depleted and NO_3^- rich conditions, but with low concentrations of reduced N as NH_4^+ or urea (Table 2; Fig. 2).

Table 4. Cell-specific (fg N cell^{-1} h^{-1}) and group-specific (ng N L^{-1} d^{-1}) uptake rates of oxidized (NO_3^- and NO_2^-) and reduced (NH_4^+ and urea) N forms measured in this study for each group of sorted cells: NFP, *Prochlorococcus* (*Pro*), and *Synechococcus*-like (*Syn*). Group-specific uptake rates were calculated multiplying the cell-specific uptake rates (fmol cell^{-1} d^{-1}) by the in situ average abundance of cells of each group (cell L^{-1}).

	Cell-specific uptake rates (fg N cell^{-1} h^{-1})				Group-specific uptake rates (ng N L^{-1} d^{-1})			
Group	NO_3^-	NO_2^-	NH_4^+*	**Urea***	NO_3^-	NO_2^-	NH_4^+*	**Urea***
NFP	**0.0022**	**0.0003**	**0.0243**	**0.0120**	**14.07**	**1.86**	**313.74**	**154.84**
Pro	**0.0003**	**0.0003**	**0.0175**	**0.0152**	**0.18**	**0.21**	**23.23**	**20.16**
	SD = 0.0003	SD = 0.00003	SD = 0.0042	SD = 0.0008	SD = 0.19	SD = 0.02	SD = 5.52	SD = 1.04
	n = 4	*n* = 2	*n* = 2	*n* = 2	*n* = 4	*n* = 2	*n* = 2	*n* = 2
Syn	**0.0005**	**0.0044**	**0.0235**	**0.0616**	**0.06**	**0.56**	**5.91**	**15.53**
		SD = 0.0004				SD = 0.05		
		n = 2				*n* = 2		

*Tracer additions resulted in initial enrichments > 50%, rates should be considered as potential uptake.

Prochlorococcus and *Synechococcus*-like numerically dominated the SCM picophytoplankton community and there were almost no detectable PPE. Apparently this pattern is a persistent characteristic of this particular environment as shown by the few previous studies in ODZs (Lavin et al. 2010; Astorga-Eló et al. 2015; Garcia-Robledo et al. 2017). The relative abundance of *Prochlorococcus* compared to the total picoplanktonic community was consistent with previously reported ranges (> 5.3%) (Lavin et al. 2010). Although the lineages of *Prochlorococcus* and *Synechococcus*-like composing the SCM community were not analyzed as part of this study, they have been previously identified using cloning and sequencing, and terminal restriction fragment length polymorphism analyses applied to the 16S–23S rRNA internal transcribed spacer region (Lavin et al. 2010). Lavin and colleagues found that > 90% of total *Prochlorococcus* in the SCM was composed by the lineage LLIV and two novel lineages termed LLV and LLVI. On other hand, *Synechococcus* was mainly represented by clade I and VI, but with very low abundances.

Assimilative N metabolism in ODZ picocyanobacteria

Natural abundance samples

The measurements of δ^{15}N-NO_3^- reported in the literature for the ODZs range from 12.4‰ to 17.2‰, and from −16.0‰ to −17.8‰ for δ^{15}N-NO_2^-, showing a difference up to 35‰ between both nitrogen sources (Casciotti and McIlvin 2007). These differences are considered a consequence of isotope fractionation during the processes of denitrification (Casciotti and McIlvin 2007) and nitrite oxidation (Peters et al. 2016). NH_4^+ and urea exhibit very low (nanomolar) concentrations in the ocean (for our study sites, see Table 2) and it has not been possible to measure their δ^{15}N to date, as the most sensitive methods require concentrations of at least 0.5 μmol L^{-1} (Zhang et al. 2007). However, NH_4^+ and urea would have an estimated value close to 7‰ (min = 1.3‰; max = 14.4‰; SD = 4.2‰) considering the average of 10‰ for PON_{sus} in the SCM (Supporting Information Table S7) or close to 5.1‰ if the NH_4^+ and urea come mainly by the degradation of sinking material as fecal pellets and/or marine snow (PON_{sk} ~ 8.1‰ in the ODZ; Fuchsman et al. 2018) (Table 3).

The δ^{15}N-PON_{sus} for the SCM samples was always positive, with values ranging from 4.3‰ to 16.6‰ (Fig. 3). The explanation for these relative high δ^{15}N could be the result of the assimilation of high δ^{15}N (as NO_3^-) by the community composing the SCM or the release of low δ^{15}N (as the case of anammox or denitrification) Thus, the δ^{15}N-PON_{sus} for the SCM represents a mixture of the δ^{15}N of diverse source pools, both living and nonliving. The relative contributions of the different components vary among stations, with δ^{15}N values that can be low for some components and high for others.

Another source of variability of δ^{15}N-PON_{sus} from SCMs at different stations may due to the potential variability in the composition of NFP. Although we identified a very abundant and consistent picophytoplankton component (*Prochlorococcus* and *Synechococcus*-like) in samples collected from the SCM, NFP including heterotrophic or chemoautotrophic bacteria and archaea were far more abundant and may vary greatly in functional composition in SCM samples from different stations (e.g., ETNP/ETSP or coastal/oceanic). Differences in the bacterial or archaeal composition may be reflected in differences in the nutritional preferences of the dominant bacterial or archaeal members and this may be reflected in their δ^{15}N. As the δ^{15}N-PON_{sus} in the SCM presented much higher values than their components (Fig. 3), part of the variability presented and heavy isotopic signature could also be due to the contribution of nonliving particulate material sinking from the surface with high δ^{15}N. That could be the case for stations sampled in the ETSP, where measurements of δ^{15}N-PON_{sus} for the SCM exceeding by 6.5‰, 10.0‰, 3.3‰, and 3.5‰ the values measured for the δ^{15}N-PON_{sus} in the PCM (Supporting Information Table S7, bold font). Thus, sinking particles can be experiencing degradation by both bacteria and zooplankton, which preferentially degrade low δ^{15}N-PON to NH_4^+, leaving the residual PON enriched in ^{15}N. Accordingly, these results emphasize the importance of the use of flow cytometry cell sorting to distinguish the living and nonliving components of the community and their contribution to the bulk δ^{15}N signature.

The δ^{15}N observed for sorted *Prochlorococcus* cells from the SCM ranged from −4.0‰ to 13.0‰ (range = 17‰), higher than the range previously observed for *Prochlorococcus* cells from the Sargasso Sea with values ranging from −4‰ to −1‰ (range = 3‰) (Fawcett et al. 2011). The smaller range in δ^{15}N values from the Sargasso Sea *Prochlorococcus* group may be due to a more stable nutrient environment relative to an ODZ SCM. *Prochlorococcus* from the Sargasso Sea preferentially assimilates recycled N sources such as NH_4^+ or amino acids (Fawcett et al. 2011). The highest δ^{15}N observed in ODZ *Prochlorococcus* was only seen once in a coastal station in the ETSP (cruise NBP1305, Sta. BB2) and may have been due to use of NO_3^- (Table 3) as the main N source. The lowest δ^{15}N value (−4.0‰) for *Prochlorococcus* was observed at a more oceanic station in the ETSP (cruise AT2626, Sta. 8). Since neither *Prochlorococcus* nor *Synechococcus* has the genes to fix N_2 (Latysheva et al. 2012), low δ^{15}N values could be evidence of NO_2^- assimilation, as NO_2^- is the only N source with negative δ^{15}N values. Fifty percent of the *Prochlorococcus* δ^{15}N values ranged from −2.1‰ to 2.6‰ (median of −0.6‰), suggesting that ODZ SCM *Prochlorococcus* is most likely assimilating a mixture of N sources with positive δ^{15}N as ammonium, urea, and/or NO_3^-, while assimilation of N sources with negative δ^{15}N such as NO_2^- may lower cellular δ^{15}N. Similar to *Prochlorococcus*, *Synechococcus*-like cells isolated from the ODZ SCM had δ^{15}N values ranging from −4.0‰ to 8.1‰ (range = 12.1) and had a broader range than values observed for Sargasso Sea *Synechococcus*, which ranged from −3‰ to −1‰ (range = 2) (Fawcett et al. 2011). Apparently both picocyanobacteria have similar nutritional preferences in the ODZ SCM.

No photosynthetic picoeukaryotes were observed in the ODZ SCM, while those found in the PCM presented $\delta^{15}N$ values ranging from −0.3‰ to 2.4‰, with 50% of the data (n = 5) ranging from 0.5‰ to 1.2‰. These values are one-order of magnitude lower than those reported for PPE in the Sargasso Sea at 100 m depth ($\delta^{15}N$ = 12.7‰), where PPE seems to be assimilating upwelled NO_3^- from below the euphotic zone, but close to those reported for lower depths ($\delta^{15}N$ between 1‰ and 5‰) where most phytoplankton growth is thought to be supported by NH_4^+ (Fawcett et al. 2011).

The question remains whether the high variability $\delta^{15}N$ of *Prochlorococcus* and *Synechococcus*-like might be explained by environmental factors such as light and/or nutrient concentration. It can be hypothesized that higher light availability might increase the probability that *Prochlorococcus* uses NO_3^- because it would have more energy available needed for NO_3^- assimilation. However, there was no significant correlation of $\delta^{15}N$ with light percentage, but instead a significant negative correlation with NO_3^- and positive correlations with NH_4^+ (Supporting Information Table S6). A negative correlation

Table 5. Comparison of cell-specific uptake rates (fg N cell^{-1} h^{-1}) by picophytoplankton in various regions of the ocean. ND indicates it was not detected.

	Cell-specific uptake rate (fg N cell^{-1} h^{-1})						
Microorganism	**Urea**	**NH_4^+**	**NO_3^-**	**NO_2^-**	**Estimated total N rates***	**Environment**	**Reference**
Prochlorococcus	0.0152	0.0175	0.0003	0.0003	—	ODZ	This study
Synechococcus-like	0.0616	0.0235	0.0005	0.0044	—	ODZ	This study
NF picoplankton	0.0120	0.0243	0.0022	0.0003	—	ODZ	This study
Picophytoplankton	—	—	—	—	0.0711	SCM ODZ ETNP	Garcia-Robledo et al. (2017)
Picophytoplankton	—	—	—	—	0.0326	SCM ODZ ETNP	Garcia-Robledo et al. (2017)
Picophytoplankton	—	—	—	—	0.1304	SCM ODZ ETNP	Garcia-Robledo et al. (2017)
Picophytoplankton	—	—	—	—	ND	SCM ODZ ETNP	Garcia-Robledo et al. (2017)
Picophytoplankton	—	—	—	—	0.6521	SCM ODZ ETNP	Garcia-Robledo et al. (2017)
Picophytoplankton	—	—	—	—	0.2304	SCM ODZ ETNP	Garcia-Robledo et al. (2017)
Picophytoplankton	—	—	—	—	0.2642	SCM ODZ ETNP	Garcia-Robledo et al. (2017)
Picophytoplankton	—	—	—	—	0.3098	SCM ODZ ETNP	Garcia-Robledo et al. (2017)
Picophytoplankton	—	—	—	—	0.2260	SCM ODZ ETNP	Garcia-Robledo et al. (2017)
Picophytoplankton	—	—	—	—	0.6711	SCM ODZ ETNP	Garcia-Robledo et al. (2017)
Picophytoplankton	—	—	—	—	0.2785	SCM ODZ ETNP	Garcia-Robledo et al. (2017)
Picophytoplankton	—	—	—	—	0.2144	SCM ODZ ETNP	Garcia-Robledo et al. (2017)
Prochlorococcus	—	—	—	—	0.0150	ST. ALOHA, 75 m	Björkman et al. (2015)
Prochlorococcus	—	—	—	—	0.0650	ST. ALOHA, 75 m	Björkman et al. (2015)
Prochlorococcus	—	—	—	—	0.0038	North Atlantic, 60 m	Li (1994)
Prochlorococcus	—	—	—	—	0.0338	North Atlantic, 60 m	Li (1994)
Prochlorococcus	—	—	—	—	0.1013	North Atlantic, 1 m	Li (1994)
Prochlorococcus	—	—	—	—	0.1500	Northeast Atlantic, surface	Jardillier et al. (2010)
Prochlorococcus	—	—	—	—	0.0463	Atlantic Northern Gyre, 20 m	Hartmann et al. (2014)
Prochlorococcus	—	—	—	—	0.1063	Atlantic equatorial region, 20 m	Hartmann et al. (2014)
Prochlorococcus	—	—	—	—	0.0550	Atlantic Southern Gyre, 20 m	Hartmann et al. (2014)
Prochlorococcus	—	—	—	—	0.0625	Atlantic southern temperate waters, 20 m	Hartmann et al. (2014)
Synechococcus	—	—	—	—	0.0238	North Atlantic, 60 m	Li (1994)
Synechococcus	—	—	—	—	0.1025	North Atlantic, 60 m	Li (1994)
Synechococcus	—	—	—	—	0.9600	North Atlantic, 1 m	Li (1994)
Synechococcus	—	—	—	—	0.4250	Northeast Atlantic, surface	Jardillier et al. (2010)
Synechococcus	—	—	—	—	2.1375	Northeast Atlantic, surface	Jardillier et al. (2010)
Synechococcus	—	—	—	—	0.6188	Atlantic Northern Gyre, 20 m	Hartmann et al. (2014)
Synechococcus	—	—	—	—	0.8338	Atlantic equatorial region, 20 m	Hartmann et al. (2014)
Synechococcus	—	—	—	—	0.5675	Atlantic Southern Gyre, 20 m	Hartmann et al. (2014)
Synechococcus	—	—	—	—	0.2800	Atlantic Southern temperate waters, 20 m	Hartmann et al. (2014)

between $\delta^{15}N$ of *Prochlorococcus* with NO_3^- concentration might be explained by the isotope discrimination during the NO_3^- assimilation. In general, at the top of the ODZ, where the SCM is developed, the NO_3^- concentration is always high, although variable among stations. At lower NO_3^- concentrations, the NO_3^- remaining would be enriched in ^{15}N due to fractionation during assimilation, enriching the signal in *Prochlorococcus* that are still assimilating this NO_3^-. This possibility is supported by the results of $\delta^{15}N$ for *Prochlorococcus* in the coastal Sta. BB2 where the SCM is shallower (68–88 m depth) and the concentration of NO_3^- is lower compared with the oceanic stations where the SCMs are found at greater depths with higher concentration of NO_3^- (*see* Supporting Information Fig. S3). In the case of *Synechococcus*-like, $\delta^{15}N$ did not have any significant correlations with either the percentage of light or the concentrations of nutrients. In summary, our $\delta^{15}N$ natural abundance data from sorted groups of *Prochlorococcus* and *Synechococcus*-like suggest that these groups are using a mixture of different sources of N, mainly as NH_4^+ and urea, while in some instances NO_2^- or NO_3^- may be used preferentially to satisfy their N requirements.

Nitrogen assimilation rates

The cell-specific uptake rates of oxidized and reduced N forms for the different sorted groups (*Prochlorococcus*, *Synechococcus*-like and NFP) were compared with total N uptake rates reported for picophytoplankton in several study sites (Table 5). The results indicate that *Prochlorococcus* and *Synechococcus*-like are using NO_3^- and NO_2^- in the SCM at extremely low rates for their N requirements and that the potential rates for NH_4^+ and urea are comparable at least to some of the study sites listed in Table 5. It is also important to point out that this list in Table 5 shows high variability in the uptake rates (*see* Garcia-Robledo et al. 2017 for measurements for different stations in the SCM) and that our results are within this variability. The uptake rates obtained for the reduced N forms also support the data obtained for the natural abundance values of $\delta^{15}N$, where most of the natural abundance data for the picocyanobacteria were consistent with the $\delta^{15}N$ of NH_4^+/urea or a mixture of these sources including NO_3^- and NO_2^-. However, the results here are not yet sufficient to provide understanding of what controls the use of the different N sources.

Our results indicate that although ODZ *Prochlorococcus* have retained the capacity to use NO_3^- (Astorga-Eló et al. 2015; Widner et al. 2018*a*), they appear not to rely on NO_3^- as a principal N source. This suggests that ODZ *Prochlorococcus* are not under the high pressure for genome streamlining that other picocyanobacterial lineages experience. These findings are consistent with the basal characteristic of ODZ *Prochlorococcus* lineages linking this group with marine *Synechococcus* (Lavin et al. 2010), which has also not experienced significant genome streamlining (Dufresne et al. 2005; Partensky and Garczarek 2010). Thus, the ecological and evolutionary basis for the apparently strong niche preference of the ODZ *Prochlorococcus* for the low-light anoxic conditions of the SCM remains mysterious.

Implications for the ODZs

The fate of all nitrogen sources taken up by cyanobacteria is to be metabolized to NH_4^+, which is finally incorporated into the carbon backbones through glutamine synthetase-glutamate synthetase pathway, a key step to conversion from inorganic N forms to organic N forms such as amino acids or nucleic acids (García-Fernández and Diez 2004; Flores and Herrero 2005). Since all N sources other than NH_4^+ require intracellular conversion to NH_4^+, it is usually assumed that the most reduced forms of N (NH_4^+, urea, amino acids) will be the preferred N sources by cyanobacteria, as they require a lower energy expenditure for use. This is even more important in zones where the energy available is limited, as in the SCM (< 0.1% of the incident light) and where the oxidized N sources are abundant and the reduced ones are scarce. Then the selection of one or another N source is a balance between the energy needed to utilize that source and N availability in the environment.

ODZs present an active N cycle where processes like denitrification, anammox, and nitrification are known for the use and/or production of different forms of N (Lam and Kuypers 2011; Stewart et al. 2012). The low NH_4^+ concentrations have been explained by a coupling between the NH_4^+ produced during organic matter respiration by heterotrophic denitrification and a high anammox activity that converts NH_4^+ to N_2 (Richards et al. 1965; Devol 2003). However, it has recently been demonstrated that ODZ *Prochlorococcus* can contribute to aerobic metabolisms in the ODZs, such as nitrification and aerobic organic matter oxidation, through cryptic O_2 production in these zones (Garcia-Robledo et al. 2017). In that study, (meta)transcriptional analysis indicated a low anammox activity (possibly inhibited by *Prochlorococcus* O_2 production) and high NO_2^- and organic matter oxidation. These results can be interpreted as a possible NH_4^+ production due to organic matter oxidation, a decreased NH_4^+ consumption by the anammox bacteria and/or archaea (low transcripts), leaving available NH_4^+ for *Prochlorococcus* assimilation with no accumulation of NH_4^+ in the water column and explaining the high uptake rates of reduced N forms. However, NH_4^+ is still scarce, so NO_2^-, which is most abundant in the SCM, could represent the source of N needed for at least a percentage of the group of *Prochlorococcus* inhabiting the ODZ. Therefore, the uptake of NO_2^- by *Prochlorococcus* would mean an eventual competition for this nutrient with the highly active nitrite oxidizing bacteria in the SCM (Garcia-Robledo et al. 2017).

Conclusions

In summary, our results suggest that ODZ *Prochlorococcus* cyanobacteria are using a mixture of reduced and oxidized forms of N to satisfy their requirements. Nevertheless when NH_4^+ and urea are available, *Prochlorococcus* preferentially use

those nutrients even though their genetic repertoire permits the use of oxidized forms. The selection of reduced forms of N can be explained by the low energy needed to assimilate those N forms, important in the SCM (<0.1% of the incident light), but not for the availability of these nutrients in the SCM since they are scarce in ODZ. Perhaps the oxygen production by *Prochlorococcus* is stimulating aerobic respiration by heterotrophic bacteria and producing the NH_4^+ that *Prochlorococcus* needs with no accumulation in the SCM. Finally, our results suggest that ODZ picocyanobacteria might thus represent potential competitors with anammox bacteria or ammonia-oxidizing archaea for NH_4^+ and/or with nitrite oxidizing bacteria for NO_2^-.

References

Astorga-Eló, M., S. Ramírez-Flandes, E. F. DeLong, and O. Ulloa. 2015. Genomic potential for nitrogen assimilation in uncultivated members of *Prochlorococcus* from an anoxic marine zone. ISME J. **9**: 1264–1267. doi:10.1038/ismej.2015.21

Batmalle, C. S., H.-I. Chiang, K. Zhang, M. W. Lomas, and A. C. Martiny. 2014. Development and bias assessment of a method for targeted metagenomic sequencing of marine cyanobacteria. Appl. Environ. Microbiol. **80**: 1116–1125. doi:10.1128/AEM.02834-13

Berges, J. A., and M. R. Mulholland. 2008. Enzymes and nitrogen cycling, p. 1385–1444. *In* D. G. Capone, D. A. Bronk, M. R. Mulholland, and E. J. Carpenter [eds.], Nitrogen in the marine environment. Academic Press. doi:10.1016/B978-0-12-372522-6.00032-3

Berube, P. M., and others. 2015. Physiology and evolution of nitrate acquisition in *Prochlorococcus*. ISME J. **9**: 1195–1207. doi:10.1038/ismej.2014.211

Biller, S. J., P. M. Berube, D. Lindell, and S. W. Chisholm. 2014. *Prochlorococcus*: The structure and function of collective diversity. Nat. Rev. Microbiol. **13**: 13–27. doi:10.1038/nrmicro3378

Björkman, K. M., M. J. Church, J. K. Doggett, and D. M. Karl. 2015. Differential assimilation of inorganic carbon and leucine by *Prochlorococcus* in the oligotrophic North Pacific Subtropical Gyre. Front. Microbiol. **6**: 1–14. doi:10.3389/fmicb.2015.01401

Casciotti, K. L., and M. R. McIlvin. 2007. Isotopic analyses of nitrate and nitrite from reference mixtures and application to Eastern Tropical North Pacific waters. Mar. Chem. **107**: 184–201. doi:10.1016/j.marchem.2007.06.021

Casey, J. R., M. W. Lomas, J. Mandecki, and D. E. Walker. 2007. *Prochlorococcus* contributes to new production in the Sargasso Sea deep chlorophyll maximum. Geophys. Res. Lett. **34**: 1–5. doi:10.1029/2006GL028725

Chisholm, S. W. 1992. Phytoplankton size, p. 213–237. *In* P. G. Falkowski, A. D. Woodhead, and K. Vivirito [eds.], Primary productivity and biogeochemical cycles in the sea. Environmental science research, v. **43**. Springer. doi:10.1007/978-1-4899-0762-2_12

Devol, A. H. 2003. Nitrogen cycle: Solution to a marine mystery. Nature **422**: 575–576. doi:10.1038/422575a

Dufresne, A., L. Garczarek, and F. Partensky. 2005. Accelerated evolution associated with genome reduction in a free-living prokaryote. Genome Biol. **6**: R14. doi:10.1186/gb-2005-6-2-r14

Dugdale, R. C., and F. P. Wilkerson. 1986. The use of ^{15}N to measure nitrogen uptake in eutrophic oceans; experimental considerations. Limnol. Oceanogr. **31**: 673–689. doi:10.4319/lo.1986.31.4.0673

Fawcett, S. E., M. W. Lomas, J. R. Casey, B. B. Ward, and D. M. Sigman. 2011. Assimilation of upwelled nitrate by small eukaryotes in the Sargasso Sea. Nat. Geosci. **4**: 717–722. doi:10.1038/ngeo1265

Flombaum, P., and others. 2013. Present and future global distributions of the marine cyanobacteria *Prochlorococcus* and *Synechococcus*. Proc. Natl. Acad. Sci. USA **110**: 9824–9829. doi:10.1073/pnas.1307701110

Flores, E., and A. Herrero. 2005. Nitrogen assimilation and nitrogen control in cyanobacteria. Biochem. Soc. Trans. **33**: 164–167. doi:10.1042/BST0330164

Fuchsman, C. A., A. H. Devol, K. L. Casciotti, C. Buchwald, B. X. Chang, and R. E. A. Horak. 2018. An N isotopic mass balance of the Eastern Tropical North Pacific oxygen deficient zone. Deep-Sea Res. Part II Top. Stud. Oceanogr. **156**: 137–147. doi:10.1016/j.dsr2.2017.12.013

Fuhrman, J. 2003. Genome sequences from the sea. Nature **424**: 1001–1002. doi:10.1038/4241001a

García-Fernández, J. M., N. T. de Marsac, and J. Diez. 2004. Streamlined regulation and gene loss as adaptive mechanisms in *Prochlorococcus* for optimized nitrogen utilization in oligotrophic environments. Microbiol. Mol. Biol. Rev. **68**: 630–638. doi:10.1128/MMBR.68.4.630-638.2004

García-Fernández, J. M., and J. Diez. 2004. Adaptive mechanisms of nitrogen and carbon assimilatory pathways in the marine cyanobacteria *Prochlorococcus*. Res. Microbiol. **155**: 795–802. doi:10.1016/j.resmic.2004.06.009

Garcia-Robledo, E., C. C. Padilla, M. Aldunate, F. J. Stewart, O. Ulloa, A. Paulmier, G. Gregori, and N. P. Revsbech. 2017. Cryptic oxygen cycling in anoxic marine zones. Proc. Natl. Acad. Sci. USA **114**: 8319–8324. doi:10.1073/pnas.1619844114

Garside, C. 1982. A chemiluminescent technique for the determination of nanomolar concentrations of nitrate and nitrite in seawater. Mar. Chem. **11**: 159–167. doi:10.1016/0304-4203(82)90039-1

Goericke, R., R. Olson, and A. Shalapyonok. 2000. A novel niche for *Prochlorococcus* sp. in low-light suboxic environments in the Arabian Sea and the Eastern Tropical North Pacific. Deep-Sea Res. Part I Oceanogr. Res. Pap. **47**: 1183–1205. doi:10.1016/S0967-0637(99)00108-9

Granger, J., D. M. Sigman, M. M. Rohde, M. T. Maldonado, and P. D. Tortell. 2010. N and O isotope effects during nitrate assimilation by unicellular prokaryotic and eukaryotic

plankton cultures. Geochim. Cosmochim. Acta **74**: 1030–1040. doi:10.1016/j.gca.2009.10.044

Hamersley, M. R., and others. 2007. Anaerobic ammonium oxidation in the Peruvian oxygen minimum zone. Limnol. Oceanogr. **52**: 923–933. doi:10.4319/lo.2007.52.3.0923

Hartmann, M., P. Gomez-Pereira, C. Grob, M. Ostrowski, D. J. Scanlan, and M. V. Zubkov. 2014. Efficient CO_2 fixation by surface *Prochlorococcus* in the Atlantic Ocean. ISME J. **8**: 2280–2289. doi:10.1038/ismej.2014.56

Holmes, R. M., A. Aminot, R. Kerouel, B. A. Hooker, and B. J. Peterson. 1999. A simple and precise method for measuring ammonium in marine and freshwater ecosystems. Can. J. Fish. Aquat. Sci. **56**: 1801–1808. doi:10.1139/f99-128

Jardillier, L., M. V. Zubkov, J. Pearman, and D. J. Scanlan. 2010. Significant CO_2 fixation by small prymnesiophytes in the subtropical and tropical northeast Atlantic Ocean. ISME J. **4**: 1180–1192. doi:10.1038/ismej.2010.36

Johnson, Z. I., E. R. Zinser, A. Coe, N. P. McNulty, E. M. S. Woodward, and S. W. Chisholm. 2006. Niche partitioning among *Prochlorococcus* ecotypes along ocean-scale environmental gradients. Science **311**: 1737–1740. doi:10.1126/science.1118052

Kamennaya, N. A., and A. F. Post. 2011. Characterization of cyanate metabolism in marine *Synechococcus* and *Prochlorococcus* spp. Appl. Environ. Microbiol. **77**: 291–301. doi:10.1128/AEM.01272-10

Lam, P., and M. M. M. Kuypers. 2011. Microbial nitrogen cycling processes in oxygen minimum zones. Ann. Rev. Mar. Sci. **3**: 317–345. doi:10.1146/annurev-marine-120709-142814

Latysheva, N., V. L. Junker, W. J. Palmer, G. A. Codd, and D. Barker. 2012. The evolution of nitrogen fixation in cyanobacteria. Bioinformatics **28**: 603–606. doi:10.1093/bioinformatics/bts008

Lavin, P., B. González, J. F. Santibáñez, D. J. Scanlan, and O. Ulloa. 2010. Novel lineages of *Prochlorococcus* thrive within the oxygen minimum zone of the eastern tropical South Pacific. Environ. Microbiol. Rep. **2**: 728–738. doi:10.1111/j.1758-2229.2010.00167.x

Li, W. K. W. 1994. Primary production of prochlorophytes, cyanobacteria, and eucaryotic ultraphytoplankton: Measurements from flow cytometric sorting. Limnol. Oceanogr. **39**: 169–175. doi:10.4319/lo.1994.39.1.0169

Marie, D., F. Partensky, D. Vaulot, and C. Brussaard. 1999. Enumeration of Phytoplankton, Bacteria, and Viruses in Marine Samples, p. 11.11.1–11.11.15. In J.P.E.A Robinson [ed.], Current protocols in cytometry, suppl. 10. John Wiley & Sons Inc., New York. N.Y. doi:10.1002/0471142956.cy1111s10

Martiny, A. C., A. P. K. Tai, D. Veneziano, F. Primeau, and S. W. Chisholm. 2009. Taxonomic resolution, ecotypes and the biogeography of *Prochlorococcus*. Environ. Microbiol. **11**: 823–832. doi:10.1111/j.1462-2920.2008.01803.x

McIlvin, M. R., and K. L. Casciotti. 2011. Technical updates to the bacterial method for nitrate isotopic analyses. Anal. Chem. **83**: 1850–1856. doi:10.1021/ac1028984

Moore, L. R., G. Rocap, and S. W. Chisholm. 1998. Physiology and molecular phylogeny of coexisting *Prochlorococcus* ecotypes. Nature **393**: 464–467. doi:10.1038/30965

Moore, L. R., and S. W. Chisholm. 1999. Photophysiology of the marine cyanobacterium *Prochlorococcus*: Ecotypic differences among cultured isolates. Limnol. Oceanogr. **44**: 628–638. doi:10.4319/lo.1999.44.3.0628

Moore, L. R., A. F. Post, G. Rocap, and S. W. Chisholm. 2002. Utilization of different nitrogen sources by the marine cyanobacteria *Prochlorococcus* and *Synechococcus*. Limnol. Oceanogr. **47**: 989–996. doi:10.4319/lo.2002.47.4.0989

Owens, N. J. P. 1987. Natural variations in ^{15}N in the marine environment, p. 389–451. In J. H. S. Blaxter and A. J. Southward [eds.], Advances in Marine Biology. Academic Press Inc. London, Great Britain.

Partensky, F., J. Blanchot, and D. Vaulot. 1999*a*. Differential distribution and ecology of *Prochlorococcus* and *Synechococcus* in oceanic waters: A review. Bull. l'Institut océanographique **19**: 457–475.

Partensky, F., W. R. Hess, and D. Vaulot. 1999*b*. *Prochlorococcus*, a marine photosynthetic prokaryote of global significance. Microbiol. Mol. Biol. Rev. **63**: 106–127.

Partensky, F., and L. Garczarek. 2010. *Prochlorococcus*: Advantages and limits of minimalism. Ann. Rev. Mar. Sci. **2**: 305–331. doi:10.1146/annurev-marine-120308-081034

Peters, B., R. Horak, A. Devol, C. Fuchsman, M. Forbes, C. W. Mordy, and K. L. Casciotti. 2018. Estimating fixed nitrogen loss and associated isotope effects using concentration and isotope measurements of NO_3^-, NO_2^-, and N_2 from the Eastern Tropical South Pacific oxygen deficient zone. Deep-Sea Res. Part II Top. Stud. Oceanogr. **156**: 121–136. doi:10.1016/j.dsr2.2018.02.011

Peters, B. D., A. R. Babbin, K. A. Lettmann, C. W. Mordy, O. Ulloa, B. B. Ward, and K. L. Casciotti. 2016. Vertical modeling of the nitrogen cycle in the eastern tropical South Pacific oxygen deficient zone using high-resolution concentration and isotope measurements. Global Biogeochem. Cycles **30**: 1661–1681. doi:10.1002/2016GB005415

Revsbech, N. P., L. H. Larsen, J. Gundersen, T. Dalsgaard, O. Ulloa, and B. Thamdrup. 2009. Determination of ultra-low oxygen concentrations in oxygen minimum zones by the STOX sensor. Limnol. Oceanogr.: Methods **7**: 371–381. doi:10.4319/lom.2009.7.371

Richards, F. A., J. D. Cline, W. W. Bronkow, and L. P. Atkinson. 1965. Some consequences of the decomposition of organic matter in Lake Nitinat, an anoxic fjord. Limnol. Oceanogr. **10**: 185–201. doi:104319/lo.1965.10.suppl2.r185

Rocap, G., and others. 2003. Genome divergence in two *Prochlorococcus* ecotypes reflects oceanic niche differentiation. Nature **424**: 1042–1047. doi:10.1038/nature01947

Santoro, A. E., and others. 2013. Measurements of nitrite production in and around the primary nitrite maximum in the Central California Current. Biogeosciences **10**: 7395–7410. doi:10.5194/bg-10-7395-2013

Scanlan, D. J. 2003. Physiological diversity and niche adaptation in marine *Synechococcus*. Adv. Microb. Physiol. **47**: 1–64. doi:10.1016/S0065-2911(03)47001-X

Sigman, D. M., and K. L. Casciotti. 2001. Nitrogen isotopes in the ocean, p. 1884–1894. In J. H. Steele, K. K. Turekian, and S. A. Thorpe [eds.], Encyclopedia of Ocean Sciences. Academic Press Inc. London, Great Britain.

Sigman, D. M., K. L. Casciotti, M. Andreani, C. Barford, M. Galanter, and J. K. Böhlke. 2001. A bacterial method for the nitrogen isotopic analysis of nitrate in seawater and freshwater. Anal. Chem. **73**: 4145–4153. doi:10.1021/ac010088e

Stewart, F. J., O. Ulloa, and E. F. Delong. 2012. Microbial metatranscriptomics in a permanent marine oxygen minimum zone. Environ. Microbiol. **14**: 23–40. doi:10.1111/j.1462-2920.2010.02400.x

Thamdrup, B., T. Dalsgaard, M. M. Jensen, O. Ulloa, L. Farías, and R. Escribano. 2006. Anaerobic ammonium oxidation in the oxygen-deficient waters off northern Chile. Limnol. Oceanogr. **51**: 2145–2156. doi:10.4319/lo.2006.51.5.2145

Thamdrup, B., T. Dalsgaard, and N. P. Revsbech. 2012. Widespread functional anoxia in the oxygen minimum zone of the Eastern South Pacific. Deep-Sea Res. Part I Oceanogr. Res. Pap. **65**: 36–45. doi:10.1016/j.dsr.2012.03.001

Ulloa, O., D. E. Canfield, E. F. DeLong, R. M. Letelier, and F. J. Stewart. 2012. Microbial oceanography of anoxic oxygen minimum zones. Proc. Natl. Acad. Sci. USA **109**: 15996–16003. doi:10.1073/pnas.1205009109

Ward, B. B., A. H. Devol, J. J. Rich, B. X. Chang, S. E. Bulow, H. Naik, A. Pratihary, and A. Jayakumar. 2009. Denitrification as the dominant nitrogen loss process in the Arabian Sea. Nature **461**: 78–81. doi:10.1038/nature08276

Waser, N. A. D., P. J. Harrison, B. Nielsen, S. E. Calvert, and D. H. Turpin. 1998. Nitrogen isotope fractionation during the uptake and assimilation of nitrate, nitrite, ammonium, and urea by a marine diatom. Limnol. Oceanogr. **43**: 215–224. doi:10.4319/lo.1998.43.2.0215

West, N. J., W. A. Schönhuber, N. J. Fuller, R. I. Amann, R. Rippka, A. F. Post, and D. J. Scanlan. 2001. Closely related *Prochlorococcus* genotypes show remarkably different depth distributions in two oceanic regions as revealed by in situ hybridization using 16S rRNA-targeted oligonucleotides. Microbiology **147**: 1731–1744. doi:10.1099/00221287-147-7-1731

Widner, B., C. A. Fuchsman, B. X. Chang, G. Rocap, and M. R. Mulholland. 2018*a*. Utilization of urea and cyanate in waters overlying and within the eastern tropical north Pacific oxygen deficient zone. FEMS Microbiol. Ecol. **94**: 1–15. doi:10.1093/femsec/fiy138

Widner, B., C. W. Mordy, and M. R. Mulholland. 2018*b*. Cyanate distribution and uptake above and within the Eastern Tropical South Pacific oxygen deficient zone. Limnol. Oceanogr. **63**: S177–S192. doi:10.1002/lno.10730

Zhang, L., M. A. Altabet, T. Wu, and O. Hadas. 2007. Sensitive measurement of NH_4^+ $^{15}N/^{14}N$ ($\delta^{15}NH_4^+$) at natural abundance levels in fresh and saltwaters. Anal. Chem. **79**: 5297–5303. doi:10.1021/ac070106d

Zubkov, M. V., B. M. Fuchs, G. A. Tarran, P. H. Burkill, and R. Amann. 2003. High rate of uptake of organic nitrogen compounds by *Prochlorococcus* cyanobacteria as a key to their dominance in oligotrophic oceanic waters. Microbiology **69**: 1299–1304. doi:10.1128/AEM.69.2.1299

Acknowledgments

We would like to thank chief scientists Alan Devol (NPB1305), Frank Stewart (NH1410), and Amal Jayakumar (RB1603). We would also like to thank the captains, crews, and scientific support personnel of the R/V *Nathaniel B. Palmer*, the R/V *New Horizon*, the R/V *Atlantis*, and the R/V *Ronald Brown*. We also thank Gadiel Alarcón, Marguerite Blum, and Francisco Chavez for help with the PPS; Cristian Venegas for assistance with flow cytometry analysis; and Brian Peters and Karen Casciotti for $\delta^{15}NO_3^-$ isotope data from cruise AT2626. This study was financially supported by the Millennium Science Initiative (grant IC 120019), the Chilean National Commission for Scientific and Technological Research (grant Fondecyt 1161483 to O.U.; grants Conicyt-USA 20120014 and FONDEQUIP EQM130267 to P.v.D.; and a graduate fellowship to M.A.) the National Science Foundation (grant OCE-1356056 to MRM). Additional support has been provided by REDOC project of Universidad de Concepción.

Conflict of Interest

None declared.

Submitted 11 January 2019
Revised 21 June 2019
Accepted 10 August 2019

Associate editor: James Moffett

Supplementary information

Table S1. Flow cytometric analysis of the microbial community at the peak depth of the PCM for the ETNP and ETSP, including: cruise name; station; position (latitude and longitude); peak depth of the PCM reported in meters; the percent of incident light at the PCM peak depth (Light%); *Prochlorococcus* (*Pro*), S*ynechococcus* (*Syn*), Photosynthetic Picoeukaryotes (PPE), Total Fluorescent Picoplankton (Fluor. Picoplank.= *Pro*+*Syn*+PPE), non-fluorescent picoplankton (NFP) and total Picoplanctonic Comunity (Total Picoplank.= *Pro*+*Syn*+PPE+NFP) abundances ($x10^3$ cells ml^{-1}) at the peak depth; *Prochlorococcus* relative abundance to Fluor. Picoplank. and to Total Picoplank; Fluorescence of SCM relative to PCM. NA indicates data not available.

Table S1.

ETNP

Cruise	Station	Lat. (N)	Long. (W)	Peak depth at PCM (m)	Light (%)	*Pro* (10^3 cells ml^{-1})	*Syn* (10^3 cells ml^{-1})	PPE (10^3 cells ml^{-1})	Fluor. Picoplank. (10^3 cells ml^{-1})	NFP (10^3 cells ml^{-1})	Total Picoplank. (10^3 cells ml^{-1})	Pro Rel. Ab. to Fluor. Picoplak. (%)	Pro Rel. Ab. to Total Picoplank. (%)	Fluor. of SCM relative to PCM
NH1410	T9	18.200	105.199	40	2.00	47	15.8	4.8	67.2	534	668	69	7.0	1.30
RB1603	6	18.688	104.417	30	2.34	NA	NA	NA	NA	NA	NA	NA	NA	0.58
RB1603	7	17.500	102.700	49	3.27	NA	NA	NA	NA	NA	NA	NA	NA	0.72
RB1603	8	16.251	100.843	35	3.74	NA	NA	NA	NA	NA	NA	NA	NA	0.06
RB1603	9	15.000	99.000	45	3.30	NA	NA	NA	NA	NA	NA	NA	NA	0.20
RB1603	10	15.471	101.503	76	0.63	NA	NA	NA	NA	NA	NA	NA	NA	0.36
RB1603	11	15.903	103.800	78	2.47	123	6.4	3.5	133.1	805	1071	93	11.5	0.91
RB1603	12	16.316	106.092	95	1.26	243	1.9	0.4	245.4	866	1357	99	17.9	0.45
RB1603	13	16.778	108.397	69	2.89	157	0.8	7.4	165.2	1141	1472	95	10.7	0.17
Min				**30**		**47**	**0.8**	**0.43**	**67.16**	**534**	**668**	**69**	**7.0**	**0.06**
Max				**95**		**243**	**15.8**	**7.35**	**245.37**	**1141**	**1472**	**99**	**17.9**	**1.30**
Average				**57**		**142**	**6.2**	**4.02**	**152.70**	**836**	**1142**	**89**	**11.8**	**0.53**
SD				**23**		**81**	**7**	**3**	**74**	**249**	**358**	**13**	**5**	**0**

ETSP

Cruise	Station	Lat. (S)	Long. (W)	Peak depth at PCM (m)	Light (%)	*Pro* (10^3 cells ml^{-1})	*Syn* (10^3 cells ml^{-1})	PPE (10^3 cells ml^{-1})	Fluor. Picoplank. (10^3 cells ml^{-1})	NFP (10^3 cells ml^{-1})	Total Picoplank. (10^3 cells ml^{-1})	Pro Rel. Ab. to Fluor. Picoplak. (%)	Pro Rel. Ab. to Total Picoplank. (%)	Fluor. of SCM relative to PCM
NBP1305	H9	13.002	82.199	25	4.62	16	24.3	4.74	45.3	548	638	36	2.5	0.33
NBP1305	H21	21.500	70.582	23	16.21	15	4.5	9.26	28.7	415	472	52	3.2	0.33
NBP1305	BB2	20.526	70.712	24	6.65	8	28.5	16.87	52.9	869	975	14	0.8	0.18
AT2626	1	20.002	74.005	41	3.67	50	15.9	5.57	71.3	1206	1349	70	3.7	0.31
AT2626	3	18.798	76.200	35	3.53	38	33.3	8.71	79.9	1135	1295	47	2.9	1.91
AT2626	8	11.502	81.411	40	4.81	0	27	5.82	32.6	831	897	0	0.0	0.62
AT2626	9	11.999	84.001	34	9.12	0	30	7.97	37.7	431	507	0	0.0	0.36
AT2626	10	11.998	81.198	50	6.64	36	3	3.87	42.5	241	326	85	11.0	1.12
AT2626	12	12.545	77.593	25	6.24	0	31.1	4.28	35.4	371	441	0	0.0	0.15
AT2626	14	14.198	77.499	20	1.28	0	96.0	38.16	134.2	2862	3130	0	0.0	0.02
AT2626	18	15.591	75.335	29	0.58	0	8.3	24.40	32.7	750	815	0	0.0	0.39
Min				**20**		**0**	**2.6**	**3.87**	**28.7**	**241**	**326**	**0**	**0.0**	**0.02**
Max				**50**		**50**	**96.0**	**38.16**	**134.2**	**2862**	**3130**	**85**	**11.0**	**1.91**
Average				**31**		**15**	**27.4**	**11.79**	**53.9**	**878**	**986**	**28**	**2.2**	**0.52**
SD				**9**		**18**	**25.3**	**10.74**	**31.3**	**729**	**788**	**32**	**3.3**	**0.54**

Table S2. Summary of oceans, cruises, stations and type of chlorophyll maxima (PCM/SCM) sampled in this study and the isotopic analyses available in each one (in gray). δ^{15}N-PON$_{sus}$= δ^{15}N of suspended Particulate Organic Nitrogen; δ^{15}N-*Pro*= δ^{15}N of *Prochlorococcus*; δ^{15}N-*Syn*= δ^{15}N of *Synechococcus*; δ^{15}N-PPE= δ^{15}N of Photosynthetic Picoeukaryotes; δ^{15}N-NFP= δ^{15}N of non-fluorescent picoplankton.

Ocean	**Cruise**	**Station**	**PCM/SCM**	**δ^{15}N-PON$_{sus}$**	**δ^{15}N-*Pro***	**δ^{15}N-*Syn***	**δ^{15}N-PPE**	**δ^{15}N-NFP**
ETNP	NH1410	T9	PCM			x	x	
ETNP	NH1410	T9	SCM		x	x		
ETNP	RB1603	6	SCM	x				
ETNP	RB1603	7	SCM	x				
ETNP	RB1603	8	SCM	x				
ETNP	RB1603	9	PCM	x				
ETNP	RB1603	9	SCM	x				
ETNP	RB1603	10	SCM	x	x	x		x
ETNP	RB1603	11	SCM	x	x			x
ETNP	RB1603	12	PCM	x				
ETNP	RB1603	12	SCM	x				
ETNP	RB1603	13	SCM	x				
ETSP	NBP1305	H9	SCM	x				
ETSP	NBP1305	H21	SCM	x				
ETSP	NBP1305	BB2	SCM	x	x	x		
ETSP	AT2626	1	PCM		x	x	x	
ETSP	AT2626	3	PCM		x	x	x	
ETSP	AT2626	3	SCM		x	x		
ETSP	AT2626	8	PCM	x		x	x	x
ETSP	AT2626	8	SCM	x	x	x		
ETSP	AT2626	9	SCM		x	x		
ETSP	AT2626	10	SCM	x	x	x		
ETSP	AT2626	12	PCM	x		x	x	x
ETSP	AT2626	12	SCM	x	x	x		

Table S3. Summary statistics. Kruskal-Wallis and Steel-Dwass-Critchlow-Fligner test for the comparison among δ^{15}N-PON$_{sus}$, δ^{15}N-*Pro* and δ^{15}N-*Syn* for the SCM.

Summary statistics:

Variable	Observations	Obs. with missing data	Obs. without missing data	Minimum	Maximum	Mean	Std. deviation
SCM- δ^{15}N -PON$_{sus}$	14	0	14	4.347	16.620	9.225	3.865
SCM- δ^{15}N -*Pro*	14	5	9	-4.031	12.968	1.162	5.359
SCM- δ^{15}N -*Syn*	14	7	7	-3.992	8.122	0.854	4.272

Kruskal-Wallis test / Two-tailed test:

K (Observed value)	13.998
K (Critical value)	5.991
DF	2
p-value (one-tailed)	0.001
α	0.05

H0: The samples come from the same population
Ha: The samples do not come from the same population.

As the computed *p*-value is lower than the significance level ***α*** = 0.05, one should reject the null hypothesis H0, and accept the alternative hypothesis Ha.
The risk to reject the null hypothesis H0 while it is true is lower than 0.09%.

Multiple pairwise comparisons using the Steel-Dwass-Critchlow-Fligner procedure / Two-tailed test:

Sample	Frequency	Sum of ranks	Mean of ranks	Groups
SCM- δ^{15}N -*Syn*	7	69.000	9.857	A
SCM- δ^{15}N -*Pro*	9	89.000	9.889	A
SCM- δ^{15}N -PON$_{sus}$	14	307.000	21.929	B

Pairwise comparisons:

	SCM δ^{15}N -PON$_{sus}$	SCM δ^{15}N -*Pro*	SCM δ^{15}N -*Syn*
SCM- δ^{15}N -PON$_{sus}$		**4.365**	**4.326**
SCM- δ^{15}N -*Pro*	**-4.365**		-0.225
SCM- δ^{15}N -*Syn*	**-4.326**	0.225	

***p*-values:**

	SCM δ^{15}N -PON$_{sus}$	SCM δ^{15}N -*Pro*	SCM δ^{15}N -*Syn*
SCM- δ^{15}N -PON$_{sus}$	**1**	**0.006**	**0.006**
SCM- δ^{15}N -*Pro*	**0.006**	**1**	0.986
SCM- δ^{15}N -*Syn*	**0.006**	0.986	1

Table S4. Summary statistics and Wilcoxon test for the comparison between δ^{15}N-PCM-*Prochlorococcus* and δ^{15}N-SCM-*Prochlorococcus*.

Summary statistics:

Variable	Observations	Obs. with missing data	Obs. without missing data	Minimum	Maximum	Mean	Std. deviation
PCM-*Pro*	3	0	3	-6.544	3.266	-0.695	5.170
SCM-*Pro*	12	0	12	-4.387	12.968	0.728	4.766

Sign test / Two-tailed test:

N+	1
Expected value	1.500
Variance (N+)	0.750
p-value (Two-tailed)	1.000
α	0.05

The *p*-value is computed using an exact method.

Test interpretation:

H0: The two samples follow the same distribution.

Ha: The distributions of the two samples are different.

As the computed *p*-value is higher than the significance level α = 0.05, one should no reject the null hypothesis H0.

The risk to reject the null hypothesis H0 when is it true is 100.00%.

Wilcoxon signed-rank test / Two-tailed test:

V	2
Expected value	3.000
Variance (V)	3.500
p-value (Two-tailed)	0.789
α	0.05

An approximation has been used to compute the *p*-value.

Test interpretation:

H0: The two samples follow the same distribution.

Ha: The distributions of the two samples are different.

As the computed *p*-value is higher than the significance level α = 0.05, one should no reject the null hypothesis H0.

The risk to reject the null hypothesis H0 while is true is 78.93%.

Table S5. Detection limit for cell-specific (fg N $cell^{-1}$ h^{-1}) uptake rates of oxidized (NO_3^- and NO_2^-) and reduced (NH_4^+ and urea) N forms measured in this study for each group of sorted cells: non-fluorescent picoplankton (NFP), *Prochlorococcus* (*Pro*) and *Synechococcus*-like (*Syn*).

	Detection Limit: Cell-Specific uptake rates (fg N $cell^{-1}$ h^{-1})			
Group	**NO_3^-**	**NO_2^-**	***NH_4^+**	***Urea**
NFP	0.000040	0.000030	0.000010	0.000013
Pro	0.000029 SD= 0.000027	0.000021 SD= 0.000001	0.000012 SD= 0.000001	0.000017 SD= 0.000002
Syn	0.000069	0.000429 SD= 0.000002	0.000023	0.000048

Table S6. Pearson correlation coeficients between δ^{15}N-*Prochlorococcus* (δ^{15}N-*Pro*) and δ^{15}N-*Synechococcus*-like (δ^{15}N-*Syn*) and environmental variables. Variables included nutrient concentrations (NO_3^-, NO_2^-, NH_4^+) and percent incident light (Light%). Bold values are different from 0 with a significance level $\alpha = 0.05$

Variables	δ^{15}N-*Pro*	Light%	$[NO_3^-]$	$[NH_4^+]$	$[NO_2^-]$
δ^{15}N-*Pro*	**1**	0.321	**-0.819**	**0.723**	0.194
Light%	0.321	**1**	**-0.800**	0.612	0.699
$[NO_3^-]$	**-0.819**	**-0.800**	**1**	-0.569	-0.557
$[NH_4^+]$	**0.723**	0.612	-0.569	**1**	0.149
$[NO_2^-]$	0.194	0.699	-0.557	0.149	**1**

Table S7. Estimation of δ^{15}N-NH_4^+ and δ^{15}N-urea for the PCM and SCM in ODZs. The estimation was performed assuming that NH_4^+ and urea are regenerated nitrogen sources resulting from the degradation of the organic matter (PON_{sus}). The isotope fractionation factor associated to this process is $\varepsilon \leq 3$‰ (Sigman and Casciotti, 2001).

Ocean	Cruise	Station	Lat.	Long.	Peak depth at PCM (m)	PCM δ^{15}N-PON_{sus}	Estimated δ^{15}N-NH_4^+ and δ^{15}N-urea (PCM)	Peak depth at SCM (m)	SCM δ^{15}N-PON_{sus}	Estimated δ^{15}N-NH_4^+ and δ^{15}N-urea (SCM)
ETNP	RB1603	ST6	18.688	104.417	90				7.9	4.9
ETNP	RB1603	ST7	17.500	102.700	93				4.3	1.3
ETNP	RB1603	ST8	16.251	100.843	97				5.6	2.6
ETNP	RB1603	ST9	15.000	99.000	45	9.6	6.6	98	5.6	2.6
ETNP	RB1603	ST10	15.471	101.503				128	5.9	2.9
ETNP	RB1603	ST11	15.903	103.800				115	6.8	3.8
ETNP	RB1603	ST12	16.316	106.091	95	13.9	10.9	160	8.3	5.3
ETNP	RB1603	ST13	16.778	108.397				160	6.9	3.9
ETSP	NBP1305	Hydro 9	-13.002	-82.199				110	11.0	8.0
ETSP	NBP1305	Hydro 9	-12.992	-82.198				113	10.4	7.4
ETSP	NBP1305	Hydro 21	-21.500	-70.582				70	11.4	8.4
ETSP	NBP1305	BB2	-20.553	-70.732				74	14.6	11.6
ETSP	NBP1305	BB2	-20.449	-70.675				88	17.1	14.1
ETSP	NBP1305	BB2	-20.769	-70.659				68	17.4	14.4
ETSP	AT2626	ST 08	-11.499	-81.401	38	**6.6**	3.6	112	**13.1**	10.1
ETSP	AT2626	ST 10	-11.998	-81.198				117	5.9	2.9
ETSP	AT2626	ST 12	-12.545	-77.589	25	**5.2**	2.2	127	**15.2**	12.2
ETSP	AT2626	ST 14	-14.198	-77.499	20	**8.6**	5.6	78	**11.9**	8.9
ETSP	AT2626	ST 18	-15.591	-75.335	23	**9.8**	6.8	77	**13.3**	10.3
Av.						9.0	6.0		10.1	7.1
SD						3.0	3.0		4.2	4.2
min						5.2	2.2		4.3	1.3
max						13.9	10.9		17.4	14.4
n						6.0	6		19	19

Supplementary figures.

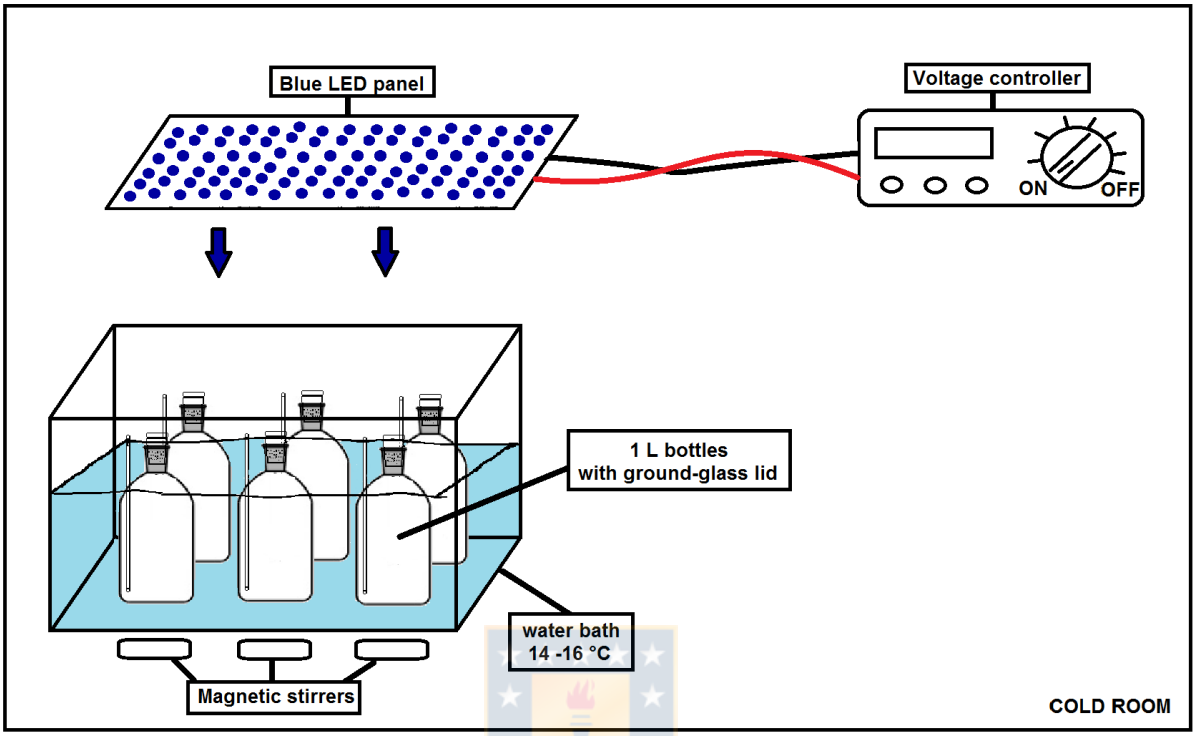

Figure S1. Experimental setup for N assimilation incubations. Standard Schott-Duran glass bottles were modified similar to the bottles used in Garcia-Robledo et al. 2017. Modifications included: 1) replacement of the screw cap with a ground-glass neck and cap. 2) the introduction of a long open glass tube (internal diameter 2.5 mm) for pressure compensation and for injection of tracers. These modified bottles were placed in a temperature controlled water bath. Blue LED lights were located over the incubator and the intensity was regulated using a voltage controller. Magnetic stirrers were installed below the water bath in order to keep the water of each bottle homogeneous.

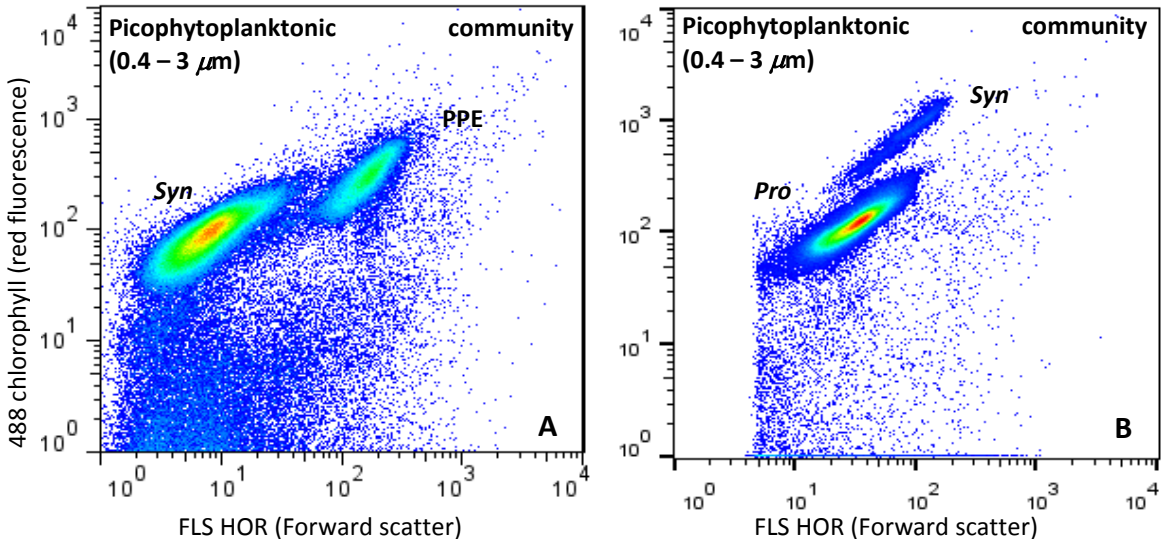

Figure S2. Typical cytogram showing autotrophic groups in samples taken from station 8 on cruise AT2626 (ETSP). The X axis (FLS HOR) represents the horizontal forward scatter and the Y axis (488 nm chlorophyll signal) represents red fluorescence. Picophytoplanktonic groups of interest are: *Synechococcus* (*Syn*), Photosyntetic Picoeukariotes (PPE) and *Prochlorococcus* (*Pro*). A) Primary chlorophyll maximum (PCM) B) Secondary chlorophyll maximum (SCM).

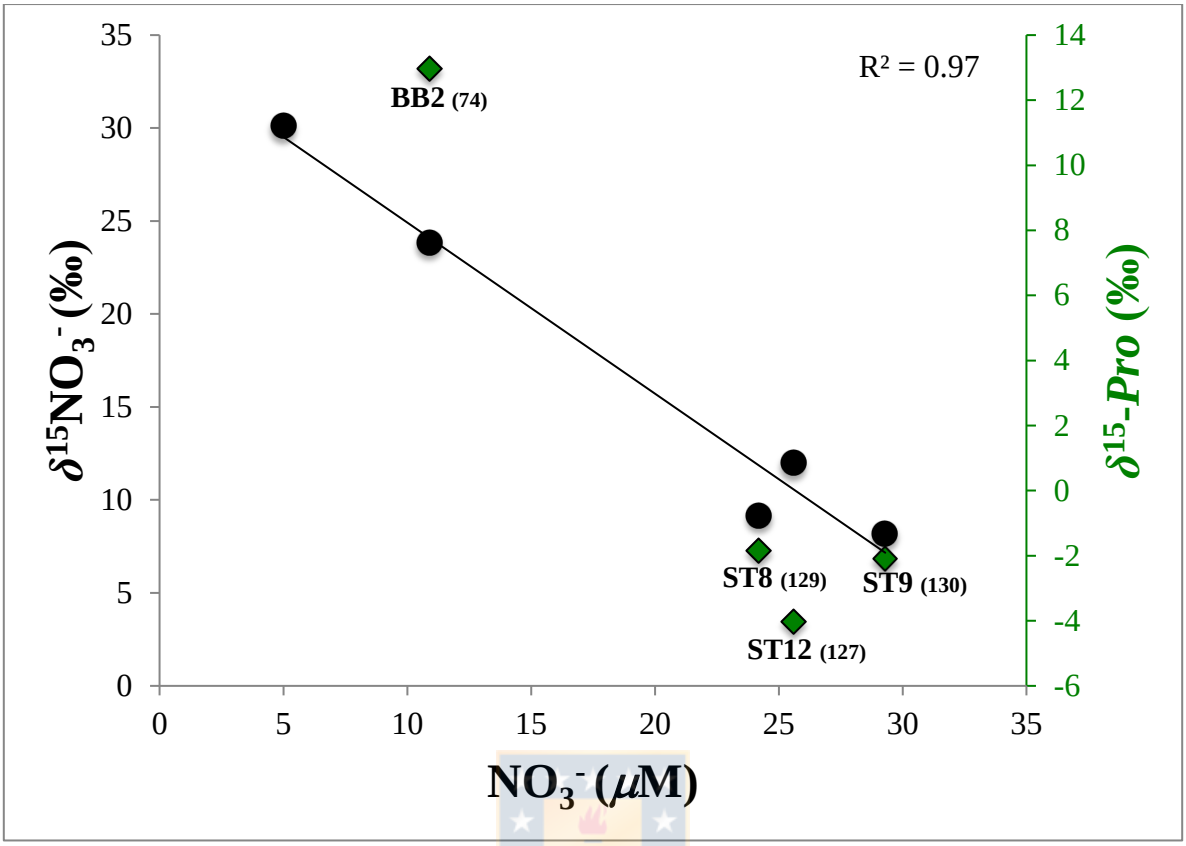

Figure S3. Dispersion plot showing the negative relationship beetween NO_3^- concentration and δ^{15}N-NO_3^- (black dots) for samples from the SCM in the ETSP: cruises NBP1305 (station BB2; data from Peters et al. 2016) and AT2626 (stations 8, 9 and 12; K. Casciotti pers. comm.). Green diamods represent the δ^{15}N values for sorted *Prochlorococcus* cells (δ^{15}N – *Pro*) in the same stations and depths. Numbers in parenthesis represent the sampling depths.

References

Peters, B. D., A. R. Babbin, K. A. Lettmann, C. W. Mordy, O. Ulloa, B. B. Ward, and K. L. Casciotti. 2016. Vertical modeling of the nitrogen cycle in the eastern tropical South Pacific oxygen deficient zone using high-resolution concentration and isotope measurements. Global Biogeochem. Cycles **30**: 1661–1681. doi:10.1002/2016GB005415

Sigman, D. M., and K. L. Casciotti. 2001. Nitrogen Isotopes in the Ocean, p. 1884–1894. *In* Encyclopedia of Ocean Sciences. Elsevier.

4.3. Capítulo 3. “Asimilación de cabono en la comunidad que habita el máximo secundario de clorofila de las zonas marinas anóxicas del Pacífico Norte y Sur oriental tropical”

Artículo científico en preparación para ser enviado a la revista “Frontiers in Marine Science”

Autores: **Montserrat Aldunate**, Peter von Dassow, Osvaldo Ulloa

Resumen

Las zonas marinas anóxicas (ZMAs) son zonas del océano que se distinguen de las zonas mínimas de oxígeno (ZMO) por la ausencia total de oxígeno detectable. En la parte superior de estas zonas, por debajo de la oxiclina, los nutrientes son abundantes y casi no existe luz (<1% luz incidente). En ciertos casos, se desarrolla un máximo de clorofila secundario (MSC), compuesto principalmente por dos ecotipos aún no cultivados de cianobacterias *Prochlorococcus* propios de las ZMAs. La gran abundancia de este grupo puede explicarse en parte por la presencia de divinil clorofila *a* (Chl a_2) como pigmento fotosintético principal, lo que los hace muy eficientes en la captura de energía solar. Sin embargo, algunos estudios genómicos sugieren una posible heterotrofia complementaria, importante debido a la posición de *Prochlorococcus* dentro de la columna de agua donde es probable que existan períodos con ausencia total de luz y, por lo tanto, falta de energía para realizar la fotosíntesis.

En este estudio utilizamos la abundancia isotópica natural del C ($\delta^{13}C$) de la comunidad picoplanctónica que habita el máximo primario y secundario de clorofila (MPC y MSC, respectivamente) complementado con tasas de asimilación de distintas fuentes de C para explorar el potencial mixotrófico de las cianobacterias *Prochlorococcus* de las ZMAs. Los resultados muestran que no hay diferencias significativas entre los valores de $\delta^{13}C$ del MSC del Pacífico Nor y Sur Oriental Tropical. Sin embargo, se encontraron diferencias significativas entre los valores de $\delta^{13}C$ entre la comunidad del MSC comparado con la que habita la parte superior de la ZMA sin desarrollo de SCM, lo que destaca la importancia que ejerce el picofitoplancton modificando el ciclo C en la capa superior de las ZMAs. Por otro lado, las tasas de asimilación de bicarbonato en el SCM fueron 28 veces más altas que las tasas de asimilación de glucosa durante las incubaciones con luz y 2 veces mayores durante las

incubaciones en oscuridad, indicando un importante rol de la luz, incluso en bajas intensidades, en las tasas de asimilación de C en el SCM. Además, no se identificaron patrones para las tasas de incorporación de acetato y no se detectó asimilación de cianato. Futuros estudios, que incorporen tasas de asimilación grupo-específicas serán importantes para determinar la importancia de cada grupo funcional que compone la comunidad SCM en las AMZ en el ciclo C.

Title: Carbon assimilation in the community inhabiting the secondary chlorophyll maximum of the anoxic marine zones of the Eastern tropical North and South Pacific.

Authors:

Montserrat Aldunate (maldunate@udec.cl)[1,2,3]

Peter von Dassow (pvondassow@bio.puc.cl)[3,4,5]

Osvaldo Ulloa (oulloa@udec.cl)[*1,3]

Affiliation:

[1]Departamento de Oceanografía, Universidad de Concepción, 4070386, Concepción, Chile.

[2]Programas de Postgrados en Oceanografía, Universidad de Concepción, 4070386, Concepción, Chile.
[3]Instituto Milenio de Oceanografía, Universidad de Concepción, 4070386, Concepción, Chile.

[4]Departmento de Ecología, Pontificia Universidad Católica de Chile, Santiago 8331150, Chile.

[5]UMI 3614, Evolutionary Biology and Ecology of Algae, Centre National de la Recherche Scientifique-UPMC Sorbonne Universités, PUCCh, UACH, Station Biologique de Roscoff, Roscoff, France.

**Corresponding author:*
Osvaldo Ulloa
Departamento de Oceanografía & Instituto Milenio de Oceanografía, Universidad de Concepción, Casilla 160-C, 4070386 - Concepción, Chile.
Phone number: (+56) 41 220 3585; Fax: (+56) 41 223 9900
e-mail: oulloa@udec.cl

Running head: Carbon metabolism in SCM AMZ.

Keywords: Carbon, SCM, AMZ, *Prochlorococcus*

Abstract

The anoxic marine zones (AMZs) are places in the ocean distinguished from other oxygen minimum zones (OMZs) by the complete absence of detectable oxygen. At the top of these zones, below the oxycline, nutrients are abundant and the light is almost absent (<1% of incident light). In certain cases, a secondary chlorophyll maximum (SCM) develops below the oxycline and is principally composed of two as yet uncultivated ecotypes of *Prochlorococcus* cyanobacteria found only in such waters. The great abundance of AMZ *Prochlorococcus* in the SCM can be explained in part by the presence of dyvinil chlorophyll *a* (Chl a_2) as the main photosynthetic pigment, very efficient in capturing solar energy at such depths. However, some genomic studies suggest a possible complementary heterotrophy for *Prochlorococcus* that would be very important due to their position within the water column where they are likely to experience long periods where the penetration of solar radiation is insufficient to perform photosynthesis.

In this study we compared measurements of $\delta^{13}C$ for particulate organic carbon (POC) from the primary and secondary chlorophyll maximum (PCM and SCM respectively) and also at the top of the AMZ layer when no SCM was present. We complemented these measurements with community C uptake rates experiments during five oceanographic cruises, in the Eastern Tropical North and South Pacific to explore the potential for mixotrophy of *Prochlorococcus* cyanobacteria, the most abundant picocyanobacteria in the SCM inhabiting the AMZs. Results shows that there are no significant differences between $\delta^{13}C$-POC from ETNP SCM vs. ETSP SCM. However, significant differences in $\delta^{13}C$-POC were found between SCMs and layers at comparative relative depths in AMZ where SCMs had not developed, highlighting the importance of picophytoplankton modifying the C cycle at the top of AMZ. In addition, bicarbonate uptake rate in the SCM exceeded uptake of glucose by 28-fold during light incubations and 2-fold during dark incubations. This last result highlights how community C and energy sources are still dominated by photoautotrophy in these very dimly lit waters. On other hand, no patterns were identified for acetate uptake rates and no uptake rates were detected for cyanate, coinciding with the fact that no genes associated to cyanate utilization have been found in AMZ *Prochlorococcus*. Incorporation of group-specific assimilation rates will be important in order to determine the importance to the C cycle of each functional group composing the SCM community in AMZs.

Introduction

The anoxic marine zones (AMZs) are places in the ocean distinguished from other oxygen minimum zones (OMZs) by the accumulation of nitrite and the complete absence of detectable oxygen using the most sensitive detectors such as the STOX oxygen sensor (detection limits 1-10 nM; Revsbech et al. 2009; Thamdrup et al. 2012; Ulloa et al. 2012). At the top of these zones, below the oxycline, nutrients are abundant and light is very low (<1% of incident light), but in certain cases, a secondary chlorophyll maximum (SCM) developes below a chlorophyll minimum within the oxycline. This AMZ SCM is mainly composed by the picocyanobacteria *Prochlorococcus*, specifically by three low ligh lineages: LLIV, LLV and LLVI (the last two found only in the ZMAs and as yet have not been successfully cultivated). In addition, a much less abundant group of *Synechoccocus* is also present and no photosynthetic picoeukaryotes have been detected (Lavin et al. 2010).

The great abundance of AMZ *Prochlorococcus* in the SCM can be explained in part by the presence of dyvinil chlorophyll *a* (Chl a_2) as main photosynthetic pigment. This pigment would make *Prochlorococcus* LL lineages very efficient in capturing the blue light energy, the dominant spectrum of light at that depths, and in its ability to fix C by photosynthesis (Garcia-Robledo et al. 2017). However, due to their position within the water column, they are likely to frequently be transported by internal waves or turbulence to depths where too little sunlight penetrates to support photosyntesis.

Because there are currently no isolates for AMZ *Prochlorococcus* lineages, what is known about C metabolism is from a very few studies. AMZ *Prochlorococcus* has the ability to fix C by photosynthesis; this fixed carbon can be recycled through the microbial loop or exported to deeper areas within the ZMAs (Garcia-Robledo et al., 2017). However, a study based on experiments on growth rates of natural samples from the Arabian Sea suggests a possible complementary heterotrophy for *Prochlorococcus* (Johnson et al., 1999). This is reinforced by some genomic studies that have found that the expression of genes related to glucose utilization increases strongly after the addition of this C source in *Prochlorococcus* cultures (Gómez-Baena et al., 2008; Muñoz-Marín et al., 2013).

In this study we compared measurements of $\delta^{13}C$ for particulate organic carbon (POC) from the primary and secondary chlorophyll maximum (PCM and SCM respectively) and also the top of the AMZ layer when no SCM was present. We complemented these measurements

with C uptake rates experiments during five oceanographic cruises, in the Eastern Tropical North Pacific and Eastern Tropical South Pacific to explore the potential for mixotrophy of *Prochlorococcus* cyanobacteria, the major constituent of the SCM inhabiting the AMZs.

Materials and methods

Sampling site and field collection. Samples were obtained from the AMZs of the Eastern Tropical North (ETNP) and South Pacific (ETSP), during four cruises: NH1410 (May, 2014) and RB1603 (April, 2016) for the ETNP, and NBP1305 (June, 2013), AT2626 (January, 2015) and LowpHOx I (November, 2015) for the ETSP. Samples were taken from the Secondary Chlorophyll Maximum (SCM) using a pump profiler system (PPS). PPS instrument pumps water directly from the desired depth while profiling the water column with an attached CTD system (Seabird SBE-19 plus for ETNP and Seabird SBE-25 for ETSP), which provides continuous determinations of salinity, temperature, depth, as well as dissolved oxygen (Seabird SBE 43 oxygen sensor; all cruises) and in vivo fluorescence (WETStar for ETNP cruise and ECO-AFL/FL for ETSP cruises, both WET Labs fluorometers). Discrete nutrient samples were analyzed using standard colorimetric methods according to the manufacturers specifications and the fluorometric method of Holmes et al. (1999). In April 2016 (ETNP; cruise RB1603) seawater was pumped into the laboratory and connected to an auto analyzer for nutrients continuous profiles for NO_3^-, NO_2^-, and NH_4^+, binned to 1 measurement per second.

Incubation experiments. Natural abundance of $^{13}C/^{12}C$ in suspended particulate organic carbon (POC_{sus}; 0.3 – 3 μm size fraction) was determined by filtering 2-3 L of seawater though a 3-μm poresize polycarbonate membrane filter and collecting the microbial biomass on a pre-combusted (500ºC for 6 h) 0.3 μm glass fiber filter (Sterlitech GF-75; 0.3 μm nominal pore size). The GF-75 filters were dried onboard or frozen in liquid nitrogen. Once in the laboratory, GF-75 filters were fumed with HCl vapors for 8 h to drive off inorganic C and then dried and encapsulated in tin capsules for analysis at the University of California Davis Stable Isotope Facility. To determine uptake rates in incubation experiments using different C sources, water was collected in a 20-L glass bottle and purged for 20 min with a mixture of 800 ppm CO_2 balanced He in order to avoid any oxygen contamination during the sampling.

This water was siphoned to 6 – 12 custom-made incubation bottles (1.1 L) and each bottle placed in a water bath inside a temperature-controlled cold van (see diagram in Aldunate et al., 2019). The incubation conditions were set to simulate *in situ* temperature (ranging between 14 and 16 ºC depending of the station) and light (blue light with intensities of 10 – 30 μmol photons m^{-2} s^{-1}). Four different ^{13}C-labeled compounds (Cambridge Isotope Laboratories) were used to assess the potential C uptake rates in the SCM. Final concentrations represented enrichments of 14.9-20.3% for ^{13}C-HCO_3^-, 17.7% for ^{13}C-glucose, 83.8% for ^{13}C-cyanate and 16.5% for ^{13}C-acetate. After 12 h of incubation, the picoplankton from each bottle was concentrated by filtration as described above for $^{13}C/^{12}C$ natural abundance measurements.

C assimilation rates calculations. Assimilation rates ($\rho^{13}C$*;* mg C L^{-1} h^{-1}) were calculated for each C source using the equation (1) (Slawyk et al. 1977):

$$\rho^{13}\mathrm{C} = \frac{\left[\frac{(R_{\mathrm{POC}} - R_n) \times \left(\frac{\mathrm{POC}}{12 \times V_f}\right)}{R_{\mathrm{C}}}\right]}{T} \qquad (1)$$

Where R_{POC} represents the ^{13}C enrichment in the filter after incubation (atom %) and R_n represent the natural abundance of ^{13}C (atom %). POC represents the amount of particulate organic carbon recovered in the filter after incubation (µg), V_f represents the incubation volume and T indicates the incubation time (hours). The excess enrichment of the tracer after its addition at the beginning of the incubation is indicated by R_C (in %) and is calculated using the equation (2):

$$R_{\mathrm{C}} = \frac{\left[\left(\frac{V^{13}\mathrm{C} \times 13\mathrm{C}}{V_b}\right) + C_i \times C_a\right] \times 100}{C_i + \frac{V^{13}C \times 13\mathrm{C}}{Vb}} \qquad (2)$$

Where $V^{13}C$ represent the volume of the ^{13}C tracer solution added to the incubation bottle (0.5 mL). 13C represents the concentration in ^{13}C of the added tracer. C_i represents the concentration of the C source in the sample before tracer addition; C_a indicates the natural abundance of ^{13}C (in absolute value) and V_b is the volume of sample bottles (1.1 L).

When the tracer additions resulted in initial enrichments exceeding 50%, rates should be considered as potential uptake.

Statistical analysis. Statistical differences among δ^{13}C-POC from the ETNP SCM, the ETSP SCM and ETSP where there are no SCM were tested using Kruskal-Wallis test. Statistical significance was set at 0.05. Correlations between δ^{13}C POC from the ETNP and ETSP and environmental variables (nutrient concentrations, light %, etc) will be calculated using Pearson's correlation analysis. The variables will be logarithmic transformed as Log_{10} (X+1) and the Pearson's correlation coefficients will be tested for significance at α = 0.05 using XLStat software (AddinSoft SARL).

Results and Discusion

The structure of the water column at all experimental stations exhibited a SCM within the upper anoxic layer at average depths of 114 m for the ETNP and 100 m for the ETSP as shown in Aldunate et al. 2019. The SCM varied in intensity with a maximum fluorescence equaling or almost doubling that of the PCM at some stations. Only in the cruise LowpHOx-I were SCMs not detected in any station.

Previous studies showed that the SCM communities in anoxic subsurface waters differed consistently from those in oxic surface waters in both abundance and composition, with phytoplanktonic communities mainly composed of *Prochlorococcus* cells (Av. Rel. Ab. 93-97%) and to a lesser extent of *Synechococcus*-like cells (yellow/orange fluorescent) and with almost no detectable PPE (Lavin et al. 2010; Garcia-Robledo et al. 2017; Aldunate et al. 2019).

δ^{13}C of POC at the depth of the PCM and SCM

δ^{13}C-POC values are indicative of the sources of dissolved organic matter. The natural abundance δ^{13}C-POC in both the PCM and SCM in the ETNP and ETSP showed a high variability. For the PCM of the ETNP, the values ranged from -30.3‰ to -28.1‰ and the distribution of the data shows that 50% of the values (n = 7) ranged from -29.4‰ to -28.5‰, with a median of -28.7‰ and an average of -29.0‰. For the PCM of the ETSP the values ranged from -28.0‰ to -21.7‰ with the 50% of the values (n = 6) ranging from -27.7‰ to -

25.1‰, with a median of -27.4‰ and an average of -26.1‰. (Fig. 1 top panel). Meanwhile, for the SMC of the ETNP these values ranged from -31.1‰ to -23.9‰ with 50% of the data (*n* = 20) distributed between -30.4‰ and -27.3‰. In the case of the ETSP SCM these values ranged from -30.7‰ to -23.9‰ with 50% or the data (*n* = 11) between -29.5‰ and -24.6‰ with a median of -24.8‰ and an average of -26.7‰ (Fig. 1 bottom panel). In the case of the samples taken during LowpHOx-I cruise where no SCM was detected (ETSP no SCM), the samples were taken from the top of the AMZ anoxic layer and the values ranged from -31.0‰ to -28.1‰ and the distribution of the data shows that 50% of the values (*n* = 5) ranged from -30.6‰ to -30.1‰, with a median of -30.5‰ and an average of -30.0‰ (Fig. 1 bottom panel).

In general, ^{13}C-depleted POC values (-30 to -24‰) are indicative of terrestrial organic matter advected off the continental shelf, meanwhile ^{13}C-enriched values (-22 to -18‰) reflect surface ocean derived materials (Barros et al., 2010; Podlaska et al. 2012). However, AMZs are known to harbor a condiderable chemoautotrophic community including anammox bacteria and sulfur-oxidizers (Stevens & Ulloa, 2008) that strongly fractionate against ^{13}C, producing ^{13}C-depleted biomass (Schouten et al., 2004). The multiple-pairwise comparisons among δ^{13}C-PON for the ETNP SCM, the ETSP SCM and ETSP no-SCM, indicate that there are no significant differences between δ^{13}C-POC from ETNP SCM vs. ETSP SCM at a 95% confidence level. However, significant differences were found between δ^{13}C-POC from ETSP SCM vs. ETSP no SCM, with ETSP SCM being 3.3‰ on average heavier. Depleted ^{13}C values in the ETSP when no SCM was present could indicate a stronger chemoautotrophic activity compared with the values in the ETSP SCM. These results, highligh the importance of picocyanobacteria modifying the C cycle at the top of AMZ (Table 1).

Carbon assimilation rates.

Rates for bicarbonate, glucose, cyanate and acetate were calculated from uptake experiments in the SCM (Fig. 2) with more station and replicates performed for bicarbonate and glucose. Carbon fixation (bicarbonate assimilation) was always higher when light was applied, as expected from the known photosynthetic activity in the SCM (Garcia-Robledo et al. 2017). These rates were higher in the ETSP station ST8 (AT) compared with other stations in ETSP (NBP1305 cruise, stations H9, H21 and BB2) and could be probably explained by a more abundant population of *Prochlorococcus* reported for station ST8 (AT) (Aldunate et al. 2019). During dark incubation, C affixation rates were very low, but present, indicating

chemoautotrophic activity, probably associated with anammox or sulfur-oxidazing bacteria, especially at station ST12 (RB), where C fixation rates in light and dark were similar (Fig 1A).

Glucose and acetate are labile dissolved organic carbon (DOC) components in the ocean and their production have been related with the increase of primary productivity in oxic zones (Hansell & Carlson, 2001) and by fermerters in anaerobic environments (Chen et al. 2017). Glucose uptake has previously been used as a proxy for heterotrophic microbial activity (Carlson & Ducklow, 1996). Regarding our results, glucose assimilation was higher in the ETSP station ST6 (cruise AT2626) with no significant difference between light and dark incubations among stations (Fig. 2B). In the case of acetate, it has been shown that across the suboxic/anoxic interface of Cariaco Basin, when chemoautotrophic production was elevated, a broad zone of high acetate uptake rate observed, with organic carbon supply as one of the major factors controlling microbial acetate uptake in the water column (Ho et al. 2002). Our results show variable acetate uptake rate, with similar variability and magnitud to that shown by Ho et al. 2002, in suboxic/anoxic interface in Cariaco Basin. However, we only have three measurements and no pattern was identified (Fig. 2C). Finally, no uptake rates were detected for cyanate, similar to that shown by Widner et al. 2018 in some stations in the ETSP, suggesting that cyanate uptake is an episodic process that depends on its availability. This is also supported with the fact that no genes associated to cyanate utilization have been found at list in AMZ *Prochlorococcus*. When we compared bicarbonate and glucose uptake rates in the only station that we have with both measurements, the results showed that bicarbonate uptake rate in the SCM exceeded uptake of glucose by 28-fold during light incubations and 2-fold during dark incubations (Fig. 2D). This last highlights the importance of light (even if it is low) in C assimilation rates in the SCM. However, both the maximum glucose and acetate uptake rates exceeded C fixation rates, supporting that often the SCM is still a net heterotrophic system. As the non-fluorescent picoplankton represent the most abundant group (5.39×10^8 cell L^{-1}) compared with *Prochlorococcus* (5.53×10^7 cell L^{-1}) and *Synechococcus*-like cyanobacteria (1.05×10^7 cell L^{-1}) (Aldunate et al. 2019), it is expected that their total assimilation rates of C are higher that picophytoplankton, explaining why in most stations glucose assimilation rates were higher than inorganic C (Fig. 2).

Conclusions

δ^{13}C-POC natural abundance in both the PCM and SCM in the ETNP and ETSP showed a high variability. Significant differences were found between δ^{13}C-POC from ETSP SCM vs. ETSP no SCM, with ETSP SCM being 3.3‰ on average heavier. Depleted ^{13}C values in the ETSP when no SCM was present could indicate a stronger chemoautotrophic activity compared with more enriched values in the ETSP when SCM was present.

On the other hand, inorganic carbon fixation (bicarbonate assimilation) was always higher when light was applied, explained by the known photosynthetic activity in the SCM (Garcia-Robledo et al. 2017). These rates were higher in the ETSP station ST8 (AT) compared with other stations in ETSP (NBP1305 cruise, stations H9, H21 and BB2) and could be probably explained by a more abundant population of *Prochlorococcus* reported for station ST8 (AT) (Aldunate et al. 2019). During dark incubations, C fixation rates were very low, but present, indicating chemoautotrophic activity, probably associated with anammox or sulfuroxidazing bacteria. Glucose assimilation rates were higher in the ETSP station ST6, cruise AT2626 with no significant difference between light and dark incubations among stations and no pattern was identified for acetate uptake rates. In addition, comparison of bicarbonate and glucose uptake rates in the same station shows that bicarbonate uptake rate in the SCM exceeded uptake of glucose by 28-fold during light incubations and 2-fold during dark incubations. This last highlights the importance of light (even if it is low) in C assimilation rates in the SCM. However, both the maximum glucose and acetate uptake rates exceeded C fixation rates, supporting that often the SCM is still a net heterotrophic system. The incorporation of group-specific assimilation rates will be important in order to determine the importance in the C cycle of each functional group composing the SCM community in AMZs.

References

Aldunate, M., Henríquez-Castillo, C., Ji, Q., Lueders-Dumont, J., Mulholland, M. R., Ward, B. B., von Dassow, P. Ulloa, O. 2019. Nitrogen assimilation in picocyanobacteria inhabiting the oxygen-deficient waters of the eastern tropical North and South Pacific. Limnology and Oceanography. doi:10.1002/lno.11315

Barros, G. V., L. A. Martinelli, T. M. Oliveira Novais, J. P. H. B. Ometto, and G. M. Zuppi. 2010. Stable isotopes of bulk organic matter to trace carbon and nitrogen dynamics in an estuarine ecosystem in Babitonga Bay (Santa Catarina, Brazil). Sci. Total Environ. **408**: 2226–2232. doi:10.1016/j.scitotenv.2010.01.060

Carlson, C., and H. Ducklow. 1996. Growth of bacterioplankton and consumption of dissolved organic carbon in the Sargasso Sea. Aquat. Microb. Ecol. **10**: 69–85. doi:10.3354/ame010069

Chen, J., Hanke, A., Tegetmeyer, H. E., Kattelmann, I., Sharma, R., Hamann, E., … Strous, M. (2017). Impacts of chemical gradients on microbial community structure. *The ISME Journal*, *11*(4), 920–931. https://doi.org/10.1038/ismej.2016.175

Eek, K. M., A. L. Sessions, and D. P. Lies. 2007. Carbon-isotopic analysis of microbial cells sorted by flow cytometry. Geobiology **5**: 85–95. doi:10.1111/j.1472-4669.2006.00094.x

Garcia-Robledo, E., C. C. Padilla, M. Aldunate, F. J. Stewart, O. Ulloa, A. Paulmier, G. Gregori, and N. P. Revsbech. 2017. Cryptic oxygen cycling in anoxic marine zones. Proc. Natl. Acad. Sci. **114**: 8319–8324.doi:10.1073/pnas.1619844114

Gómez-Baena, G., A. López-Lozano, J. Gil-Martínez, J. M. Lucena, J. Diez, P. Candau, and J. M. García-Fernández. 2008. Glucose Uptake and Its Effect on Gene Expression in Prochlorococcus C.-H. Yang [ed.]. PLoS One **3**: e3416. doi:10.1371/journal.pone.0003416

Hansell, D. A., & Carlson, C. A. (2001). Marine dissolved organic matter and the carbon cycle. *Oceanography*, *14*(4), 41–49.

Hansman, R. L., and A. L. Sessions. 2016. Measuring the in situ carbon isotopic composition of distinct marine plankton populations sorted by flow cytometry. Limnol. Oceanogr. Methods **14**: 87–99. doi:10.1002/lom3.10073

Ho, T.-Y., Taylor, G. T., Astor, Y., Varela, R., Müller-Karger, F., & Scranton, M. I. (2004). Vertical and temporal variability of redox zonation in the water column of the Cariaco Basin: implications for organic carbon oxidation pathways. *Marine Chemistry*, *86*(1–2), 89–104. https://doi.org/10.1016/j.marchem.2003.11.002

Johnson, Z., M. L. Landry, R. R. Bidigare, S. L. Brown, L. Campbell, J. Gunderson, J. Marra, and C. Trees. 1999. Energetics and growth kinetics of a deep Prochlorococcus spp. population in the Arabian Sea. Deep Sea Res. Part II Top. Stud. Oceanogr. **46**: 1719–1743. doi:10.1016/S0967-0645(99)00041-7

Lavin, P., B. González, J. F. Santibáñez, D. J. Scanlan, and O. Ulloa. 2010. Novel lineages of *Prochlorococcus* thrive within the oxygen minimum zone of the eastern tropical South Pacific. Environ. Microbiol. Rep. **2**: 728–738. doi:10.1111/j.1758-2229.2010.00167.x

Munoz-Marin, M. d. C., I. Luque, M. V Zubkov, P. G. Hill, J. Diez, and J. M. Garcia-Fernandez. 2013. Prochlorococcus can use the Pro1404 transporter to take up glucose at nanomolar concentrations in the Atlantic Ocean. Proc. Natl. Acad. Sci. **110**: 8597–8602. doi:10.1073/pnas.1221775110

Podlaska, A., S. G. Wakeham, K. A. Fanning, and G. T. Taylor. 2012. Microbial community structure and productivity in the oxygen minimum zone of the eastern tropical North Pacific. Deep Sea Res. Part I Oceanogr. Res. Pap. **66**: 77–89. doi:10.1016/j.dsr.2012.04.002

Revsbech, N. P., L. H. Larsen, J. Gundersen, T. Dalsgaard, O. Ulloa, and B. Thamdrup. 2009. Determination of ultra-low oxygen concentrations in oxygen minimum zones by the STOX sensor. Limnol. Oceanogr. Methods **7**: 371–381.doi:10.4319/lom.2009.7.371

Rijpstra, I., S. Schouten, M. Strous, and others. 2017. Stable Carbon Isotopic Fractionations Associated with Inorganic Carbon Fixation by Anaerobic Ammonium-Oxidizing ... Stable Carbon Isotopic Fractionations Associated with Inorganic Carbon Fixation by Anaerobic Ammonium-Oxidizing Bacteria. **70**: 3785–3788. doi:10.1128/AEM.70.6.3785

Slawyk, G., Y. Collos, and J.-C. Auclair. 1977. The use of the 13 C and 15 N isotopes for the simultaneous measurement of carbon and nitrogen turnover rates in marine phytoplankton1. Limnol. Oceanogr. **22**: 925–932. doi:10.4319/lo.1977.22.5.0925

Stevens, H., and O. Ulloa. 2008. Bacterial diversity in the oxygen minimum zone of the eastern tropical South Pacific. Environ. Microbiol. **10**: 1244–1259. doi:10.1111/j.1462-2920.2007.01539.x

Thamdrup, B., T. Dalsgaard, and N. P. Revsbech. 2012. Widespread functional anoxia in the oxygen minimum zone of the Eastern South Pacific. Deep Sea Res. Part I Oceanogr. Res. Pap. **65**: 36–45.doi:10.1016/j.dsr.2012.03.001

Ulloa, O., D. E. Canfield, E. F. DeLong, R. M. Letelier, and F. J. Stewart. 2012. Microbial oceanography of anoxic oxygen minimum zones. Proc. Natl. Acad. Sci. **109**: 15996–16003.doi:10.1073/pnas.1205009109

Widner, B., Mordy, C. W., & Mulholland, M. R. (2018). Cyanate distribution and uptake above and within the Eastern Tropical South Pacific oxygen deficient zone. *Limnology and Oceanography*, *63*(S1), S177–S192. https://doi.org/10.1002/lno.10730

Acknowledgments

We would like to thank to the chief scientists whose invited to us to participate in the cruises included in this study: Bess Ward and Alan Devol (NPB1305) Frank Stewart (NH1410), Margaret Mulholland (AT2626 and RB1603; NSF OCE-1356056) and Amal Jayakumar (RB1603). We also would like to thank the captain and crew of the *R/V Nathaniel B. Palmer*, the *R/V New Horizon*, the *R/V Atlantis* and NOAA vessel *Ronald Brown* for their help with the sampling. We also want to thank to Gadiel Alarcón, Marguerite Blum and Francisco Chavez

for their help with the PPS and Cristian Venegas for flow cytometry analysis. This study was financially supported by the Millennium Science Initiative (grant IC 120019), the Chilean National Commision for Scientific and Technological Research (grant Fondecyt 1161483 to O.U. and a graduate fellowship to M.A.).

Figures and Tables

Figure 1. Boxplot of δ^{13}C natural abundance from POC (0.3 – 3.0 μm size fraction) samples taken during the ETNP and ETSP cruises. PCM indicates primary chlorophyll maximum (top panel), SCM indicates secondary chlorophyll maximum and no-SCM indicates samples taken at the top of the AMZ when no SCM was present (bottom panel). *n* is the number of measurements per group.

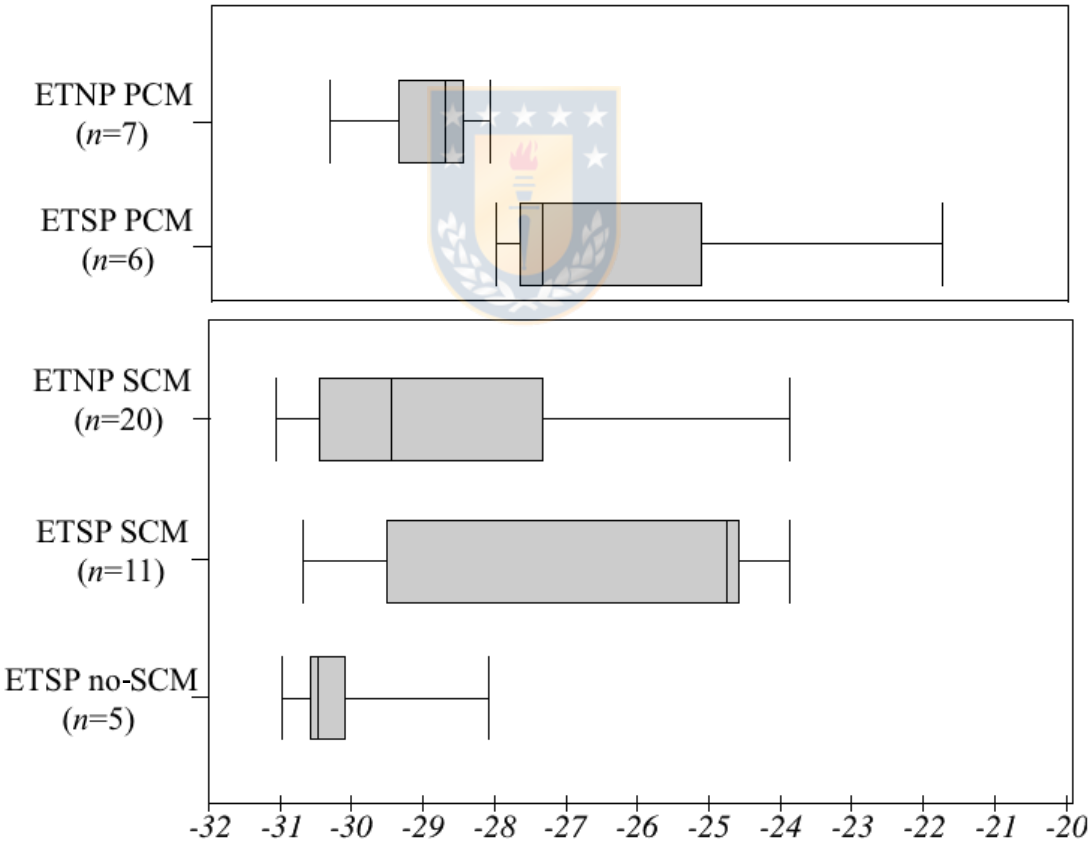

Figure 2. C assimilation rates for bicarbonate (A), glucose (B) and acetate (C) during light (grey bars) and dark (black bars) incubations for several stations at the depth of the SCM. X axis indicates the sampling station with the name of the cruise in parenthesis; NH is NH1410 cruise; RB is RB1603 cruise; AT is AT2626 cruise; NBP is NBP1305 cruise. C assimilation rates for bicarbonate and glucose (D) during light (grey bars) and dark (black bars) incubations for the SCM at the station F8 in the cruise NH1410.

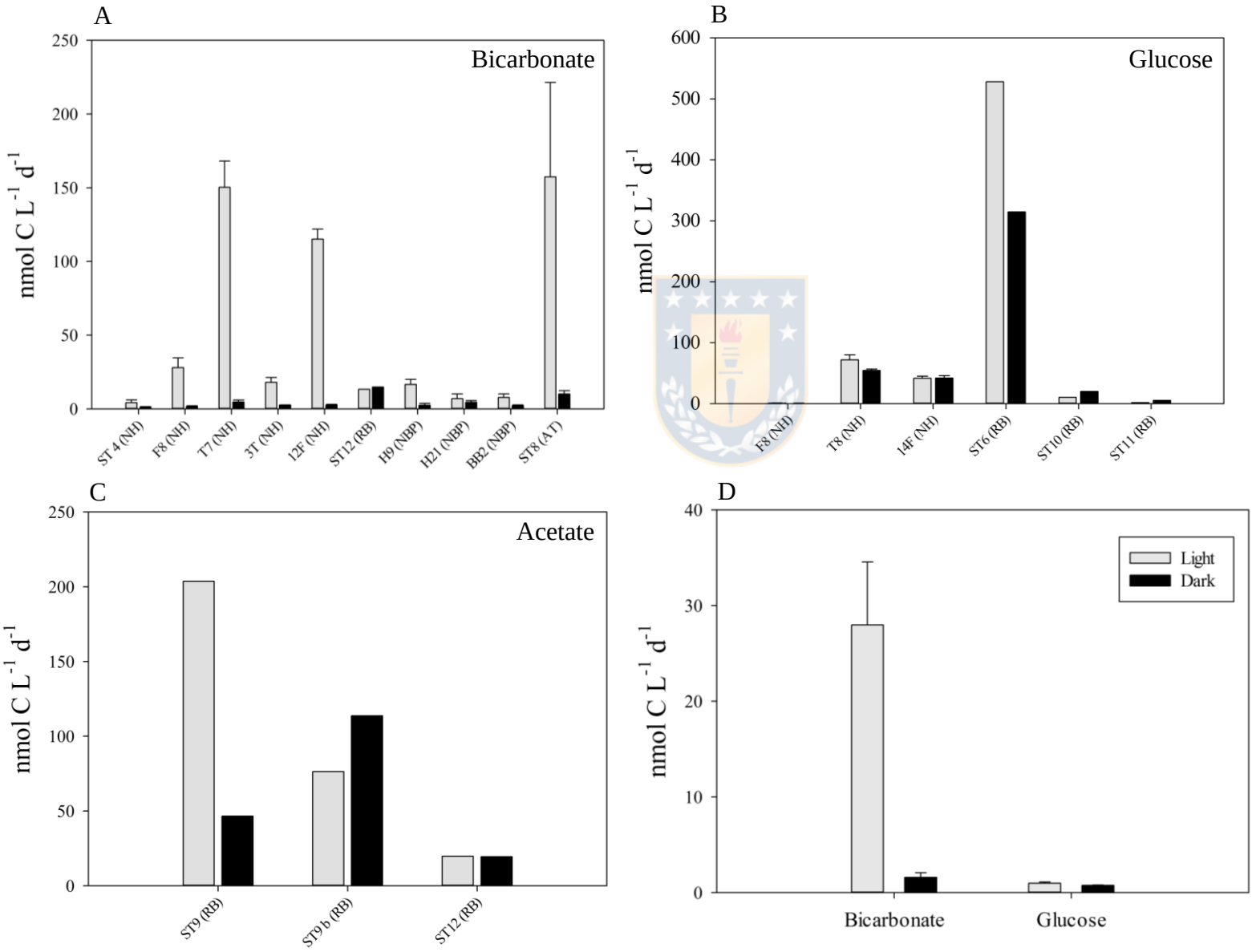

Table 1. Kruskal-Wallis test for the comparison among δ^{13}C-ETNP SCM, δ^{13}C-ETSP SCM and δ^{13}C-ETSP no-SCM.

Kruskal-Wallis test / Two-tailed test

K (observed value)	6.629
K (kritical value)	5.991
DF	2
p-value	0.036
alpha	0.05

Test interpretation:

H0: The samples are not significantly different.

Ha: The samples do not come from the same population.

As the computed p-value is lower than the significance level alpha = 0.05, one should reject the null hypothesis H0, and accept the alternative hypothesis Ha.

5. DISCUSIÓN

Picocianobacterias en las ZMAs

Las picocianobacterias son un grupo muy abundante de microorganimos importantes por representar aproximadamente un 25% de la productividad primaria marina (Flombaum et al. 2013). Estos microorganismos por lo tanto tienen importantes efectos en el ciclo global de los elementos como el O, el C y el N. Linajes no cultivados de la picocianobacteria *Prochlorococcus* habitan las ZMAs del océano Pacífico Nor y Sur oriental tropical (Lavin, et al. 2010). En estas ZMAs, el O_2 disuelto muestra condiciones de saturación en la superficie, bajo esta capa oxigenada se desarrolla una pronunciada oxiclina disminuyendo la concentración de oxígeno hasta niveles indetectables entre los 62 y 130 m de profundidad. Justamente, a la profundidad en que no se detecta O_2, se desarrolla un MSC, que en contraste con otras regiones del océano – escasas en nutrientes y saturadas en O_2 – se desarrolla en condiciones anóxicas y ricas en NO_3^-, pero con bajas concentraciones de N reducido como el NH_4^+ o la urea (Lavin et al. 2010; Widner et al. 2018a, Widner et al. 2018b).

El MSC del PNOT y el PSOT estuvo dominado numéricamente por *Prochlorococcus* y las cianobacterias tipo *Synechococcus* y casi no se detectaron PEF. La abundancia relativa de *Prochlorococcus* comparada con la comunidad picoplanctónica total fue consistente con los rangos previamente reportados (> 5,3%) (Lavin et al. 2010). Aparentemente este patrón es una característica persistente de este ambiente particular como se muestra en algunos estudios previos de estas ZMAs (Lavin et al. 2010; Astorga-Eló et al. 2015).

Aunque los linajes de *Prochlorococcus* y las picocianobacterias tipo *Synechococcus* que componen la comunidad del MSC no fueron analizados como parte de este estudio, ellos han sido previamente identificados utilizando un conjunto de análisis moleculares que incluyen clonación, secuenciación y análisis de huella genética aplicados al espaciador transcrito interno (ITS) de los genes 16S y 23S de ARNr (Lavin et al. 2010). Lavin y colaboradores encontraron que > 90% de los *Prochlorococcus* del MSC estuvo compuesto por los linajes LLIV y dos linajes nuevos llamados LLV y LLVI. Por otro lado, *Synechococcus* estuvo mayormente representado por los clados I y VI, pero con abundancia muy bajas.

Fotosíntesis oxigénica y fijación de carbono en el MSC

Los experimentos de incubación con muestras de la comunidad del MSC mostraron que la concentración de O_2 en el tiempo difiere sustancialmente entre las muestras incubadas con luz y oscuridad. La producción neta de la comunidad (NCP =balance entre la producción y consumo de O_2) incrementó gradualmente a medida que se incrementaba la irradianza. Además, esta producción neta de O_2 fue variable entre las estaciones de muestreo reflejando la variabilidad temporal y espacial de la actividad metabólica en términos de tasas de fotosíntesis y respiración. En algunas estaciones de muestreo, el consumo de O_2 neto ocurrió con todas las irradiancias aplicadas y con una clara disminución en las tasas de consumo cuando se incrementaba la luz. En otras estaciones, el incremento neto del O_2 fue medido cuando las muestras fueron expuestas a una irradiancia de 10 μmol fotones m^{-2} s^{-1}. Sin embargo, en la mayoría de las estaciones, la máxima irradiancia observada *in situ* estuvo en el rango de 2–5 μmol fotones m^{-2} s^{-1}; con esos niveles tan bajos de luz, un consumo neto de O_2 fue siempre observado.

Las tasas de producción bruta de O_2 (GCP-O_2 = NCP + respiración) fueron validadas midiendo simultáneamente la incorporación de carbono inorgánico en la biomasa microbiana (tasas de producción bruta de C o GCP-C = tasas de fijación de C). Ambas mediciones siguieron una curva clásica de fotosíntesis-irradianza con valores de producción bruta máxima (GCP-max) sobre las intensidades de saturación de la luz (E_k) de 10,5 ± 2,0 y 21,4 ± 9.3 μmol fotones m^{-2} s^{-1} (0,5 y 1% de luz incidente) para el PNOT y PSOT respectivamente. El bajo valor de E_k refleja la adaptación de *Prochlorococcus* a las bajas intensidades de luz ambiental siendo similares a los valores encontrados para la comunidad del MSC del Mar Arábigo (Johnson et al. 1999) o en ejemplares cultivados de *Prochlorococococcus* (Moore & Chisholm, 1999). Las intensidades de la luz en el MSC fueron variables y casi siempre sustancialmente bajo los 10 μmol fotones m^{-2} s^{-1}. En esas condiciones, las tasas de producción de O_2 son más bajas que la tasas de respiración y el O_2 producido es inmediatamente consumido por la comunidad microbiana, resultando en un ciclo críptico del O_2 en el ambiente aparentemente anóxico del MSC. Sin embargo, en algunas estaciones la irradianza fue similar a las intensidades de saturación de la luz (*Ek*), por lo que la detección ocacional de bajas concentraciones de O_2 en el MSC (Tiano et al. 2014, Ganesh et al. 2015) puede ser explicada por la actividad fotosintética en el MSC incrementando así las concentraciones de O_2 a niveles medibles.

Producción de O_2 y procesos microbianos

A pesar de que los niveles de O_2 son indetectables en el MSC, su producción es suficiente para mantener importantes metabolismos aeróbicos. Por medio de análisis metatranscriptómicos se detectaron transcritos que codifican para unas enzimas clave en el metabolismo aeróbico, las oxidasas terminales de alta y baja afinidad por el oxígeno (HATO y LATO respectivamente). Tanto las HATO como las LATO fueron detectadas en todas las profundidades, con un aumento en el número de secuencias en el MSC comparado con las muestras recolectadas por sobre (oxiclina) y por debajo (núcleo anóxico) del MSC, indicando la presencia de organismos que realizan respiración aeróbica.

El O_2 producido puede ser también consumido por vías metabólicas claves del ciclo del N en las ZMAs. Estudios previos han reportado que muy cerca del límite óxico/anóxico en las ZMAs existirían altas tasas de nitrificación autotrófica (oxidación de nitrito y amonio) (Galsgaard et al. 2012). En el estudio abordado en el capítulo 1 de esta tesis se encontraron transcritos afiliados a bacterias y arqueas oxidantes del amonio, aquellas que codifican la enzima amonio monooxigenasa –*amo*– que cataliza la reacción de oxidación del amonio aeróbicamente, alcanzando su máximo en la parte más alta de la oxiclina y disminuyendo su abundancia dentro del núcleo de la ZMA. En contraste, los transcritos de bacterias nitrito oxidantes, principalmente las del género *Nitrospina*, incrementaron dentro del MSC, coincidiendo en la mayoría de los casos con un enriquecimiento local en transcritos que codifican nitrito oxidoreductasas (*nxr*). Estos resultados, son apoyados por un estudio previo que muestra un aumento de las tasas potenciales de oxidación del nitrito (10,8 nmol N L^{-1} h^{-1}) en el MSC del PNOT las que representan el doble de la tasa de respiración máxima de O_2 medida en este estudio. Tomando en cuenta la estiquiometría de la oxidación de nitrito, podemos inferir entonces que la mayoría del consumo de O_2 medido puede ser debido a la oxidación de nitrito. Sin embargo, el balance entre el consumo heterotrófico de O_2 y el de las oxidantes de nitrito puede variar en función de la concentración real de O_2 medido para las distintas estaciones.

Metabolismo del C en el MSC

La variabilidad del MSC se ve reflejado también en sus valores de δ^{13}C-COP, mostrando una alta variabilidad tanto en el PNOT como en el PSOT. En el caso del crucero

LowpHOx-I (PSOT) donde no hubo desarrollo de un MSC, las muestras fueron recolectadas desde la parte superior de la capa anóxica, en la misma posición dentro de la columna de agua donde en otros momentos se desarrolla el MSC (zona anóxica justo por debajo de la oxiclina). Los valores de δ^{13}C-COP del PSOT, cuando no hubo desarrollo de un MSC, mostraron diferencias significativas cuando se compararon con los de los otros cruceros donde si hubo desarrollo de un MSC, siendo estos últimos 3.3‰ más pesados. Valores bajos de δ^{13}C-COP – en el caso del PSOT sin desarrollo de un MSC – indicarían una mayor actividad quimioautótrofa, debido a que los organismos quimioautótrofos (*e.g.* anammox, bacterias sulfuro oxidantes) fracccionan fuertemente en contra del isotopo más pesado, generando por lo tanto biomasa (COP) más liviana (Schouten et al. 2004). Así, estos resultados estarían corroborando la importancia del picofitoplancton modificando el ciclo del C en las ZMAs.

Por otro lado, las tasas de asimilación de distintas fuentes de C en el MSC indicaron que la fijación de C mediante fotosíntesis (experimentos con bicarbonato/luz) es el metabolismo preferido en el MSC. Sin embargo, existe una gran variabilidad en las tasas de fijación de C que estaría probablemente asociada a la abundancia de *Prochlorococcus*. Por ejemplo, en el caso de la estación ST8 (crucero AT2626) las mayores tasas de fijación de C coinciden con una población muy abudante de *Prochlorococcus* (Aldunate et al. 2019). Además, durante las incubaciones en oscuridad, las tasas de fijación de C fueron muy bajas, pero presentes, indicando actividad quimioautótrofa, probablemente asociada a bacterias anammox y sulfuro-oxidantes. En cuanto a las tasas de asimilación de glucosa, no se vieron diferencias significativas entre luz y oscuridad, siendo por lo tanto un proceso que podría eventualmente utilizar las picocianobacterias de las ZMAs en momentos de oscuridad. Sin embargo, estos resultados son tasas de la comunidad, por lo que no podemos diferenciar si esta asimilación de glucosa está siendo ejecutada por las picocianobacterias u otro componente del picoplancton del MSC.

Como el picoplancton no fluorescente representa el grupo más abundante de células (5,39 x10^8 células L^{-1}) en comparación con *Prochlorococcus* (5,53 x10^7 células L^{-1}) y las cianobacterias tipo *Synechococcus* (1,05 x10^7 células L^{-1}) (Aldunate et al. 2019), se espera que las tasas de asimilación de C para este grupo sean más altas que para el picofitoplancton. Sin embargo, no fue posible medir las tasas para grupos específicos dentro del MSC porque eso requiere experimentos con isótopos radiactivos, no siempre permitido en los buques de

investigación, o el uso de una técnica basada en isótopos estables que aún no se encuentra desarrollada completamente (Eek et al. 2007; Hansman & Sessions, 2015).

Metabolismo asimilativo del N en las picocianobacterias de las ZMAs

El destino de todas las fuentes de N tomada por las cianobacterias es ser metabolizadas a NH_4^+, el cual es finalmente incorporado a través de los esqueletos de carbono a través de la vía glutamina sintetasa – glutamato sintetasa, un paso clave en la conversión desde formas inorgánica de N hacia formas orgánicas de N como aminoácidos o ácidos nucleicos (García-Fernández & Diez, 2004; Flores & Herrero, 2005). Debido a que todas las fuentes de N diferentes al NH_4^+ requieren de una conversión intracelular a NH_4^+, es usualmente asumido que las formas reducidas de N (NH_4^+, urea, aminoácidos) serán las fuentes de N preferidas por las cianobacterias, debido a que ellas requieren un menor gasto energético para su uso. Esto es incluso más importante en zonas donde la energía disponible es limitada, como en el MSC (< 1% de luz incidente) y donde las fuentes de N oxidadas son abundantes y las reducidas escasas. Así, la selección de una u otra fuente de N es un balance entre la energía necesaria para utilizar esa fuente y la disponibilidad de esa fuente de N en el ambiente.

Las fuentes de N, además de encontrarse en distintas concentraciones en el ambiente, poseen distintas señales isotópicas, las que son transferidas a los organismos que las consumen. Cuando consideramos la comunidad picoplanctónica total que habita el MSC, representado por el PON_{sus}, se puede apreciar que la señal isotópica fue siempre positiva con valores de $\delta^{15}N$ altamente variables y que oscilan entre 4,3 y 16,6‰ (Fig. 3, capítulo 2). Valores de $\delta^{15}N$ relativamente altos, como los aquí presentados, pueden ser el resultado de la asimilación de alto $\delta^{15}N$ (como NO_3^-) o la liberación de bajo $\delta^{15}N$ (como en el caso de anammox o desnitrificación). Como los miembros de esta comunidad poseen distintos metabolismos, el $\delta^{15}N$-PON_{sus} para el MSC representa así una mezcla de los $\delta^{15}N$ de sus componentes los que pueden variar también entre distintas estaciones de muestreo. Aunque en el MSC hemos identificado un componente picofitoplanctónico muy abundante y consistente (*Prochlorococcus* y células tipo *Synechococcus*), esta comunidad también incluye bacterias y arqueas heterotróficas o quimiautotróficas (PNF) mucho más abundantes y que pueden variar dependiendo de la estación de muestreo (*e.g.* MSC en el PNOT vs PSOT o costero vs oceánico). Cambios en la composición del PNF puede producir diferencias en las preferencias

nutricionales de los miembros de bacterias y arqueas dominantes y de esta forma reflejarse en el δ^{15}N de la comunidad. Como el δ^{15}N-PON$_{sus}$ en el MSC presenta valores mucho más altos que los componentes aislados y analizados en esta tesis (*Prochlorococcus*, cianobacterias tipo *Synechococcus*, PNF; Fig. 3, capítulo 2), parte de la variabilidad presentada y la marca isotópica pesada puede ser explicada por la contribución de material particulado no vivo con un alto δ^{15}N. Esto puede ser el caso de las estaciones muestreadas en el PSOT, dónde las mediciones de δ^{15}N-PON$_{sus}$ del MSC exceden por 6,5‰, 10,0‰, 3,3‰ y 3,5‰ los valores medidos para el δ^{15}N-PON$_{sus}$ en el MPC (Tabla S7, capítulo 2). Así, las partículas que se hunden pueden estar degradándose por bacterias que prefieren partículas de bajo δ^{15}N dejando el PON residual enriquecido en ^{15}N. De acuerdo con esto, los resultados enfatizan la importancia del uso de citometría de flujo y el aislamiento de grupos celulares "cell-sorting" para distinguir los componentes vivos y muertos de la comunidad y su contribución a la marca isotópica del δ^{15}N total.

Los valores de δ^{15}N observados para las células aisladas de *Prochlorococcus* desde el MSC variaron de -4,0‰ a 13,0‰ (rango = 17‰), este rango es mayor y con δ^{15}N mucho más pesados que los datos previamente observados para las células de *Prochlorococcus* aisladas desde el Mar de los Sargazos que reportaron valores entre -4‰ y -1‰ (rango = 3‰) (Fawcett et al. 2011). La mayor variabilidad en los datos de *Prochlorococcus* del de las ZMAs puede deberse a que las concentraciones de nutrientes en las ZMAs son mucho más variables que en el Mar de los Sargazos, siendo este último un ambiente más estable con un grupo de *Prochlorococcus* que asimila preferentemente fuentes de N recicladas tales como NH_4^+ o aminoácidos (Fawcett et al. 2011). Los valores más altos observados (13.0‰) se vieron solo una vez en la estación más costera del PSOT (Crucero NBP1305, Estación BB2) y pueden ser explicados por el uso de NO_3^- como fuente principal de N (Table 3), mientras que los más bajos (-4,0‰) fueron observados en la estación más oceánica del PSOT (Crucero AT2626, Estación 8). Debido a que ni *Prochlorococcus* ni *Synechococcus* tienen los genes para fijar N_2 (Latysheva et al. 2012), los valores bajos pueden ser evidencia de asimilación de NO_2^-, debido a que el NO_2^- es la única fuente de N con valores de δ^{15}N negativos. El 50% de los valores de δ^{15}N observados para *Prochlorococcus* estuvieron en el rango de –2,1 y 2,6‰ (media de -0,6‰), sugiriendo que los *Prochlorococcus* del MSC en las ZMAs estarían mayormente asimilando una mezcla de fuentes de N, con valores positivos de δ^{15}N como el NH_4^+, urea y/o

NO_3^-, mientras que la asimilación de fuentes de N con valores negativos de $\delta^{15}N$ como el NO_2^- pueden estar disminuyendo el valor de $\delta^{15}N$ de las células. Similar a lo que pasa con *Prochlorococcus*, las células tipo *Synechococcus* aisladas desde el MSC de las ZMAs tienen valores de $\delta^{15}N$ que van desde -4,0‰ a 8,1‰ (rango = 12,1) y tienen un rango más amplio que las observadas en el Mar de Los Sargazos que van desde -3‰ a -1‰ (rango = 2) (Fawcett et al. 2011). Aparentemente ambas picocianobacterias tienen preferencias nutricionales similares en el MSC de las ZMAs.

En el MSC de las ZMAs no se observaron PEF, pero si se detectaron en el MPC con valores observados de $\delta^{15}N$ entre -0,3‰ y 2,4‰, con un 50% de los datos entre 0,5‰ y 1,2‰ (n = 5). Estos valores fueron un orden de magnitud más bajo que los reportados para los PEF del Mar de Los Sargazos a 100 m de profundidad ($\delta^{15}N$ =12,7‰), dónde los PEF parecen estar asimilando NO_3^- que aflora por debajo de la zona fótica, pero cercanos a los reportados a menores profundidades ($\delta^{15}N$ entre 1‰ y 5‰) dónde la mayoría del crecimiento del fitoplancton se cree es en base a NH_4^+ (Fawcett et al. 2011).

A pesar de los datos expuestos, aun queda la duda si la alta variabilidad en los valores de $\delta^{15}N$ para *Prochlorococcus* y las células tipo *Synechococcus* es explicada por los factores ambientales como la luz y/o la concentración de nutrientes. Se ha hipotetizado que una mayor disponibilidad de luz puede incrementar la probabilidad de que *Prochlorococcus* use NO_3^- debido a que tendría una mayor cantidad de energía disponible necesaria para su asimilación. Sin embargo, no hubo correlaciones significativas entre los valores de $\delta^{15}N$ y el porcentaje de luz incidente en el MSC, aunque si hubo una correlación negativa con la concentración de NO_3^- y positiva con el NH_4^+ (Table S6). Una correlación negativa entre el $\delta^{15}N$ de *Prochlorococcus* con la concentración de NO_3^- puede ser explicada por la discriminación isotópica durante la asimilación de NO_3^-. En general, en el límite superior de las ZMAs donde se desarrolla el MSC, la concentración de NO_3^- fue siempre alta, aunque variable entre estaciones de muestreo. A concentraciones menores de NO_3^-, el NO_3^- remanente se enriquece en ^{15}N debido al fraccionamiento durante la asimilación, enriqueciendo la señal en *Prochlorococcus* que aun está asimilando este nutriente. Esta posibilidad es apoyada por los resultados de $\delta^{15}N$ para *Prochlorococcus* en la estación costera BB2 donde el MSC fue más superficial (68 a 88 m de profundidad) y la concentración de NO_3^- fue más baja comparada con las estaciones oceánicas dónde los MSCs se encuentran a mayores profundidades con

concentraciones de NO_3^- más altas (Ver Fig. S3). En el caso de las células tipo *Synechococcus*, el $\delta^{15}N$ no tuvo ninguna correlación significativa ni con el porcentaje de luz ni con la concentración de nutrientes. En resumen nuestros datos de abundancia natural de $\delta^{15}N$ para las células aisladas de *Prochlorococcus* y tipo *Synechococcus* sugieren que estos grupos están utilizando una mezcla de diferentes fuentes de N, mayormente como el NH_4^+ y la urea, mientras que en ciertos casos el NO_2^- o NO_3^- pueden ser utilizados preferentemente para satisfacer sus requerimientos de N.

Estas conclusiones son apoyadas por las tasas de asimilación grupo específicas (*Prochlorococcus*, células tipo *Synechococcus* y PNF) de distintas formas de N (NH_4^+, urea NO_3^- y NO_2^-). Los resultados indican que *Prochlorococcus* y las células tipo *Synechococcus* están utilizando NO_3^- y NO_2^- en el MSC a tasas extremadamente bajas para sus requerimientos de N y que las tasas potenciales de asimilación de NH_4^+ y de urea son comparables con las tasas reportadas para el picofitoplancton de algunos sitios de estudio listados en la Tabla 5, capítulo 2. Es importante también indicar que los valores en la Tabla 5 muestran también una alta variabilidad en las tasas de asimilación (ver Garcia-Robledo et al. 2017 para las mediciones para diferentes estaciones en el MSC) y que nuestros resultados están dentro de esta variabilidad.

Implicancias para las ZMAs

Las ZMAs presentan un ciclo del N activo donde procesos como la desnitrificación, anammox y nitrificación son conocidos por usar y/o producir diferentes formas de N (Lam and Kuypers, 2011; Stewart et al. 2011). Las bajas concentraciones de NH_4^+ en estas zonas han sido explicadas por un acoplamiento entre el NH_4^+ producido durante la respiración de la materia orgánica a través de la desnitrificación heterotrófica y una alta actividad anammox que convierte el NH_4^+ a N_2 (Richards et al. 1965; Devol 2003). Sin embargo, el MSC constituido principalmente por las picocianobacterias del género *Prochlorococcus* representa una fuente importante de O_2 contribuyendo así al metabolismo aeróbico en las ZMAs. Los análisis metatranscriptómicos indican una alta oxidación de NO_2^- y de materia orgánica y una baja actividad anammox (posiblemente inhibida por la producción de O_2 en el MSC). Así, el NH_4^+ producido por la oxidación de la materia orgánica y un menor consumo de NH_4^+ por las bacterias y/o arqueas anammox (bajos transcritos) puede dejar disponible el NH_4^+ para la

asimilación en *Prochlorococcus* explicando las altas tasas de asimilación de las formas reducidas de N. Sin embargo, el NH_4^+ sigue siendo escaso, por lo que el NO_2^-, el cual es más abundante en el MSC podría representar la fuente de N necesaria para por lo menos un porcentaje del grupo de *Prochlorococcus* que habita las ZMAs. Por lo tanto, la captación de NO_2^- por *Prochlorococcus* significaría una eventual competencia por este nutriente con las bacterias oxidantes de nitrito altamente activas en el MSC.

El MSC es también una fuente de carbono fijado (0,15–0,95 y 0,02–0,87 mmol C m^{-2} d^{-1} para el PNOT y el PSOT, respectivamente) y a pesar de que la producción primaria en las aguas superficiales excede ampliamente a los valores del MSC, la gran mayoría de la producción superficial es remineralizada antes de alcanzar el núcleo de la ZMA (Lee et al. 2004). La producción de C en el MSC puede proveer entre un 5-47% y el 2-20% de la materia organica suministrada hacia las aguas anóxicas del PNOT y el PSOT respectivamente, dónde parte de esta es remineralizada por los proceso de reducción desasimilatoria del NO_3^- a NO_2^- y desnitrificación (Ganesh et al. 2015, Babbin et al. 2014, Kalvelage et al. 2013, Ward, 2013).

Se espera que el calentamiento global produzca una somerizacion de la oxiclina en las ZMAs y una expansión en el volumen de las ZMAs (Gilly et al. 2013). Procesos de mesoescala, tales como la surgencia local y los remolinos anticiclónicos, somerizan los bordes oxicos-anóxico intensificando el desarrollo de los MSCs (Goericke et al. 2000, Cepeda-Morales et al. 2009). Con una oxiclina más somera, es más probable que la luz alcance los núcleos anóxicos de las ZMAs, estimulando potencialmente la comunidad fotosintética. Se esperarían entonces, áreas más extensas y con altas tasas de actividad biológica del MSC, con ciclos diarios óxicos/anóxicos e influenciando así la productividad marina y el ciclo acoplado del N global.

6. CONCLUSIONES

1. El desarrollo de un MSC en la parte superior de las ZMAs —con concentraciones altas en NO_3^- y bajas en N reducido— es un atributo que se repite con variable intensidad en las ZMAs del PNOT y PSOT. Este MSC está dominado numéricamente por las picocianobacterias *Prochlorococcus* y tipo *Synechococcus* y casi no se detectan PEF.
2. Los bajos valores de saturación de la luz (E_k = 10,5 ± 2,0 y 21,4 ± 9,3 μmol fotones m^{-2} s^{-1} para el PNOT y PSOT respectivamente) calculados desde nuestros experimentos, reflejan la adaptación de *Prochlorococcus* a las bajas intensidades de luz ambiental (<1% de luz incidente) siendo similares a los valores encontrados para la comunidad del MSC del Mar Arábigo o en ejemplares cultivados de *Prochlorococcus*.
3. Las intensidades de la luz en el MSC son variables y presentan generalmente valores por debajo de los 10 μmol fotones m^{-2} s^{-1}. Bajo esas condiciones, otros metabolismos también podrían ser importantes, como la asimilación de glucosa, una potencial fuente de C para las picocianobacterias de las ZMAs.
4. Las tasas de producción de O_2 en el MSC son más bajas que las tasas de respiración, y el O_2 producido es inmediatamente consumido por la comunidad microbiana, resultando en un ciclo críptico del O_2 en el ambiente aparentemente anóxico del MSC. A pesar de que en el MSC los niveles de O_2 son indetectables, existe una producción de O_2 suficiente para mantener metabolismos aeróbicos como la oxidación de nitrito y de la materia orgánica. Sin embargo, el balance entre el consumo heterotrófico de O_2 y el de las oxidantes de nitrito puede variar en función de la concentración real de O_2 medido para las distintas estaciones.
5. El MSC es también una fuente de C fijado. A pesar de que la producción primaria en las aguas superficiales excede ampliamente estos valores, la gran mayoría de la producción superficial es remineralizada antes de alcanzar el núcleo de la ZMA. La producción de C en el MSC puede proveer un 5-47% y 2-20% de la materia orgánica suministrada hacia las aguas anóxicas del PNOT y el PSOT, respectivamente, dónde parte de esta es remineralizada por los proceso de reducción desasimilatoria del NO_3^- a NO_2^- y desnitrificación.

6. Aunque los linajes de *Prochlorococcus* de las ZMAs han retenido la capacidad de utilizar NO_3^- ellos parecen no depender de este nutriente como fuente principal de N. Los linajes de *Prochlorococcus* de las ZMAs están utilizando una mezcla de formas oxidadas y reducidas de N para satisfacer sus requerimientos nutricionales. Sin embargo, cuando el NH_4^+ y la urea están disponibles, *Prochlorococcus* usa preferentemente estos nutrientes a pesar de que su repertorio genómico permite el uso de formas oxidadas. La producción de O_2 por *Prochlorococcus* podría estar estimulando la respiración aeróbica por bacterias heterotróficas, produciendo así el NH_4^+ que *Prochlorococcus* necesita sin acumulación en el MSC.
7. Las picocianobacterias de las ZMAs podrían representar potenciales competidoras con las bacterias anammox y las arqueas oxidantes del amonio por el NH_4^+ y/o con bacterias nitrito oxidantes por el NO_2^-.

Una posible somerización de la oxiclina en las ZMAs y una expansión del volumen de esta agua anóxicas permitiría una mayor exposición de luz solar en los núcleos anóxicos, estimulando potencialmente la comunidad fotosintética en el MSC, con ciclos diarios óxicos/anóxicos en estos MSCs influenciando así la productividad marina y el ciclo acoplado del N global.

Perspectivas

La presencia de un MSC en la parte superior de las ZMAs es un atributo que se repite con variable intensidad, sin embargo, en algunas ocasiones el MSC se encuentra ausente a pesar de que hay suficiente luz para el desarrollo de las picocianobacterias que lo componen. Mayor investigación en la que se relacionen las variables físicas, químicas y biológicas como también fenómenos de gran escala como El Niño o remolinos de mesoescala con la presencia/ausencia del MSC podrían ayudar a establecer los componentes principales que determinan la presencia/ausencia del MSC en las ZMAs.

Trabajos futuros que comprendan experimentos con comunidades naturales y tasas célula-específicas de utilización de distintas fuentes de C ayudarían a determinar cuál es la contribución de cada uno de los grupos funcionales que componen la comunidad del MSC al ciclo del C. Finalmente, mayores esfuerzos conducentes a aislar representantes de

Prochlorococcus que habitan las ZMAs podrían ayudar a tener una visión más completa de la biología y ecología de estos ecotipos.

En resumen, en esta tesis:

Se acepta parcialmente la H_1: "La picocianobacteria *Prochlorococcus* LL que habita en el MSC de las ZMAs posee un metabolismo del C basado en la fijación de C y una heterotrofía complementaria que les permitiría vivir en zonas de baja luminosidad y bajo oxígeno". Efectivamente, *Prochlorococcus* tiene un metabolismo del C basado en la fijación de C, pero no se pudo comprobar la utilización de fuentes de C alternativas específicamente para *Prochlorococcus,* pero si para la comunidad del MSC.

Se rechaza la H_2: "La picocianobacteria *Prochlorococcus* LL que habita en el MSC de las ZMAs posee un metabolismo del N basado en la utilización de NO_3^-, a diferencia del conocido para los linajes que habitan las zonas óxicas iluminadas que está basado principalmente en amonio". Debido a que a pesar de que *Prochlorococcus* utiliza NO_3^-, lo hace en tasas muy bajas y basa su metabolismo en fuentes reducidas de N y/o NO_2^-.

7. REFERENCIAS

Aldunate, M., Henríquez-Castillo, C., Ji, Q., Lueders-Dumont, J., Mulholland, M. R., Ward, B. B., von Dassow, P. Ulloa, O. 2019. Nitrogen assimilation in picocyanobacteria inhabiting the oxygen-deficient waters of the eastern tropical North and South Pacific. Limnology and Oceanography. doi:10.1002/lno.11315

Astorga-Eló, M., S. Ramírez-Flandes, E. F. DeLong, and O. Ulloa. 2015. Genomic potential for nitrogen assimilation in uncultivated members of *Prochlorococcus* from an anoxic marine zone. ISME J. **9**: 1264–1267.doi:10.1038/ismej.2015.21

Babbin, A. R., R. G. Keil, A. H. Devol, and B. B. Ward. 2014. Organic Matter Stoichiometry, Flux, and Oxygen Control Nitrogen Loss in the Ocean. Science (80-.). **344**: 406–408. doi:10.1126/science.1248364

Berglund, M. & Wieser, M. 2011. Isotopic compositions of the elements 2009 (IUPAC Technical Report). *Pure and Applied Chemistry*, 83(2), pp. 397-410. Retrieved 7 Oct. 2019, from doi:10.1351/PAC-REP-10-06-02

Berube, P. M., S. J. Biller, A. G. Kent, J. W. Berta-Thompson, S. E. Roggensack, K. H. Roache-Johnson, M. Ackerman, L. R. Moore and others. 2015. Physiology and evolution of nitrate acquisition in *Prochlorococcus*. ISME J. **9**: 1195–1207.doi:10.1038/ismej.2014.211

Bibby, T. S., I. Mary, J. Nield, F. Partensky, and J. Barber. 2003. Low-light-adapted Prochlorococcus species possess specific antennae for each photosystem. Nature **424**: 1051–1054. doi:10.1038/nature01933

Biller, S. J., P. M. Berube, D. Lindell, and S. W. Chisholm. 2015. Prochlorococcus: the structure and function of collective diversity. Nat. Rev. Microbiol. **13**: 13–27. doi:10.1038/nrmicro3378

Canfield, D. E., F. J. Stewart, B. Thamdrup, L. De Brabandere, T. Dalsgaard, E. F. Delong, N. P. Revsbech, and O. Ulloa. 2010. A cryptic sulfur cycle in oxygen-minimum-zone waters off the Chilean coast. Science (80-.). **330**: 1375–8. doi:10.1126/science.1196889

Casey, J. R., M. W. Lomas, J. Mandecki, and D. E. Walker. 2007. *Prochlorococcus* contributes to new poduction in the Sargasso Sea deep chlorophyll maximum. Geophys. Res. Lett. **34**: 1–5.doi:10.1029/2006GL028725

Cepeda-Morales, J., E. Beier, G. Gaxiola-Castro, M. F. Lavín, and V. Godínez. 2009. Effect of the oxygen minimum zone on the second chlorophyll maximum. Ciencias Mar. **35**: 389–403. doi:10.7773/cm.v35i4.1622

Chisholm, S. W. 1992. Phytoplankton Size, p. 213–237. *In* P.G. Falkowski, A. Woodhead, and K. Vivirito [eds.], Primary Productivity and Biogeochemical Cycles in the Sea. Springer US.

Dalsgaard, T., B. Thamdrup, L. Farías, and N. P. Revsbech. 2012. Anammox and denitrification in the oxygen minimum zone of the eastern South Pacific. Limnol. Oceanogr. **57**: 1331–1346. doi:10.4319/lo.2012.57.5.1331

Davey, H. M., and D. B. Kell. 1996. Flow cytometry and cell sorting of heterogeneous microbial populations: the importance of single-cell analyses. Microbiol. Rev. **60**: 641–96.

Devol, A. H. 2003. Nitrogen cycle: Solution to a marine mystery. Nature **422**: 575–576. doi:10.1038/422575a

Dufresne, A., L. Garczarek, and F. Partensky. 2005. Accelerated evolution associated with genome reduction in a free-living prokaryote. Genome Biol. **6**: R14. doi:10.1186/gb-2005-6-2-r14

Dugdale, R. C., and F. P. Wilkerson. 1986. The use of 15N to measure nitrogen uptake in eutrophic oceans; experimental considerations1,2. Limnol. Oceanogr. **31**: 673–689.doi:10.4319/lo.1986.31.4.0673

Fawcett, S. E., M. W. Lomas, J. R. Casey, B. B. Ward, and D. M. Sigman. 2011. Assimilation of upwelled nitrate by small eukaryotes in the Sargasso Sea. Nat. Geosci. **4**: 717–722.doi:10.1038/ngeo1265

Flombaum, P., J. L. Gallegos, R. A. Gordillo, J. Rincón, L. L. Zabala, N. Jiao, D. M. Karl, W. K. W. Li and others. 2013. Present and future global distributions of the marine Cyanobacteria *Prochlorococcus* and *Synechococcus*. Proc. Natl. Acad. Sci. **110**: 9824–9829.doi:10.1073/pnas.1307701110

Flores, E., and A. Herrero. 2005. Nitrogen assimilation and nitrogen control in cyanobacteria: Figure 1. Biochem. Soc. Trans. **33**: 164–167. doi:10.1042/BST0330164

Fuchsman, C. A., H. I. Palevsky, B. Widner, and others. 2019. Cyanobacteria and cyanophage contributions to carbon and nitrogen cycling in an oligotrophic oxygen-deficient zone. ISME J. doi:10.1038/s41396-019-0452-6

Ganesh, S., L. A. Bristow, M. Larsen, N. Sarode, B. Thamdrup, and F. J. Stewart. 2015. Size-fraction partitioning of community gene transcription and nitrogen metabolism in a marine oxygen minimum zone. ISME J. **9**: 2682–2696. doi:10.1038/ismej.2015.44

García-Fernández, J. M., and J. Diez. 2004. Adaptive mechanisms of nitrogen and carbon assimilatory pathways in the marine cyanobacteria Prochlorococcus. Res. Microbiol. **155**: 795–802. doi:10.1016/j.resmic.2004.06.009

Gilly, W. F., J. M. Beman, S. Y. Litvin, and B. H. Robison. 2013. Oceanographic and Biological Effects of Shoaling of the Oxygen Minimum Zone. Ann. Rev. Mar. Sci. **5**: 393–420. doi:10.1146/annurev-marine-120710-100849

Goericke, R., R. Olson, and A. Shalapyonok. 2000. A novel niche for *Prochlorococcus* sp. in low-light suboxic environments in the Arabian Sea and the Eastern Tropical North Pacific. Deep Sea Res. Part I Oceanogr. Res. Pap. **47**: 1183–1205.doi:10.1016/S0967-0637(99)00108-9

Gómez-Baena, G., A. López-Lozano, J. Gil-Martínez, J. M. Lucena, J. Diez, P. Candau, and J. M. García-Fernández. 2008. Glucose Uptake and Its Effect on Gene Expression in Prochlorococcus C.-H. Yang [ed.]. PLoS One **3**: e3416. doi:10.1371/journal.pone.0003416

Grob, C., O. Ulloa, W. Li, G. Alarcón, M. Fukasawa, and S. Watanabe. 2007. Picoplankton abundance and biomass across the eastern South Pacific Ocean along latitude 32.5°S. Mar. Ecol. Prog. Ser. **332**: 53–62. doi:10.3354/meps332053

Hess, W. R., G. Rocap, C. S. Ting, F. Larimer, S. Stilwagen, J. Lamerdin, and S. W. Chisholm. 2001. The photosynthetic apparatus of Prochlorococcus : Insights through comparative genomics. 53–71.

Huang, S., S. W. Wilhelm, H. R. Harvey, K. Taylor, N. Jiao, and F. Chen. 2012. Novel lineages of Prochlorococcus and Synechococcus in the global oceans. ISME J. **6**: 285–297. doi:10.1038/ismej.2011.106

Jardillier, L., M. V Zubkov, J. Pearman, and D. J. Scanlan. 2010. Significant CO2 fixation by small prymnesiophytes in the subtropical and tropical northeast Atlantic Ocean. ISME J. **4**: 1180–1192. doi:10.1038/ismej.2010.36

Johnson, Z., M. L. Landry, R. R. Bidigare, S. L. Brown, L. Campbell, J. Gunderson, J. Marra, and C. Trees. 1999. Energetics and growth kinetics of a deep Prochlorococcus spp. population in the Arabian Sea. Deep Sea Res. Part II Top. Stud. Oceanogr. **46**: 1719–1743. doi:10.1016/S0967-0645(99)00041-7

Kalvelage, T., G. Lavik, P. Lam, and others. 2013. Nitrogen cycling driven by organic matter export in the South Pacific oxygen minimum zone. Nat. Geosci. **6**: 228–234. doi:10.1038/ngeo1739

Knapp AN, Sigman DM & Lipschultz F (2005) N isotopic composition of dissolved organic nitrogen and nitrate at the Bermuda Atlantic Time-series Study site. Global Biogeochem. Cycles 19: 1-15.

Lam, P., and M. M. M. Kuypers. 2011. Microbial Nitrogen Cycling Processes in Oxygen Minimum Zones. Ann. Rev. Mar. Sci. **3**: 317–345.doi:10.1146/annurev-marine-120709-142814

Latysheva, N., V. L. Junker, W. J. Palmer, G. A. Codd, and D. Barker. 2012. The evolution of nitrogen fixation in cyanobacteria. Bioinformatics **28**: 603–606. doi:10.1093/bioinformatics/bts008

Lavin, P., B. González, J. F. Santibáñez, D. J. Scanlan, and O. Ulloa. 2010. Novel lineages of *Prochlorococcus* thrive within the oxygen minimum zone of the eastern tropical South Pacific. Environ. Microbiol. Rep. **2**: 728–738. doi:10.1111/j.1758-2229.2010.00167.x

Lee, C., S. Wakeham, and C. Arnosti. 2004. Particulate Organic Matter in the Sea: The Composition Conundrum. AMBIO A J. Hum. Environ. **33**: 565–575. doi:10.1579/0044-7447-33.8.565

Li, W. K. W. 1994. Primary production of prochlorophytes, cyanobacteria, and eucaryotic ultraphytoplankton: Measurements from flow cytometric sorting. Limnol. Oceanogr. **39**: 169–175. doi:10.4319/lo.1994.39.1.0169

Liu, H., H. Nolla, and L. Campbell. 1997. Prochlorococcus growth rate and contribution to primary production in the equatorial and subtropical North Pacific Ocean. Aquat. Microb. Ecol. **12**: 39–47. doi:10.3354/ame012039

Lomas MW, Bronk D a & van den Engh G (2011) Use of flow cytometry to measure biogeochemical rates and processes in the ocean. Ann. Rev. Mar. Sci. 3: 537–566.

Malmstrom, R. R., A. Coe, G. C. Kettler, A. C. Martiny, J. Frias-Lopez, E. R. Zinser, and S. W. Chisholm. 2010. Temporal dynamics of Prochlorococcus ecotypes in the Atlantic and Pacific oceans. ISME J. **4**: 1252–1264. doi:10.1038/ismej.2010.60

Marie, D., F. Partensky, D. Vaulot, and C. Brussaard. 2001. Enumeration of Phytoplankton, Bacteria, and Viruses in Marine Samples, p. 1–15. *In* Current Protocols in Cytometry. John Wiley & Sons, Inc.

Martiny, A. C., A. P. K. Tai, D. Veneziano, F. Primeau, and S. W. Chisholm. 2009. Taxonomic resolution, ecotypes and the biogeography of *Prochlorococcus*. Environ. Microbiol. **11**: 823–832.doi:10.1111/j.1462-2920.2008.01803.x

Moore LR, Chisholm SW (1999) Photophysiology of the marine cyanobacterium Prochlorococcus: Ecotypic differences among cultured isolates. Limnol Oceanogr 44: 628–638. 22.

Moore, L. R., A. F. Post, G. Rocap, and S. W. Chisholm. 2002. Utilization of different nitrogen sources by the marine cyanobacteria *Prochlorococcus* and *Synechococcus*. Limnol. Oceanogr. **47**: 989–996.doi:10.4319/lo.2002.47.4.0989

Munoz-Marin, M. d. C., I. Luque, M. V Zubkov, P. G. Hill, J. Diez, and J. M. Garcia-Fernandez. 2013. Prochlorococcus can use the Pro1404 transporter to take up glucose at

nanomolar concentrations in the Atlantic Ocean. Proc. Natl. Acad. Sci. **110**: 8597–8602. doi:10.1073/pnas.1221775110

Painter, S., R. Sanders, H. Waldron, M. Lucas, and S. Torres-Valdes. 2008. Urea distribution and uptake in the Atlantic Ocean between 50°N and 50°S. Mar. Ecol. Prog. Ser. **368**: 53–63. doi:10.3354/meps07586

Partensky, F., J. Blanchot, and D. Vaulot. 1999. Differential distribution and ecology of Prochlorococcus and *Synechococcus* in oceanic waters: a review. Bull. l'Institut océanographique **19**: 457–475.

Partensky, F., and L. Garczarek. 2010. *Prochlorococcus*: Advantages and Limits of Minimalism. Ann. Rev. Mar. Sci. **2**: 305–331.doi:10.1146/annurev-marine-120308-081034

Revsbech, N. P., L. H. Larsen, J. Gundersen, T. Dalsgaard, O. Ulloa, and B. Thamdrup. 2009. Determination of ultra-low oxygen concentrations in oxygen minimum zones by the STOX sensor. Limnol. Oceanogr. Methods **7**: 371–381.doi:10.4319/lom.2009.7.371

Rocap, G., F. W. Larimer, J. Lamerdin, S. Malfatti, P. Chain, N. A. Ahigren, A. Arellano, M. Coleman and others. 2003. Genome divergence in two *Prochlorococcus* ecotypes reflects oceanic niche differentiation. Nature **424**: 1042–1047.doi:10.1038/nature01947

Richards, F.A., J.D. Cline, W.W. Bronkow and L. P. Atkinson. 1965. Some consequences of the decomposition of organic matter in Lake Nitinat, an anoxic fjord. Limnol. Oceanogr. (suppl.) 10: 185–201.

Scanlan, D. J., M. Ostrowski, S. Mazard, and others. 2009. Ecological genomics of marine picocyanobacteria. Microbiol. Mol. Biol. Rev. **73**: 249–299. doi:10.1128/MMBR.00035-08

Shapiro H. 2003. Practical Flow Cytometry.Hoboken,NewJersey:Wiley. 529 pp. 4ta ed.

Sigman, D. M., K. L. Casciotti, M. Andreani, C. Barford, M. Galanter, and J. K. Böhlke. 2001. A bacterial method for the nitrogen isotopic analysis of nitrate in seawater and freshwater. Anal. Chem. **73**: 4145–53.

Stewart, F. J., O. Ulloa, and E. F. Delong. 2011. Microbial metatranscriptomics in a permanent marine oxygen minimum zone. Environ. Microbiol. **2**. doi:10.1111/j.1462-2920.2010.02400.x

Thamdrup, B., T. Dalsgaard, and N. P. Revsbech. 2012. Widespread functional anoxia in the oxygen minimum zone of the Eastern South Pacific. Deep Sea Res. Part I Oceanogr. Res. Pap. **65**: 36–45.doi:10.1016/j.dsr.2012.03.001

Tiano L, et al. (2014) Oxygen distribution and aerobic respiration in the north and south eastern tropical Pacific oxygen minimum zones. Deep Sea Res Part I Oceanogr Res Pap 94:173–183

Tyrrell, T. 1999. The relative in Influences of nitrogen and phosphorus on oceanic primary production. Nature **400**: 525–531.

Ulloa, O., D. E. Canfield, E. F. DeLong, R. M. Letelier, and F. J. Stewart. 2012. Microbial oceanography of anoxic oxygen minimum zones. Proc. Natl. Acad. Sci. **109**: 15996–16003.doi:10.1073/pnas.1205009109

Ward, B. B. 2013. How Nitrogen Is Lost. Science (80-.). **341**: 352–353. doi:10.1126/science.1240314

Ward, B. B., a H. Devol, J. J. Rich, B. X. Chang, S. E. Bulow, H. Naik, A. Pratihary, and a Jayakumar. 2009. Denitrification as the dominant nitrogen loss process in the Arabian Sea. Nature **461**: 78–81.doi:10.1038/nature08276

Widner, B., C. W. Mordy, and M. R. Mulholland. 2018a. Cyanate distribution and uptake above and within the Eastern Tropical South Pacific oxygen deficient zone. Limnol. Oceanogr. **63**: S177–S192. doi:10.1002/lno.10730

Widner, B., C. A. Fuchsman, B. X. Chang, G. Rocap, and M. R. Mulholland. 2018b. Utilization of urea and cyanate in waters overlying and within the eastern tropical north Pacific oxygen deficient zone. FEMS Microbiol. Ecol. **94**: 1–15. doi:10.1093/femsec/fiy138

Zhaxybayeva, O., W. F. Doolittle, R. T. Papke, and J. P. Gogarten. 2009. Intertwined Evolutionary Histories of Marine Synechococcus and Prochlorococcus marinus. Genome Biol. Evol. **1**: 325–339. doi:10.1093/gbe/evp032

Zubkov, M. V, B. M. Fuchs, G. A. Tarran, P. H. Burkill, and R. Amann. 2003. High Rate of Uptake of Organic Nitrogen Compounds by *Prochlorococcus* cyanobacteria as a key to their dominance in oligotrophic oceanic waters. Microbiology **69**: 1299–1304.doi:10.1128/AEM.69.2.1299

Zubkov, M. V., G. a. Tarran, and B. M. Fuchs. 2004. Depth related amino acid uptake by Prochlorococcus cyanobacteria in the Southern Atlantic tropical gyre. FEMS Microbiol. Ecol. **50**: 153–161. doi:10.1016/j.femsec.2004.06.009

Zwirglmaier, K., L. Jardillier, M. Ostrowski, and others. 2007. Global phylogeography of marine Synechococcus and Prochlorococcus reveals a distinct partitioning of lineages among oceanic biomes. Environ. Microbiol. **0**: 070928214009001-??? doi:10.1111/j.1462-2920.2007.01440.x